DURBAN UNIVERSITY of TECHNOLOGY

Use of Evaporative Coolers for Close Circuiting of the Electroplating Process

Submitted in fulfilment of the requirements of the degree of Master of Technology: Chemical Engineering in the Faculty of Engineering and the Built Environment at the Durban University of Technology

Megashnee Munsamy

BTech: Chemical Engineering

April 2011

Promoter: Dr. V.N. Ndinisa

Co-Promoter: Dr. A. Telukdarie

DECLARATION

I, Megashnee Munsamy hereby declare that this dissertation has been done solely by me.

……..

Megashnee Munsamy

18 April 2011

Johannesburg

ABSTRACT

The South African electroplating industry generates large volumes of hazardous waste water that has to be treated prior to disposal. The main source of this waste water has been the rinse system. Conventional end-of-pipe waste water treatment technologies do not meet municipality standards. The use of technologies such as membranes, reverse osmosis and ion exchange are impractical, mainly due to their cost and technical requirements. This study identified source point reduction technologies, close circuiting of the electroplating process, specific to the rinse system as a key development. Specifically the application of a low flow counter current rinse system for the recovery of the rinse water in the plating bath was selected. However, the recovery of the rinse tank water was impeded by the low rates of evaporation from the plating bath, which was especially prevalent in the low temperature operating plating baths.

This master's study proposes the use of an induced draft evaporative cooling tower for facilitation of evaporation in the plating bath. For total recovery of the rinse tank water, the rate of evaporation from the plating bath has to be equivalent to the rinse tanks make up water requirements. A closed circuit plating system mathematical model was developed for the determination of the mass evaporated from the plating bath and the cooling tower for a specified time and the equilibrium temperature of the plating bath and the cooling tower.

The key criteria in the development of the closed circuit plating system model was the requirement of minimum solution specific data as this information is not readily available. The closed circuit plating system model was categorised into the unsteady state and steady state temperature regions and was developed for the condition of water evaporation only. The closed circuit plating system model was programmed into Matlab and verified.

The key factors affecting the performance of the closed circuit plating system were identified as the plating solution composition and operational temperature, ambient air temperature, air flow rate and cooling tower

packing surface area. Each of these factors was individually and simultaneously varied to determine their sensitivity on the rate of water evaporation and the equilibrium temperature of the plating bath and cooling tower. The results indicated that the upper limit plating solution operational temperature, high air flow rates, low ambient air temperature and large packing surface area provided the greatest water evaporation rates and the largest temperature drop across the height of the cooling tower in the unsteady state temperature region. The final equilibrium temperature of the plating bath and the cooling tower is dependent on the ambient air temperature. The only exception is that at low ambient air temperatures the rate of water evaporation from the steady state temperature region is lower than that at higher ambient air temperatures. Thus the model will enable the electroplater to identify the optimum operating conditions for close circuiting of the electroplating process.

It is recommended that the model be validated against practical data either by the construction of a laboratory scale induced draft evaporative cooling tower or by the application of the induced draft evaporative cooling tower in an electroplating facility.

DEDICATION

This dissertation is dedicated to my family for their continuous and unwavering support and love.

ACKNOWLEDGEMENTS

The following people are thanked for their work, support and guidance.

Dr. A. Telukdarie

Dr. N. V. Ndinisa

Wei Zhang

Mohamed Jaafar Bux

TABLE OF CONTENTS

LIST OF FIGURES

LIST OF TABLES

CHAPTER 1: INTRODUCTION

1.1 Overview

The focus of this master's study was the electroplating industry where large volumes of hazardous waste water, primarily from the rinse system, are generated requiring treatment prior to disposal. The objective of this master's study is to provide the electroplater with a solution for the elimination of the generation of rinse tank waste water. The scope of the study, from the identification to the application of the proposed solution, is detailed and the outputs are identified. The structure of the thesis is provided with a brief description of each chapter.

1.2 Background

The metal finishing industry is involved in the deposition of a metallic coating onto a metallic surface via varying processes such as electroplating, powder coating, hot dip coating, anodising, etc. The coatings are applied to metallic surfaces such tyre rims, exhaust pipes, lighting fixtures, plumbing fixtures, etc. The metallic coatings can be for aesthetic or protective purposes.

The electroplating process can be categorised into two phases; the cleaning phase and the electroplating phase. The cleaning phase which consists of the degreasing phase and acid cleaning phase is for the removal of oil and rust from the metal surface, respectively. The electroplating phase is the electro-deposition of the coating onto the metallic surface via an electrochemical reaction.

Prior to entering the degreasing, acid and electroplating bath, the metal pieces pass through a single or a series of rinse tanks for the removal of chemicals carried over from the previous bath. An electroplating process with a single rinse system is illustrated in Figure 1.

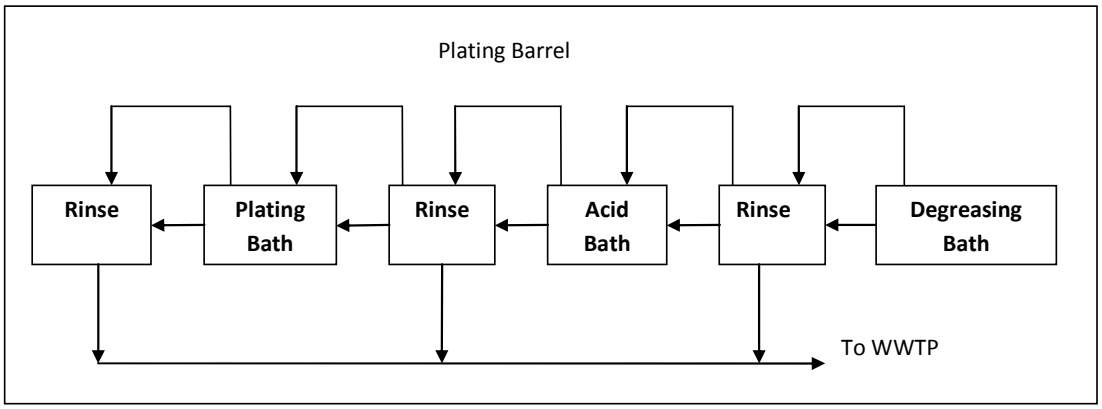

Figure 1: Diagrammatic representation of a plating line

The electroplating process consumes large amounts of hazardous chemicals and water and generates large amounts of waste water[1,2]. The waste water is hazardous and contains heavy metals, oils, acid/alkali fumes, hexavalent chrome, etc[3,4]. The primary source of waste water from an electroplating process is the rinse tanks[4].

Cleaner production (CP) is a tool utilised by industries to reduce their environmental impact by optimising the process, recycling, improved housekeeping, etc[5]. A CP initiative was sponsored by the Danish Cooperation of Environment and Development (DANCED) for the metal finishing industry in Durban, South Africa (SA). The study identified the water system as one of the primary areas for improvement[4]. For the optimisation of the water system the following measures were identified; optimising the rinse system, flow control and counter rinse flow[4].

For the purpose of this master's study, the focus was on the electroplating industry with the application of CP technologies for the reduction in the waste water generation from the rinse system.

1.3 Challenges Encountered by the Electroplating Industry

Disposal and handling of the toxic and hazardous waste water generated is problematic and costly. As South Africa's waste water disposal laws become more stringent, the local electroplaters need to identify innovative and cost effective ways of handling and treating the waste water to meet municipality waste water standards.

The majority of electroplaters in SA are small to medium enterprises (SME's). Due to their financial and technical constraints, the purchasing and application of technologies such as membrane separation, ion exchange, etc for the treatment of the waste water seems an unlikely possibility[4,6].

As proven downstream waste water treatment technologies are currently not a feasible option, solutions for waste water reduction at the source need to be identified and implemented. As the rinse system was identified as the primary source of waste water generation, possible methodologies for the reduction of the generation of rinse tank waste water were considered. Close circuiting of the electroplating process was identified as a viable option. Close circuiting of the electroplating process will enable the recovery of the rinse tank water into the plating bath, thus resulting in almost zero waste water discharge from the rinse system.

From the DANCED initiative, the low flow counter current rinse system was identified as a solution for close circuiting of the electroplating system[4]. Refer to Figure 2 for an illustration of a low flow counter current rinse system.

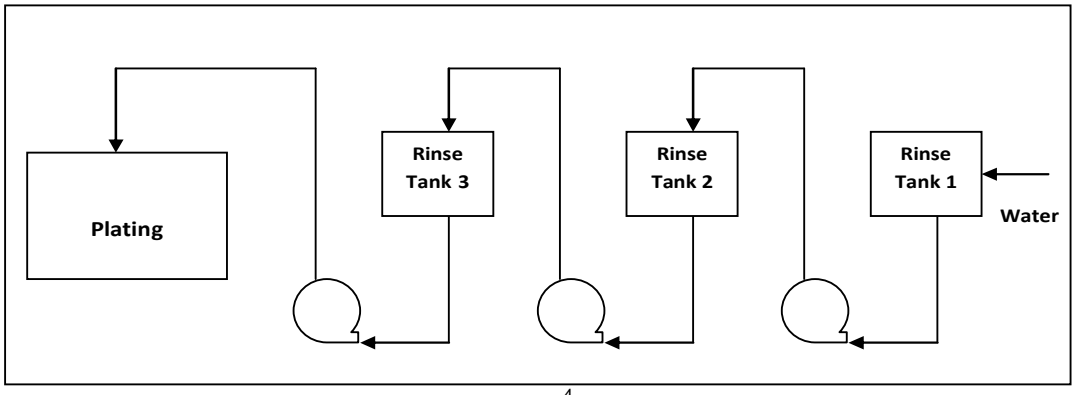

Figure 2: Low flow counter current rinse system[4]

However, close circuiting of the electroplating system was impeded by the low rates of water evaporation from the plating baths, which was especially prevalent in the low temperature operating plating baths. These low evaporation rates significantly reduced the volumes of rinse waste water that could be recovered.

To overcome the low evaporation rates in the low temperature operating plating bath, this master's study proposes the use of an induced draft evaporative cooling tower for facilitating evaporation in the plating bath. The evaporative cooler will be continuously circulated with the plating bath solution to promote evaporation.

1.4 Project Scope

Close circuiting of the electroplating process can only be achieved provided the rate of evaporation from the plating bath is equivalent to the rinse system make-up water requirements. Thus the plating bath together with the cooling tower has to be optimised to achieve the required evaporation rates.

In this master's study a mathematical model for the identification of the operating conditions for close circuiting of the electroplating process is developed. The model will predict the equilibrium temperatures and the mass of water evaporated from the cooling tower and the plating bath for a specified time period based on user specified inputs. The model developed is programmed into Matlab.

The mathematical model developed is based on evaporative cooling theory and the principles of heat and mass transfer from an open tank. The key parameters of the plating bath and cooling tower affecting the rate of evaporation will be identified and a sensitivity analysis conducted. The results of the sensitivity analysis will enable the electroplater to identify the optimum operating parameters for the cooling tower and the plating bath for recovery of the rinse water into the plating bath.

Thus the aims of this master's study are to provide electroplaters with a solution for close circuiting of the plating process, the use of evaporative cooling towers, and a tool, the Matlab model that will enable the identification of the optimum operating conditions of the plating bath and cooling tower for the elimination of the generation of rinse waste water.

1.5 Thesis Outline

The break down of the thesis excluding this chapter is as follows:

- Chapter 2: Literature Review
  This chapter provides a background on the key functional areas of the study; the metal finishing industry, the electroplating process, waste water treatment in the electroplating industry, cooling tower theory and the methodology for the model development.

- Chapter 3: Mathematical Model Development for the Closed Circuit Plating System
  This chapter details the equations and the mathematical set-up of the CCPS model.

- Chapter 4: Experimental Methodology for the Determination of the Interfacial Partial Pressure of the Diffusing Component
  This chapter details the gas diffusion experimental methodology. A statistical analysis of the experimental results is performed, for the establishment of a mathematical relationship for the prediction of the rate of diffusion of water from a plating solution.

- Chapter 5: Closed Circuit Plating System Model Verification
  This chapter details the methodology followed for the verification of the CCPS model.

- Chapter 6: Application of the Closed Circuit Plating System Model
  This chapter demonstrates the application of the CCPS model for the determination of the optimum operating conditions of the plating process.

- Chapter 7: Conclusion and Recommendations
  This chapter details the findings of the study undertaken.

CHAPTER 2: LITERATURE REVIEW

2.1 Introduction

The purpose of this chapter is to provide a background and motivation for undertaking the study. It introduces the metal finishing industry and its status in South Africa, focusing on the electroplating industry and the challenges being encountered with waste water generation and treatment. Cleaner production and the implementation of the concept of closed circuit plating for the elimination of waste water generation by the rinse system are discussed. A background on cooling towers and the methodology for the development of the CCPS model are detailed.

2.2 The Metal Finishing Industry

The metal finishing industry deposits a preservating/ decorative metallic coating onto a base metallic surface. The coatings are applied via varying processes, which categorises the various sectors within the metal finishing industry; namely electroplating, powder coating, anodising, polishing, etc. Typical metallic coatings applied to metallic surfaces are zinc, copper, tin, nickel, etc.

Upon completion of the fabrication of the metal component, the metal finishing process begins. The first phase in the metal finishing process is surface preparation, to ensure adhesion of the coating onto the metal surface[7]. Various surface preparation techniques are employed such as abrasive blasting, acid washes, alkaline cleaning, emulsion cleaning, and etc[7]. The next phase is the actual deposition of the metallic coating onto the metallic surface via a specific process. Refer to Figure 3 for an illustration of the metallic finishing process.

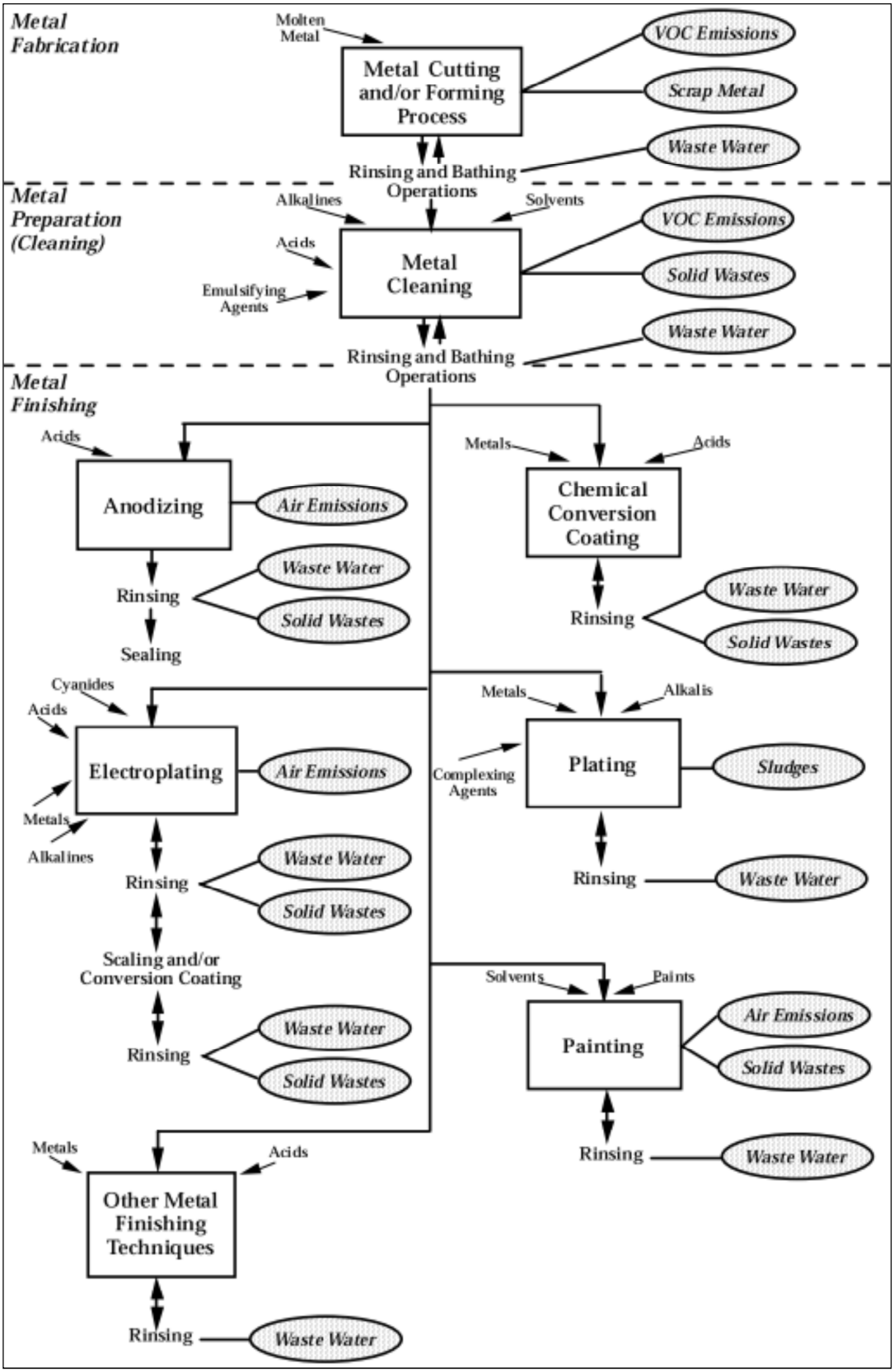

Figure 3: Workflow for a metal finishing process[7]

Table 1 provides a summarized version of the typical inputs and outputs from a metal finishing process.

Table 1: Summary of inputs and outputs from a metal finishing process[7]

Process	Material Input	Air Emission	Process Wastewater	Solid Waste
Metal Shaping				
Metal Cutting and/or Forming	Cutting oils, degreasing and cleaning solvents, acids, alkalis, and heavy metals	Solvent wastes (e.g., 1,1,1-trichloroethane, acetone, xylene, toluene, etc.)	Waste oils (e.g., ethylene glycol) and acid (e.g., hydrochloric, sulfuric, nitric), alkaline, and solvent wastes	Metal chips (e.g., scrap steel and aluminum), metal-bearing cutting fluid sludges, and solvent still-bottom wastes
Surface Preparation				
Solvent Degreasing and Emulsion, Alkaline, and Acid Cleaning	Solvents, emulsifying agents, alkalis, and acids	Solvents (associated with solvent degreasing and emulsion cleaning only)	Solvent, alkaline, and acid wastes	Ignitable wastes, solvent wastes, and still bottoms
Surface Finishing				
Anodizing	Acids	Metal-ion-bearing mists and acid mists	Acid wastes	Spent solutions, wastewater treatment sludges, and base metals
Chemical Conversion Coating	Metals and acids	Metal-ion-bearing mists and acid mists	Metal salts, acid, and base wastes	Spent solutions, wastewater treatment sludges, and base metals
Electroplating	Acid/alkaline solutions, heavy metal bearing solutions, and cyanide bearing solutions	Metal-ion-bearing mists and acid mists	Acid/alkaline, cyanide, and metal wastes	Metal and reactive wastes
Plating	Metals (e.g., salts), complexing agents, and alkalis	Metal-ion-bearing mists	Cyanide and metal wastes	Cyanide and metal wastes
Painting	Solvents and paints	Solvents	Solvent wastes	Still bottoms, sludges, paint solvents, and metals
Other Metal Finishing Techniques (Including Polishing, Hot Dip Coating, and Etching)	Metals and acids	Metal fumes and acid fumes	Metal and acid wastes	Polishing sludges, hot dip tank dross, and etching sludges

From Figure 3 and Table 1 it can be seen that there are various sources of waste (solid, liquid and gas) production in the metal finishing process. Hamid et al stated, “The metal finishing industry is chemically intensive. The vast majority of the chemicals are currently accumulated as “waste”.”[(8)] Fresner et al stated that, “German researchers estimated the amount of sludge from galvanizing plants in 2002 to be 80,000 tons. For Austria, 40,000 tons in 2003.”[(9)] Waste water discharge from German anodizing companies was found to be approximately one million cubic meters per year[9].

2.2.1 The metal finishing industry in South Africa

The metal finishing industry in South Africa cannot be accurately quantified as many are backyard operating facilities[4]. Koefoed et al stated that there are approximately 600-1000 metal finishers in SA[10]. Telukdarie et al stated that, "... over 90% of the metal finishing shops are SMEs; the majority have less than 50 employees. Of these, 20% have <10employees and 60% have <50 employees."[4] In SA the metal finishers are predominantly located in Gauteng, Kwa-Zulu Natal and the Western Cape, respectively[4,10]. Table 2 identifies the various metal finishing sectors in South Africa and indicates that the electroplating sector is the largest.

Table 2: Survey of the metal finishing industry in South Africa[4]

Proportion of Total (%)					
Electroplating	Powder Coating	Wet Painting	Hot Dip Coating	Polishing	Anodising
42	29	18	13	12	7

The metal finishing industry is characteristically polluting, with the SA metal finishing industry being no different[4,10]. The electroplating industry was identified as consuming large volumes of water, a consumption rate of 400L/m^2[4,10]. The rinse process consumes approximately 80 percent of the annual water requirements[4].

Due to the large consumption of water, large volumes of hazardous waste water are generated. The South African metal finishing industry typically uses end-of-pipe technologies to treat the waste water to conform to local municipality waste water discharge limits[4]. This has resulted in the generation of increased volumes of toxic sludge requiring disposal[4]. Thus both privately owned and government owned disposal sites have become overloaded and costly[4].

For the purposes of this master's study, the focus will be on the electroplating industry, which is water intensive and generates large volumes of hazardous waste water.

2.3 The Electroplating Process

Electroplating is the deposition of a metallic coating onto an object, by inducing a negative charge onto the object whilst immersing it in a plating solution containing ions of the metal to be coated. The electroplating process can be broken down into two phases; the cleaning/preparation phase and the plating phase.

The cleaning phase can categorised into the degreasing phase and the acid cleaning phase. In the degreasing phase the oil is removed from the metal surface by using a degreaser solution. The oil has either been used as a corrosion prevention measure or has been left behind during the manufacturing process[11]. The degreaser solution is dumped once the oil content renders the solution ineffective. In the acid phase, oxides on the metal surface are removed[7]. The acid cleaning process is also referred to as pickling[7]. The acid solution is dumped once the metal content renders the solution ineffective.

In the plating phase the actual electro-deposition of either a single metal or multi-metal layer onto a metal surface takes place[7]. The plating takes place in a plating bath, which is designed to last for extended periods of time. Refer to Figure 4 for a typical set up of an electroplating bath.

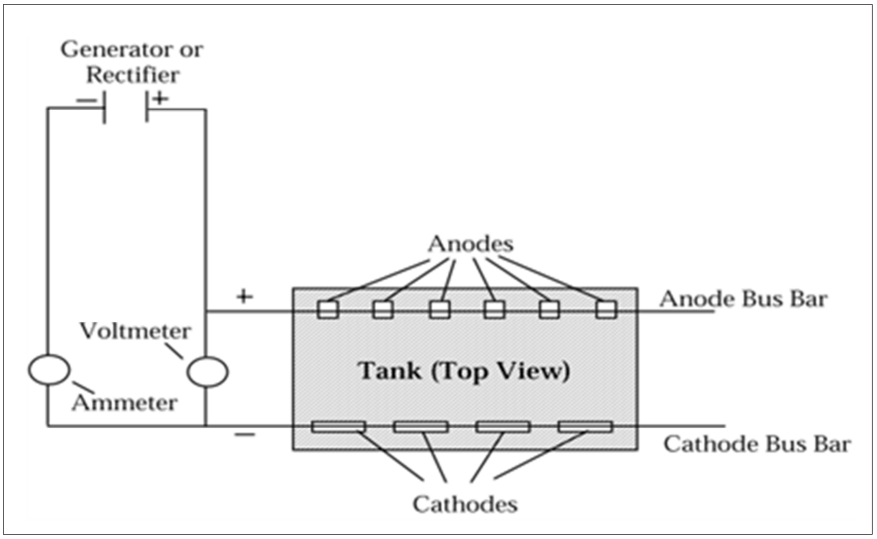

Figure 4: Electroplating bath[7]

After each of the above processes, the metal to be plated passes through a single rinse tank or a series of rinse tanks to remove the chemicals from the metal surface and to prevent drag out[9]. The tanks are either static or running rinses depending on the process requirements. Below is a diagrammatic representation of a typical electroplating process line with a single rinse system.

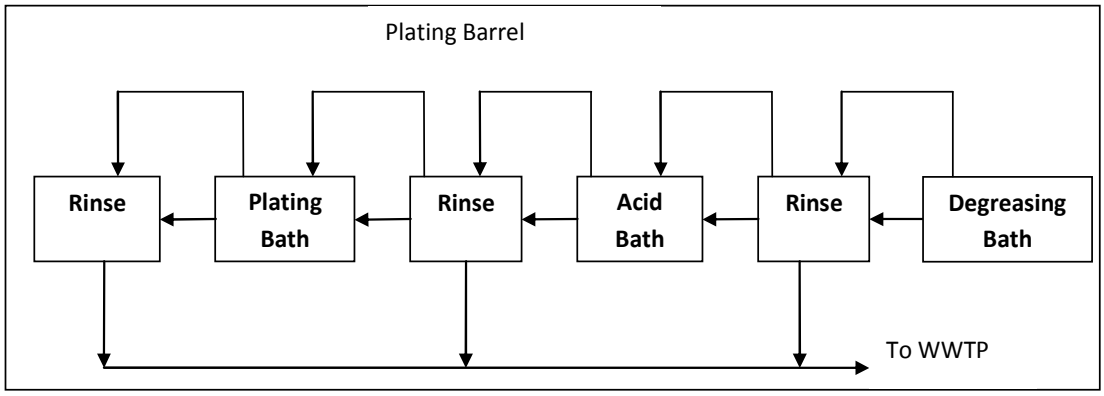

Figure 5: Diagrammatic representation of a plating line

2.4 Challenges Encountered by the Electroplating Industry

The electroplating industry utilises toxic and hazardous chemicals while simultaneously consuming and generating large amounts of water and waste water, respectively[1,2,4]. The rinse process produces the largest volume of waste water[4]. Qin et al states that, "... the typical daily consumption of a small enterprise with less than 100 employees is in the region of 1000m^3 for rinsing purpose."[3]

The waste water contaminants may include solvents, oil and grease, hexavalent chrome, cyanide, paint residue, organic compounds and heavy metals[3,4]. The sources of water contamination are: the water-in-oil emulsions, the spent bath solutions and the rinse water[12]. Alvarez-Ayuso et al identified chromium, nickel, zinc, copper and cadmium as "priority metals"[13]. In SA zinc, nickel, copper and hard chromium make up 25, 21, 16 and 13 percent of the electroplating industry, respectively[4,10]. This represents four of the five identified "priority metals."

These toxic heavy metals can have a detrimental effect on human, animal and marine life due to their toxicity and carcinogenic properties[14,15]. However,

the treatment of electroplating rinse water is a challenge with a few of the reasons highlighted below:

- They cannot be sent directly to conventional water treatment facilities, as the presence of these heavy metals can affect the biological treatment process[16].
- The possible formation of toxic hydrogen cyanide, by the mixing of cyanide and acidic waste water streams[17].
- The impedance of metal precipitation by high concentrations of oil and grease[17].

The typical end-of-pipe-technologies utilised by electroplaters for the treatment of waste water will be discussed in the next section.

2.5 Waste Water Treatment in the Electroplating Industry

There are various methods for the treatment of electroplating waste water, such as physiochemical, ion exchange resins, membranes, solvent extraction, adsorption, etc[13,15]. However, the most commonly used technique is the physiochemical process due to its capability to handle large volumes of metal laden waste water at low costs[13]. The physiochemical treatment process consists of; pH adjustment for precipitation, flocculation, clarification and filtration[16]. Pre-treatment is required for cyanide and chromium containing waste water[13]. The cyanide undergoes oxidation while hexavalent chrome is reduced to trivalent chrome[18]. A brief description of the function of each stage of the physiochemical treatment process is detailed below:

- Precipitation

  The pH required for hydroxide precipitation is typically in the range of 8.5 - 11, as in this pH range the metal hydroxide solubility is reduced[17,15]. Typically lime is utilised but sodium hydroxide and calcium hydroxide are also used[15]. Sulphide precipitation can also be used for the removal of heavy metals[15,16]. The solubility of sulphide precipitates is lower than that of hydroxide precipitates and can thus achieve greater removal of metal ions[15].

- Flocculation

  The purpose of flocculation is to facilitate the agglomeration of particles for ease of removal[15]. Fenglian Fu et al states, “Today many kinds of flocculants, such as PAC, polyferricsulfate (PFS) and polyacrylamide (PAM), are widely used in the treatment of waste water, however, it is nearly impracticable to remove heavy metal very well from waste water directly by these current flocculants.”[15]

- Clarification

  Clarifiers are used for the removal of suspended solids, based on the density difference between the solids and the water[19]. The waste water is slowly fed into a settling tank, where the denser solids collect at the bottom of the tank and the water at the top[19]. The water is extracted from the top of the tank while the solids are drained from the bottom. Refer to Figure 6 for a system depicting flocculation and clarification.

- Filtration

  Filtration is an optional step based on the final treated water requirements. Sand filters have been used as the final step in the treatment of electroplating waste water[16].

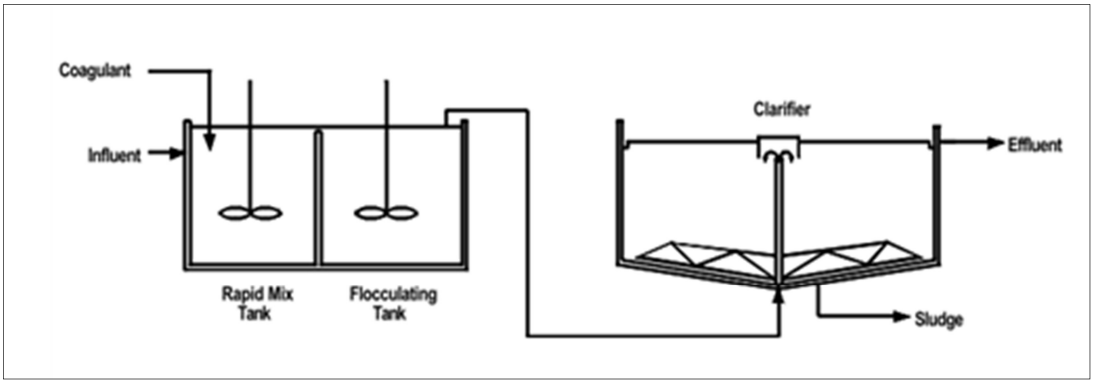

Figure 6: Diagrammatic representation of a flocculation and clarification system[19]

Some of the draws back of the physiochemical process are its inability to meet regulatory standards and the generation of large volumes of sludge[13].

The other available technologies for removal of heavy metal from waste water are membranes, ion exchange, precipitation-filtration, etc[6]. These technologies also have their drawbacks, such as high cost and high technical

capabilities[6]. As majority of the electroplaters in SA are SME's, they have financial and technical constraints, which make installation and application of the above technologies difficult and in some cases unfeasible.

These end-of-pipe waste water treatment technologies do not solve the problem of the generation of large volumes of toxic waste water, but rather treats it. Thus source point reduction technologies need to be identified, which would reduce and/or eliminate the generation of electroplating waste water. One of the environmental strategies that focus on point source reduction is CP.

2.6 Cleaner Production

Fresner defined CP as, "Cleaner production is a strategy to prevent emissions at the source and to initiate a continuous preventive improvement of environmental performance of organizations".[5] Morgan et al stated that "Hirschhorn (1993) predicted that companies failing to refocus from end-of-pipe pollution control to P2 will not remain competitive in the global marketplace [2]."[20] CP is a tool that assists a process/company to minimise its environmental impact, which works in conjunction with ISO 14001[(5)].

The key areas identified for implementation of CP were[5]:

- Housekeeping
- Employee training
- Chemical and process optimization
- Recycling

A three year CP demonstration project, in the SA metal finishing industry was sponsored by DANCED. The aim of the project was to demonstrate the implementation of CP in the metal finishing industry and the improved efficiencies, cost saving and environmental impact reduction that can be achieved[4]. Table 3 shows a summary of the results of the implementation of the CP project. This project has resulted in the following[4]:

- Establishment of the South African Metal Finishing Association (SAMFA), which serves as a central body for knowledge transfer, training, development, governance, etc.
- Establishment of four waste minimisation clubs.
- Development of the metal finishing industries guidelines by the Ethekwini Metro waste and waste water department and the metal finishing industry representatives.

Table 3: Saving achieved by the application of CP[4]

Company name	Process description	Total CP investment	CPMFI Project subsidy	Total savings	Payback period (months)	Chemical savings per year		Water savings per year	
						%	Rand	%	Rand
Aberdare cables	Tin plating copper wire	617,880	75,000	667,204	11	41	546,690	99	120,514
Anodising systems	Aluminium anodising	134,600	67,300	70,732	23	37	57,460	79	13,272
Cascolor	Chrome plating	245,040	49,008	86,125	34	36	75,695	91	10,430
Defy appliances	Nickel–chrome	384,000	75,000	329,050	14	45	282,394	91	46,656
Durban wire	Zinc phosphating	205,806	41,161	165,766	15	57	132,252	98	33,514
Euro industrials	Nickel–chrome	183,250	75,000	93,057	24	25	91,580	57	1477
Fascor	Zinc and nickel	383,740	75,000	234,047	20	33	178,452	78	55,595
Federal mogul	Hard chrome plating	320,566	64,112	321,150	12	89	307,555	75	13,595
Frontier metal processing	Copper plating	226,000	45,200	165,024	16	26	159,144	58	5880
Malben engineering	Alkaline zinc plating	395,000	75,000	240,000	20	82	234,960	60	5040
MPS/AES	Alkaline zinc plating	395,744	75,000	181,569	26	26	160,957	98	20,612
Natal electroplaters	Nickel–chrome	192,960	75,000	91,506	25	30	90,460	84	1046
Pinetown EP	nickel, chrome	226,150	75,000	80,767	34	71	77,743	90	3024
Pinclip Industries	Pre-treatment (degreasing)	347,000	68,560	126,180	33	89	123,655	40	2525
Total savings		*4,257,736*	*935,341*	*2,852,177*	*22*	*49*	*2,518,997*	*78*	*333,180*

As identified earlier, the area of concern in the electroplating industry is the rinse system due to its generation of large volumes of waste water. One the technologies identified by the CP demonstration project, for the reduction of waste water generation by the rinse system, was close circuiting of the plating process by the application of a low flow counter current rinse system[4].

2.7 Close Circuit Plating System

The aim of a CCPS is to recover the rinse tank water in the plating bath, such that the only source of waste water generation will be the spent plating, degreasing and acid baths. Overflow of the rinse tank occurs when clean make water is periodically added to the system to maintain the purity of the rinse tanks. A diagrammatic representation of a three stage low flow counter current rinse system is illustrated in Figure 7.

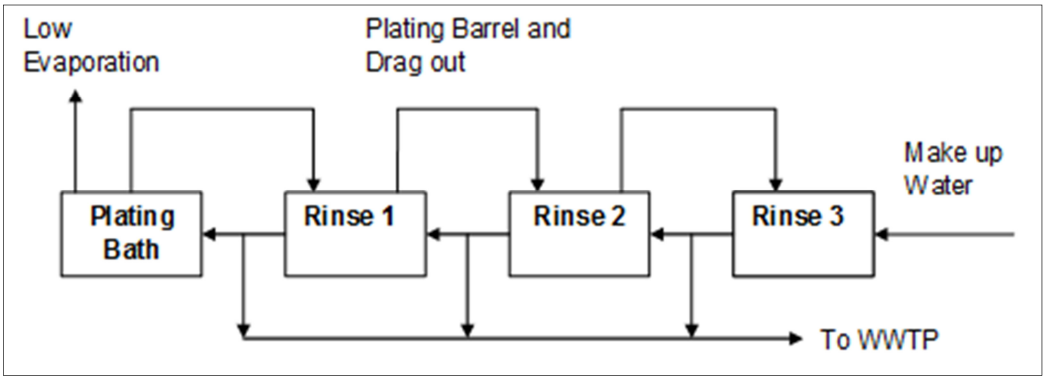

Figure 7: Three stage low flow counter current rinse system

The challenge in close circuiting the plating system, with a three stage low flow counter current rinse process, was the low rates of evaporation achieved by the low temperature operating plating baths. As these are low temperature operating plating baths, heating to induce evaporation was not an option. Thus alternative methodologies for the promotion of water evaporation in the plating bath had to be identified.

2.8 Use of an Evaporative Cooler for Close Circuiting a Low Flow Counter Current Rinse Plating Process

This master's study proposes the use of an induced draft evaporative cooler for close circuiting the three stage low flow counter current rinse plating system. A diagrammatic illustration of the proposed system is given in Figure 8.

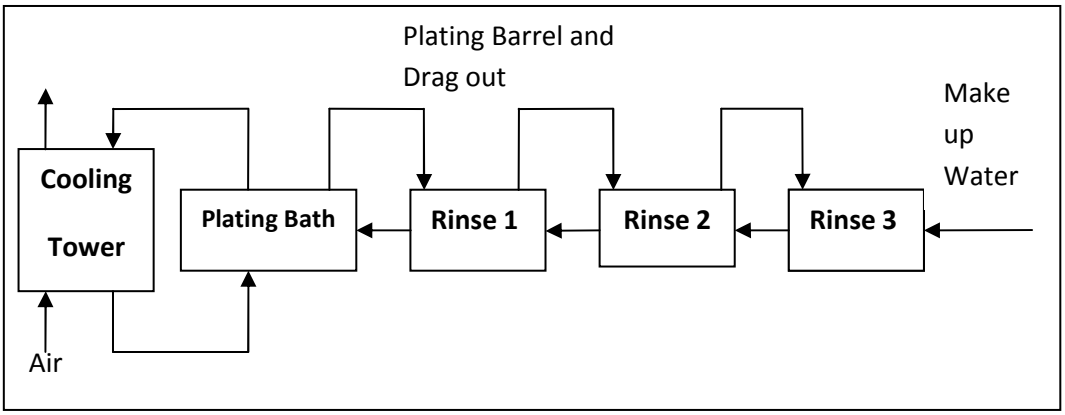

Figure 8: Proposed system with an evaporative cooler

In the proposed CCPS, the plating solution will continuously be re-circulated through a cooling tower to promote evaporation of water in the plating bath. Evaporative cooling has two potential benefits; increasing the rate of water

evaporation in the plating bath while simultaneously maintaining the plating bath temperature. The expected decrease in temperature and increase in water evaporation is based on the principles of heat and mass transfer through a cooling tower, which is discussed in the following sections. The recovery of the rinse water in the plating bath will reduce the amount of waste water sent to the waste water treatment plant (WWTP) to near zero. Thus it is a source point waste reduction technology.

2.9 Cooling Towers

Temperature control is required by majority of processes; metal finishing, power generation, refrigeration and air conditioning, petrochemical, thus cooling towers are now familiar sights at industrial facilities[21,22]. Of all the plating processes, temperature control is critical for the zinc plating process[23]. A common cooling technique employed by electroplaters is the circulation of the plating solution through coils in the rinse tanks[23]. In extreme cases and in large plating shops cooling towers or refrigeration units are used[23].

Cooling towers can be classified as either wet or dry cooling. In wet cooling towers the stream to be cooled is in direct contact with the air. In dry cooling towers the stream to be cooled is indirectly contacted with the air. The mechanisms for heat transfer in a wet cooling tower are by evaporation and sensible heat transfer, while that for dry cooling towers are by convection and radiation[24]. However, the mostly widely used of the two is the wet cooling towers[24].

Wet cooling towers can be categorised as either natural draft or mechanical draft cooling towers[24]. The selection between the two is dependent on a number of factors, such as volume of water to be cooled, operational and maintenance costs, range of temperature control, etc[24]. Mohiuddin et al provides the following decision matrix as a guide for the selection of the type of wet cooling required, refer to Figure 9[(24)]. There are two types of natural circulation towers; atmospheric and natural drafts. In atmospheric towers the ambient air enters through one side of the tower at a time[25]. Natural draft

cooling towers operate on a density gradient; hot air has a lower density than cold air. This density gradient pushes the cold air in at the bottom of the tower and forces out the hot air at the top of the tower[25].

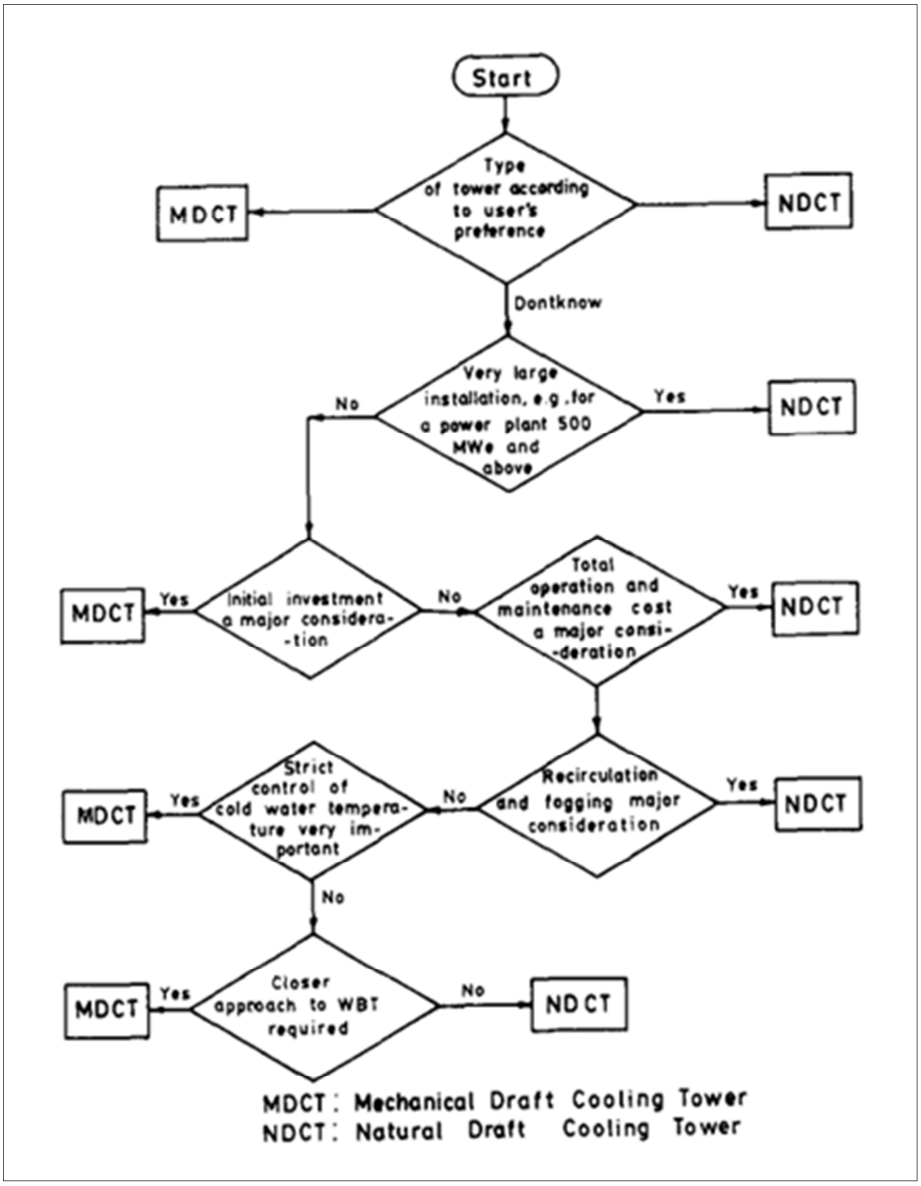

Figure 9: Decision matrix for the selection of the type of wet cooling tower[24]

In a mechanical draft cooling tower, the hot water typically flows down the tower while an electrically powered fan is used to either push or pull in the ambient air[22]. Mechanical draft cooling towers can operate in two different ways, namely induced draft and forced draft. In induced draft, the air is pulled in by a fan located at the top of the tower through louvers at the bottom[22,24]. For forced draft towers, the air is pushed in by a fan located at the bottom of the tower and discharged at the top[22,24]. The direction of air flow in a cooling

tower can either be cross flow or counter flow. In cross flow and counter flow operation the air flows horizontally and vertically against the direction of the water, respectively[24]. Mohiuddin et al provides the following decision matrices, as a guide for the selection of the mode of operation and the air flow direction of the mechanical draft cooling tower, refer to Figures 10 and 11 respectively[24].

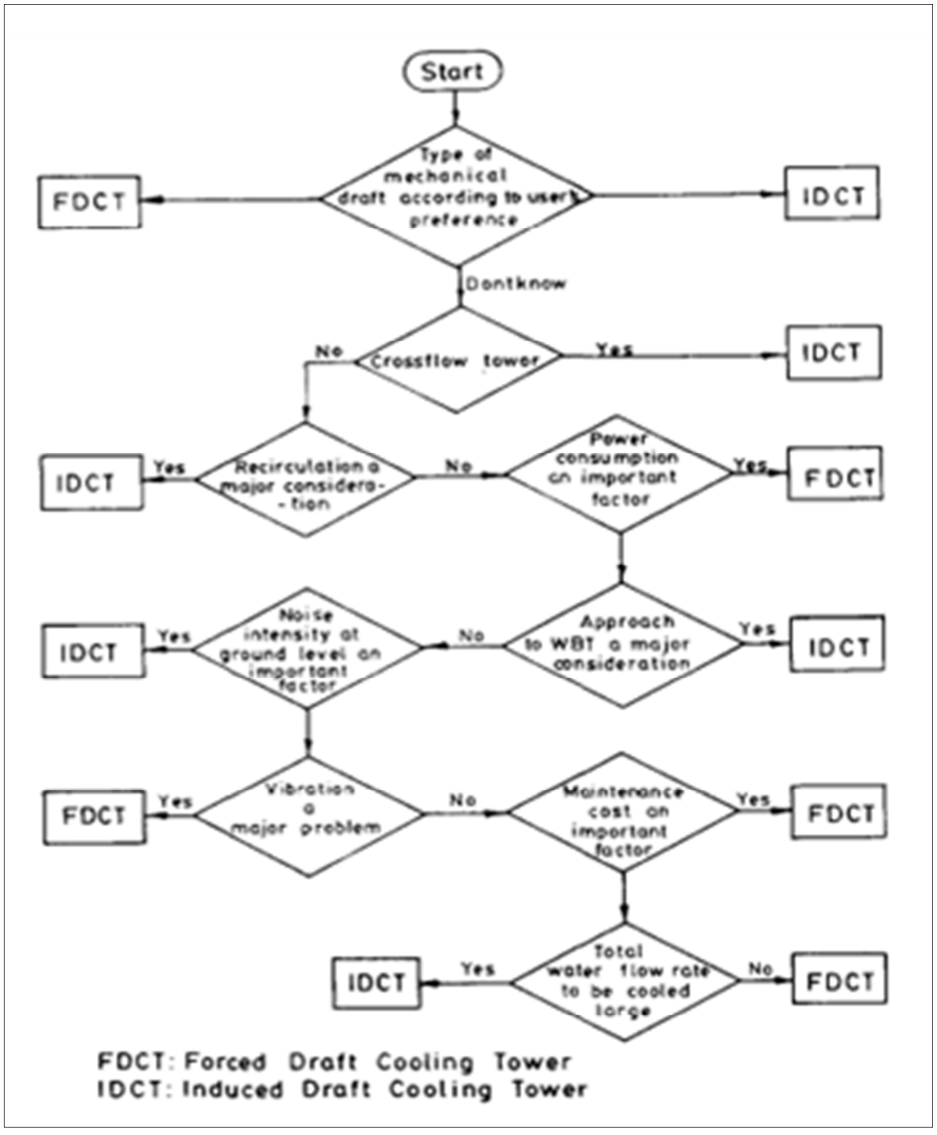

Figure 10: Decision matrix for selection of mode of operation[24]

Figure 11: Decision matrix for selection of air flow direction[24]

A diagrammatic representation of a counter flow cooling tower is given in Figure 12.

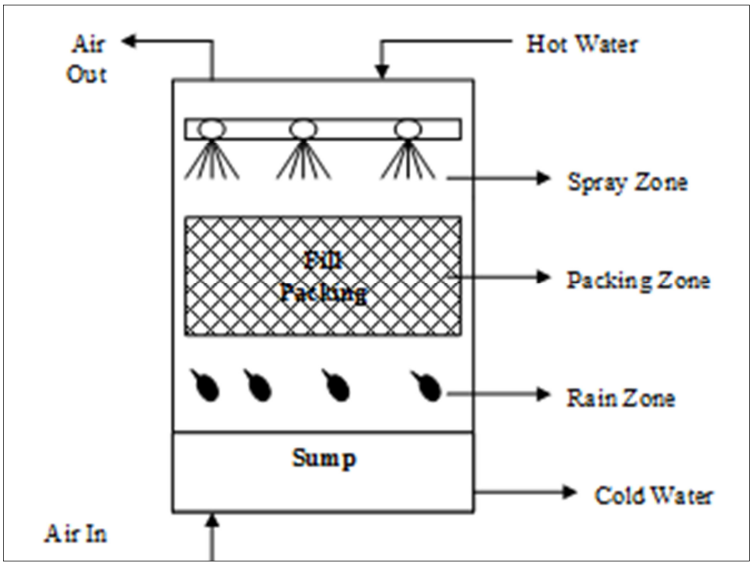

Figure 12: Diagrammatic representation of a counter flow cooling tower[22]

A cooling tower has three zones; the spray, packing and rain zones, as shown in Figure 12[(22)]. The spray zone allows for the formation of the spray pattern, where a height of 0.45m between the nozzles and the top of packing is required[22]. Nozzles are used for atomizing the water and spraying it over the packing material. Qureshi et al stated that "Kroger [7] indicated that up to 15% of the cooling might actually occur in the spray zones of large cooling towers."[22]

Cooling towers are filled with packing material, which provides a large contact surface area between the air and water thus facilitating heat and mass transfer. Qureshi et al also stated, "Davis [8] indicated that the cooling achieved in one foot of fill can be more than the cooling achieved in ten feet of free fall of water and, as a consequence, is an ineffective use of pump energy.''[22]

The purpose of the rain zone is to ensure uniform air flow into the packing[22]. Approximately 10-20 percent of the total heat and mass transfer can occur in the rain zone for large cooling towers but is insignificant for small cooling towers[22]. Uniform water and air flow through the packing will facilitate improved heat and mass transfer, thus improving the efficiency of the cooling tower.

A concentration and temperature profile of the upper part of a cooling tower is represented in Figure 13. At the gas liquid interface there is equilibrium between the phases[26]. The humidity gradient between the interface and the bulk air facilitates the diffusion of water vapour from the interface to the bulk air[26]. The driving force for the temperature drop in the bulk water is due the temperature gradient existing between the bulk water and the interface[26]. In the lower part of the cooling tower, the bulk water temperature may be lower than the air dry bulb temperature, resulting in a temperature loss in the opposite direction than that shown in Figure 13[(26)].

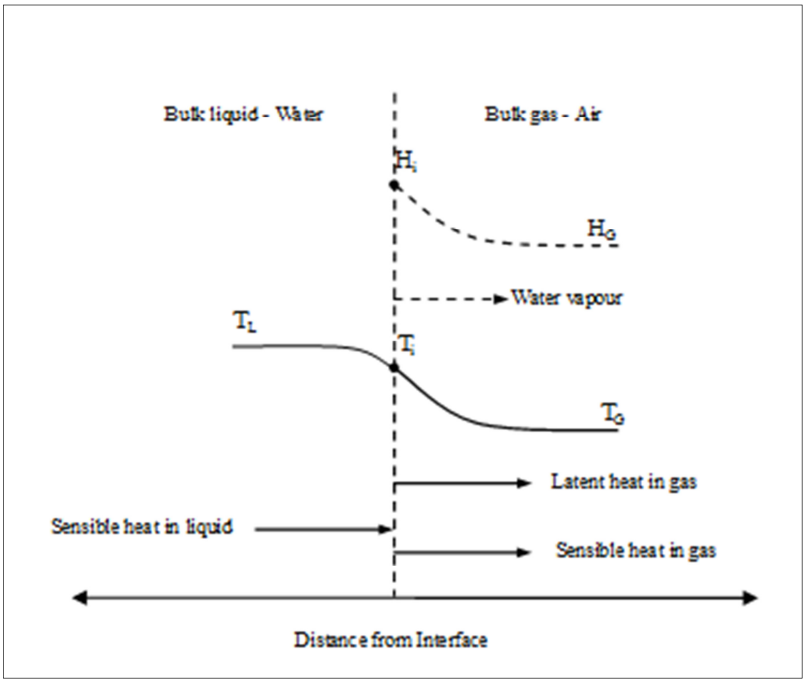

Figure 13: Temperature and concentration profile in the top part of the cooling tower[26]

Diffusion is defined as[25], "When a movement of material is promoted between two phases by a vapor pressure (or concentration) difference, it is diffusion and it is characterized by the fact that the material is transferred from one phase to another or between phases". Diffusion is also called mass or material transfer[25]. Convective mass transfer is defined as, "... the transport of material between a boundary surface and a moving fluid or between two relatively immiscible moving fluids."[27] There are two types of convective mass transfer, forced convection and natural convection. Forced convection occurs when a mechanical device, such as a pump causes the movement of the fluid[27]. Natural convection occurs when movement of the fluid is due to density differences[27].

Qi et al identified the following drawbacks of the cooling tower; lower temperature drops, blockages of fills, difficulty in the cleaning and replacement of the fills, etc[28]. Some of the advantages of evaporative cooling are ease of operation, low maintenance costs, etc[29].

The previous sections have detailed the motivation for the selection of this master's study and provided an overview of the relevant literature. In the next section the scope and the methodology of the master's study will be detailed.

2.10 Scope and Methodology for the Master's Study

The proposed solution of the use of evaporative coolers for close circuiting of the three stage low flow counter current rinse plating system, has to be optimised such that the rate of evaporation from the plating bath is equivalent to the rinse tank make-up water requirements. This will ensure zero generation of waste water from the rinse system.

Thus, one of the aims of this study is to develop a mathematical model for the identification of the operating conditions for close circuiting the three stage low flow counter current rinse plating process. The CCPS model will determine the mass of water evaporated and the equilibrium temperatures of the plating bath and the cooling tower, for minimum plating solution specific input data, for a specified time period. With the CCPS model, the electroplater can identify the quantity and frequency of make water addition to the CCPS, such that the rinse waste water generated can be reduced to almost zero.

The mathematical model for the CCPS was developed based on cooling tower theory and on the mechanisms of heat and mass transfer from an open tank. The primary challenge encountered in the development of the CCPS model, was the scarcity of information on the physical and thermodynamic characteristics of the plating solution. To overcome the data scarcity empirical correlations and experimental methodology were used, which are detailed in Chapters 3 and 4 respectively. Saturation enthalpy curves for a salt solution and specifically that for a plating solution are limited. The development of empirical correlations and experimental methodology for the construction of plating solution saturation enthalpy curves, where outside the scope of this study. Thus the primary limitation of the model is that it is based on the evaporation of water only.

The inputs for the model were determined from literature and based on current electroplating operational practices, where possible. The primary literature sources were journals, suppliers of plating solution chemicals and

books on cooling design and operation and the principles of heat and mass transfer.

The following methodology was followed for the development of the CCPS model:

- Set up of the model in Microsoft excel.
- Programming of the model in Matlab.
- Verification of the Matlab model.
- Sensitivity analysis of the model based on single input variable changes.
- Sensitivity analysis of the model based on multiple input variable changes.

2.11 Conclusion

This chapter has provided an overview of the relevant literature for the master's study. The development, verification and application of the CCPS model are detailed in the following chapters.

CHAPTER 3: MATHEMATICAL MODEL DEVELOPMENT FOR THE CLOSED CIRCUIT PLATING SYSTEM

3.1 Introduction

The purpose of this chapter is to detail the development of the mathematical model for the CCPS depicted below (system enclosed within the highlighted area). The model will identify the optimum operating conditions for the CCPS such that the rate of evaporation from the CCPS is equivalent to the make up water requirements of the CCPS. This will facilitate the process to operate with almost zero waste water generation enabling the electroplating process to be more environmentally friendly.

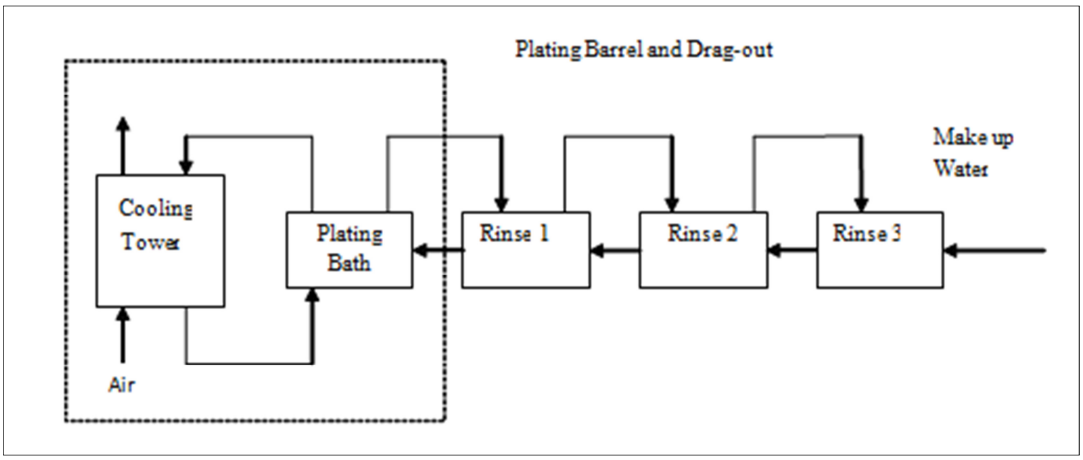

Figure 14: Closed circuit plating system

The CCPS model will determine the mass evaporated and the equilibrium temperatures based on minimum plating solution specific input data.

This chapter comprises of three sections:

- Model Criteria – Details the design basis for the CCPS model.
- Model Development for Region 1: Details the methodology for the development of the model in the unsteady state temperature region.
- Model Development for Region 2: Details the methodology for the development of the model in the steady state temperature region.

3.2 Model Criteria

The CCPS model was developed based on evaporative cooling theory and the mechanisms of heat and mass transfer from an open tank. The CCPS model was developed around the operational characteristics of an induced draft counter flow wet cooling tower. The design basis used to develop the model was:

- Water is the only diffusing component from the plating solution, as ionic diffusion is very slow[30].
- The diffusion coefficient (D_{AB}) for a specific system, in this case an air-water system, is constant across the height of the cooling tower.
- Radiation heat transfer from the plating bath is ignored as it is negligible as compared to those of convection and conduction.
- The height of the cooling tower will be an input variable into the model.

The cooling of the plating solution is divided into two regions, see Figure 15.

Region 1: The unsteady state temperature region, which is characterised from the start of cooling until equilibrium is achieved. Equilibrium conditions are defined as constant output temperature from the cooling tower and plating bath.

Region 2: The steady state temperature region, which is characterised by constant temperature.

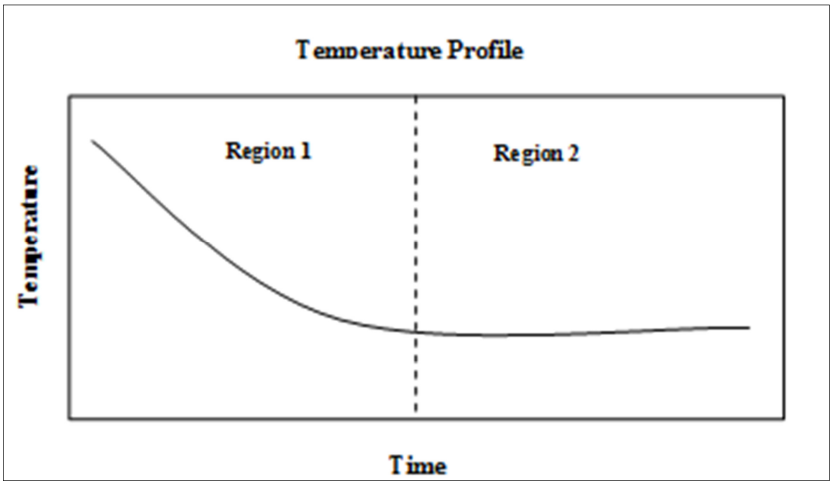

Figure 15: Temperature profile of the CCPS

For the purpose of the model development, the following schematic and naming convention was utilised, refer to Figure 16. The flow rate of air and plating solution passing through the system are represented by G and L, respectively. The humidity of the air stream and the temperature of the plating solution and air are represented by X, T_L and T_G, respectively. Air entering and exiting the cooling tower are represented by the subscripts one and two, respectively. The plating solution entering and exiting the cooling tower are represented by the subscripts two and one, respectively.

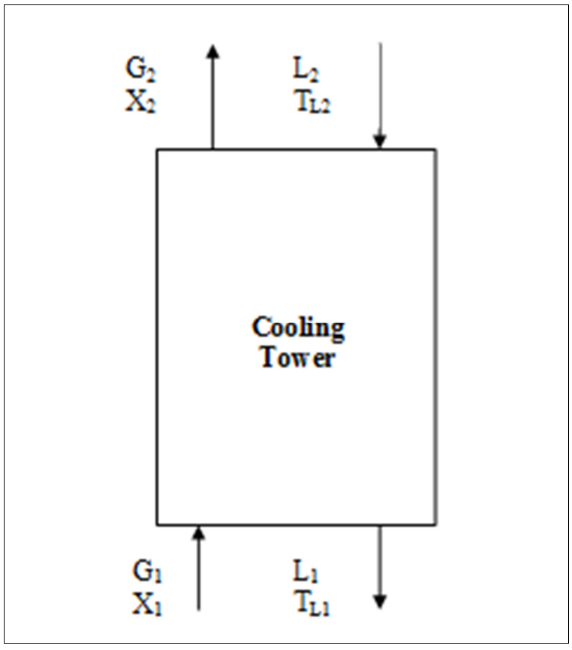

Figure 16: Schematic of counter flow cooling tower

3.3 Model Development for Region 1: Unsteady State Temperature

3.3.1 Model for calculation of exit temperature from cooling tower

Traditional models for evaporative cooling towers have been based on calculating the required cooling tower height for a specific cooling range. For the model developed the height of the cooling tower is specified while the cooling range achievable for that specific height is calculated. A frequently used correlation is that given by Geankoplis as illustrated below[26]:

$$z = \frac{G}{M_B k_G a P} \int_{H_{y1}}^{H_{y2}} \frac{dH_y}{H_{yi} - H_y} \qquad (1)$$

Where z = Cooling tower height (m)

M_B = Molecular mass of non-diffusing component (kg/kmol)

k_G = Individual gas phase mass transfer coefficient (kmol/s.m^2.Pa)

a = Surface area of packing per unit volume of packing (m^2/m^3)

P = System pressure (Pa)

G = Air mass flux (kg/s.m^2)

H_y = Enthalpy (J/kg)

From evaporative cooling theory one of the key factors affecting the rate of evaporation is the mass transfer coefficient. Mass transfer can be expressed in terms of the overall mass transfer coefficients (K_G, K_L) or the individual film transfer coefficients (k_G, k_L). For this study the individual gas phase mass transfer co-efficient (k_G) was used, as defined in equation (1), as the overall mass transfer co-efficient for a plating solution is not quantified. The individual mass transfer co-efficient can be represented in various forms, such as k_G, k_C, k_G', but all are interrelated and can be converted from one to the other[2].

Chapter 2 states that convective mass transfer occurs between two immiscible flowing fluids. In the cooling tower heat and mass transfer occurs between the air and water, which are immiscible. Thus it was assumed that convective mass transfer occurs. Convective mass transfer was assumed to occur under the conditions of turbulent flow inside wetted-wall towers[2]. Geankoplis provides the following correlation for the gas phase mass transfer co-efficient for turbulent flow inside wetted wall towers[26],

$$k_C^{'} = \frac{N_{SH} D_{AB}}{D} \qquad (2)$$

Where $k_C^{'}$ = Individual gas phase mass transfer coefficient (m/s)

N_{SH} = Sherwood number

D_{AB} = Diffusion coefficient (m^2/s)

D = Diameter (m)

Equation (2) holds for the conditions; Schmidt number (N_{SC}) of 0,6 to 3000 for gases and Reynolds number (N_{Re}) > 2100. Geankoplis provides the

following correlation for the calculation of the Schmidt and Reynolds number[26].

$$N_{SC} = \frac{\mu}{\rho\, D_{AB}} \tag{3}$$

Where N_{SC} = Schmidt number
ρ = Density of air (kg/m^3)
μ = Viscosity of air (kg/m.s)

$$N_{\mathrm{Re}} = \frac{Du\rho}{\mu} \tag{4}$$

Where N_{Re} = Reynolds number
u = Velocity of air (m/s)

The dimensionless Sherwood number (N_{SH}) was calculated using the following correlation as represented by Geankoplis for turbulent flow inside wetted wall towers[26].

$$N_{SH} = 0.023\left(\frac{Du\rho}{\mu}\right)^{0.83}\left(\frac{\mu}{\rho\, D_{AB}}\right)^{0.33} \tag{5}$$

The diffusion coefficient, D_{AB}, was calculated using the following correlation where A is the diffusing component and B the non-diffusing component[26],

$$D_{AB} = \frac{10^{-7} * T_{L2}^{1.75} * \left((1/M_A) + (1/M_B)\right)^{0.5}}{P * \left(v_A^{1/3} + v_B^{1/3}\right)^2} \tag{6}$$

Where M_A = Molecular mass of diffusing component (kg/kmol)
V_A = Molar volume coefficient for diffusing component A
V_B= Molar volume coefficient for non-diffusing component B
T_{L2} = Temperature of plating solution entering cooling tower (K)
P = System pressure (atm)

Substitution of equation (5) into equation (2) results in the following equation for k'$_C$,

$$k'c = \frac{\left[0.023\left(\frac{Du\,\rho}{\mu}\right)^{0.83}\left(\frac{\mu}{\rho\,D_{AB}}\right)^{0.33}\right]D_{AB}}{D} \quad (7)$$

In equation (2) the individual mass transfer co-efficient is written in terms of k'_C, but equation (1) requires the individual mass transfer co-efficient in terms of k_G. The units of k'_C is m/s while that of k_G, is kmol/(s.m^2.Pa). For the conversion of k'_C to k_G, the following correlation was used[26],

$$k_G = \frac{k'_C P}{RT_{G1}P_{BM}} \quad (8)$$

Where k_G = Individual gas phase mass transfer coefficient

R = Universal gas constant (8314 m^3.Pa/kmol.K)

T_{G1} = Temperature of air entering the cooling tower (K)

P_{BM} = Log mean pressure (Pa)

Substitution of equation (7) into equation (8), presents the final correlation for the calculation of k_G,

$$k_G = \frac{\left(\left(0.023*(Du\rho/\mu)^{0.83}(\mu/\rho D_{AB})^{0.33}*D_{AB}\right)/D\right)*P}{RT_{G1}P_{BM}} \quad (9)$$

Diffusion of water was assumed to occur under the conditions of stagnant A (water) diffusing through non diffusing B (air). The log mean pressure differential was written in terms of air (B), where one represents the condition at the gas liquid interface and two in the bulk air[26].

$$p_{BM} = \frac{P_{B2} - P_{B1}}{\ln(P_{B2}/P_{B1})} \quad (10)$$

Where P_{B1} = Interfacial partial pressure of air (Pa)

P_{B2} = Partial pressure of air in the bulk air (Pa)

Expanding the above equation and rewriting it in terms of the water and the total pressure,

$$p_{BM} = \frac{(P - P_{A2}) - (P - P_{A1})}{\ln((P - P_{A2})/(P - P_{A1}))} = \frac{P_{A1} - P_{A2}}{\ln((P - P_{A2})/(P - P_{A1}))} \quad (11)$$

$$P = P_{A1} + P_{B1}$$

$$P = P_{A2} + P_{B2}$$

Where P_{A1} = Interfacial pressure of water (Pa)

P_{A2} = Partial pressure of water in the bulk air (Pa)

As partial pressure is a function of the concentration of the component in the mixture, P_{A2} was assumed to be zero. The concentration of water in the bulk air will be negligible in comparison to that in the plating solution. Due to the scarcity of information, the interfacial partial pressure of water, P_{A1}, had to be determined from experimental methodology. The gas diffusion experimental methodology was followed to determine P_{A1}. The gas diffusion trials were conducted under the conditions of water diffusing through a stagnant air film into a moving air film. The gas diffusion experimental methodology and results analysis will be discussed in Chapter 4.

The statistical analysis of the experimental results provided the following optimised equation for the prediction of the change in height of the zinc plating solution in the capillary tube, under the experimental conditions specified in Chapter 4[31].

$$\Delta h = \left(\frac{1}{7.08 + (0.29C) + (0.34E) - (0.61AD) - (0.77BC) - (0.49DE) - (0.41B^2)} \right)^2 \quad (12)$$

Where Δh = Change in height of the zinc plating solution in the capillary tube (mm)

A = Zinc concentration factor

B = NaOH concentration factor

C = Dimension A concentration factor

D = Conditioner concentration factor

E = Temperature of plating solution factor

The rate of diffusion of a substance was calculated using the following equation as stated in the Diffusion Coefficient Practical[32].

$$\dot{m}_A = -D_{AB} A \left[\frac{M_A}{RT} \right] \frac{dP_A}{dx} \tag{13}$$

For the determination of the interfacial partial pressure of water, equation (13) was integrated. The limits of the integration were between the level of fluid in the capillary tube and the top of the capillary tube (open to bulk air), represented numerically by one and two respectively.

$$m_A (x_2 - x_1) = -D_{AB} * A * \left(\frac{M_A}{RT_{L2}} \right) * (P_{A2} - P_{A1}) \tag{14}$$

Where m_A = Rate of mass transfer of diffusing component (kg/s)
A = Cross sectional area of capillary tube (m^2)
x_1 = Initial level of plating solution in capillary tube (m)
x_2 = Top level of capillary tube (m)

The rate of diffusion of water from the zinc plating solution was calculated using the following equation,

$$m_A = \frac{\rho_A V_A}{t} \tag{15}$$

Where ρ_A = Density of water (kg/m^3)
V_A = Volume of water diffused (m^3)
t = Diffusion time (s)

The following equation was used to calculate the vapour density of water.

$$\rho_A = \frac{M_A P_{A0}}{RT_{L2}} \tag{16}$$

Where P_{A0} = Vapour pressure of water at plating solution temperature (Pa)

The volume of water diffused was calculated using the following equation,

$$V_A = \pi * r^2 * \Delta h \tag{17}$$

Where r^2 = Radius of capillary tube (m)

Re-arranging equation (14) and substituting equations (12), (16) and (17) into equation (14), results in the following equation for the calculation of P_{A1}.

$$P_{A1} = P_{A2} + \left(\frac{\left(\frac{M_A P_{A0}}{RT_{L2}} \right) \left(\pi r^2 * \left(\frac{1}{7.08 + 0.29C + 0.34E - 0.61AD - 0.77BC - 0.49DE - 0.41B^2} \right)^2 \right) (x_1 - x_0)}{t * A * D_{AB} * \left(\frac{M_A}{RT_{L2}} \right)} \right) \tag{18}$$

Substitution of equation (18) into equation (11) results in the following equation for P_{BM},

$$P_{BM} = \frac{\left[P_{A2} + \left(\frac{\left(\frac{M_A P_{AO}}{RT_{L2}} \right) * \pi r^2 * \left(\frac{1}{7.08 + 0.29C + 0.34E - 0.61AD - 0.77BC - 0.49DE - 0.41B^2} \right)^2 * (x_1 - x_0)}{t * A * D_{AB} * \frac{M_A}{RT_{L2}}} \right) \right] - P_{A2}}{Ln \frac{P - P_{A2}}{P - \left[P_{A2} + \left(\frac{\left(\frac{M_A P_{AO}}{RT_{L2}} \right) * \pi r^2 * \left(\frac{1}{7.08 + 0.29C + 0.34E - 0.61AD - 0.77BC - 0.49DE - 0.41B^2} \right)^2 * (x_1 - x_0)}{t * A * D_{AB} * \frac{M_A}{RT_{L2}}} \right) \right]}} \tag{19}$$

Equation (19) was substituted into equation (9) for the final representation of k_G.

$$k_G = \frac{\left(\left(0.023*\left(Du\rho/\mu\right)^{0.83}\left(\mu/\rho D_{AB}\right)^{0.33}*D_{AB}\right)\Big/D\right)*P}{R*T_{G1}*\left(\frac{\left[P_{A2}+\left(\frac{\left(\frac{M_A P_{AO}}{RT_{L2}}\right)*\pi r^2*\left(\frac{1}{7.08+0.29C+0.34E-0.61AD-0.77BC-0.49DE-0.41B^2}\right)^2*\left(x_1-x_0\right)}{t*A*D_{AB}*\frac{M_A}{RT_{L2}}}\right)\right]-P_{A2}}{Ln\frac{P-P_{A2}}{P-\left[P_{A2}+\left(\frac{\left(\frac{M_A P_{AO}}{RT_{L2}}\right)*\pi r^2*\left(\frac{1}{7.08+0.29C+0.34E-0.61AD-0.77BC-0.49DE-0.41B^2}\right)^2*\left(x_1-x_0\right)}{t*A*D_{AB}*\frac{M_A}{RT_{L2}}}\right)\right]}}\right)}$$

(20)

Equation (20) was substituted into equation (1) which resulted in the following equation.

$$z = \frac{G}{M_B*a*P*\left(\frac{\left(0.023\left(Du\rho/\mu\right)^{0.83}*\left(\mu/\rho D_{AB}\right)^{0.33}*D_{AB}\right)}{D}\right)*P}{R*T_{G1}*\left(\frac{\left[P_{A2}+\frac{\frac{M_A P_{AO}}{RT_{L2}}*\pi r^2*\left(\frac{1}{7.08+0.29C+0.34E-0.61AD-0.77BC-0.49DE-0.41B^2}\right)^2*\left(x_1-x_0\right)}{t*A*D_{AB}*\frac{M_A}{RT_{L2}}}\right]-P_{A2}}{Ln\frac{P-P_{A2}}{P-\left[P_{A2}+\frac{\frac{M_A P_{AO}}{RT_{L2}}*\pi r^2*\left(\frac{1}{7.08+0.29C+0.34E-0.61AD-0.77BC-0.49DE-0.41B^2}\right)^2*\left(x_1-x_0\right)}{t*A*D_{AB}*\frac{M_A}{RT_{L2}}}\right]}}\right)} \int_{H_{y1}}^{H_{y2}} \frac{dH_y}{H_{yi}-H_y}$$

(21)

From equation (21), the only unknown variable is the cooling tower exit temperature, T_{L1}. For the calculation of T_{L1}, the enthalpy integral had to be evaluated. Graphical methodology was selected for the evaluation of the enthalpy integral. The enthalpy integral was evaluated between the limits of the wet bulb temperature, T_{L1_min} and hot plating solution temperature, T_{L2}. Temperature T_{L1} was solved iteratively until the equilibrium temperature was reached. Equilibrium conditions were defined as no change in temperature of

T_{L1} and T_{L2}. However temperature T_{L1} need not be equivalent to temperature T_{L2}.

For the graphical solution of the enthalpy integral in equation (21), a saturated enthalpy-temperature diagram was constructed using enthalpy equation (22) for an air-water system[26]. For an alternate system, not air-water, alternate correlations will have to be utilised for the construction of the saturated enthalpy temperature diagram.

$$H_y = (1.005 + 1.88H)(T_{G1} - 0) + 2501.4 * H \qquad (22)$$

Where H = Humidity of air stream (kg_{H2O}/kg_{air})

3.3.2 Mass balance across the plating bath

A mass balance was performed around the plating bath, as represented by Figure 17, for the calculation of the plating bath mass after each pass through the cooling tower.

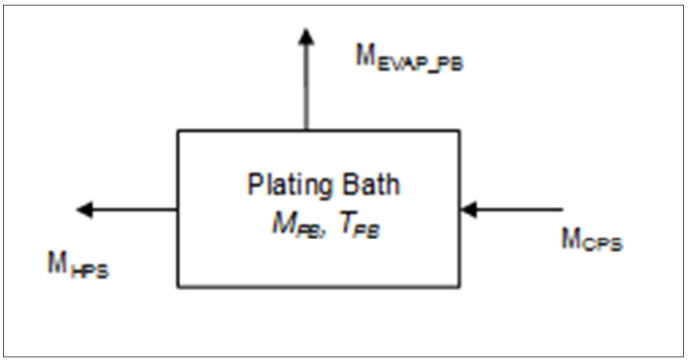

Figure 17: Mass balance around the plating bath

The mass balance around the plating bath was represented as:

$$Accumulation = Mass\ In - Mass\ Out$$

$$M_{PB_{t=2}} - M_{PB\,t=1} = M_{CPS}\Delta t - M_{HPS}\Delta t - M_{EVAP\_PB}\Delta t \qquad (23)$$

Rearranging equation (23), the mass of the plating bath after each cooling tower cycle was calculated.

$$M_{PB_{t=2}} = M_{CPS}\Delta t - M_{HPS}\Delta t - M_{EVAP\_PB}\Delta t + M_{PB\,t=1} \quad (24)$$

Where M_{PB} = Mass of plating bath (kg)

M_{CPS} = Mass flow rate of cold plating solution (kg/s)

M_{HPS} = Mass flow rate of hot plating solution (kg/s)

M_{EVAP_PB} = Rate of water evaporation from the plating bath (kg/s)

Δt = Time for which the mass change occurs (s)

Mass loss of the plating solution occurs due to the evaporation of water from the plating bath and the cooling tower. As mass loss occurs in the cooling tower, the flow rates of the plating solution entering and exiting the plating bath are not equal. Thus the mass flow rate of the cold plating solution entering the plating bath is:

$$M_{CPS} = M_{HPS} - M_{EVAP\_CT} \quad (25)$$

Where M_{EVAP_CT} = Rate of water evaporation from the cooling tower (kg/s)

The evaporative loss across the cooling tower was calculated by equation (26) as represented by Perry's Chemical Engineering Handbook[33].

$$R_{EVAP\_CT} = 0.00085 R_{HPS}\left(T_{L2} - T_{L1}\right) \quad (26)$$

Where R_{EVAP_CT} = Rate of water evaporation from the cooling tower (gal/min)

R_{HPS} = Flow rate of hot plating solution (gal/min)

T_{L1} = Temperature of plating solution exiting the cooling tower (^{0}F)

T_{L2}= Temperature of plating solution entering the cooling tower (^{0}F)

The evaporative losses from the plating bath was calculated using the equation below[34],

$$R_{EVAP\_PB} = 0.352 * e^{-\left(7.2-0.032*\left(\left(T_{PB}*9/5\right)\right)+32\right)} \quad (27)$$

Where R_{EVAP_PB} = Rate of water evaporated from the plating bath (L/m^2.hr)

T_{PB} = Temperature of plating bath (^{0}C)

3.3.3 Energy balance across the plating bath

An energy balance was performed around the plating bath, as represented by Figure 18, to determine the plating bath temperature, T_{PB}, for each pass through the cooling tower. This temperature is equivalent to the temperature of the plating solution entering the cooling tower, T_{L2}.

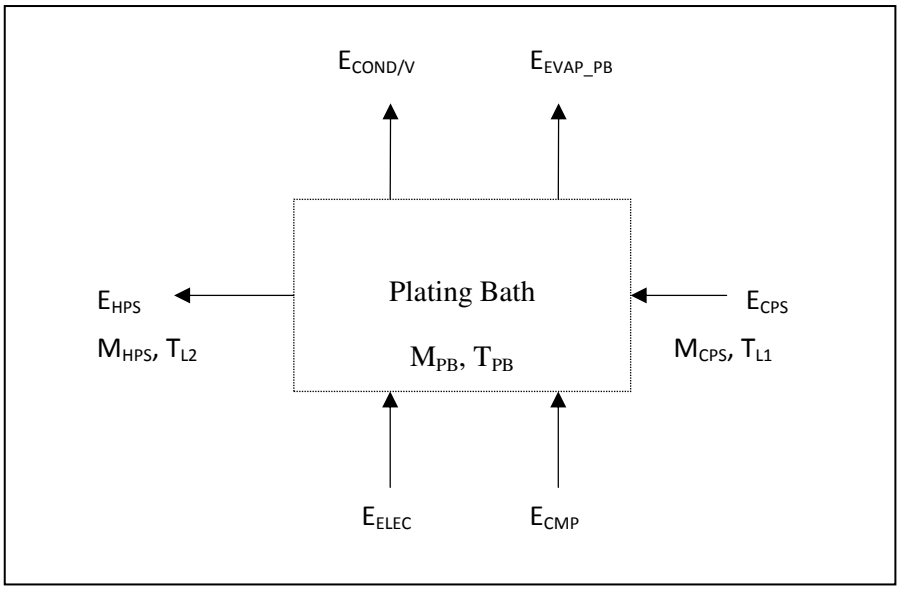

Figure 18: Energy balance across the plating bath solution

The energy balance across the plating bath was represented as,

$$Accumulation = Energy\ In - Energy\ Out$$

$$M_{PB}Cp\left(T_{PB} - T_{REF}\right)\Big|_{t=2} - M_{PB}Cp\left(T_{PB} - T_{REF}\right)\Big|_{t=1} = E_{CPS}\Delta t + E_{ELEC} + E_{CMP} - E_{COND/V}\Delta t - E_{EVAP\_PB}\Delta t - E_{HPS}\Delta t \quad (28)$$

Where Cp = Specific heat capacity of plating bath (KJ/kg.K)

E_{ELEC} = Electrical energy (KJ)

E_{CPS} = Energy of cold plating solution entering the plating bath (KJ)

$E_{COND/V}$ = Conduction and convection energy losses (KJ)

E_{CMP} = Energy of cold metal parts immersed in plating solution (KJ)

E_{HPS} = Energy of hot plating solution leaving the plating bath (KJ)

E_{EVAP_PB} = Energy lost due to evaporation from the plating bath (KJ)

Δt = Time for which the temperature change occurs (s)

The electrical energy input into the system was calculated using the following equation[34],

$$E_{ELEC} = CD*V*Time_{CT}*MetalPiece_{SM}*MetalPiece_{No.} \quad (29)$$

Where CD = Amperage per square meter (A/m^2)
V = Volts (V)
$Metal\ Piece_{SM}$ = Square meter of individual metal pieces (m^2)
$Metal\ Piece_{No}$ = Number of metal pieces in plating barrel
$Time_{CT}$ = Time for plating solution to pass through the tower (s)

The energy lost by the plating bath solution due to the immersion of the cold metal pieces in the solution was calculated using the following equation[34],

$$E_{CMP} = \rho_{CMP}*Cp_{CMP}*Metal\ Piece_{thick}*Metal\ Piece_{SM}*(T_{PB}-T_{AMB})*Metal\ Piece_{No} \quad (30)$$

Were ρ_{CMP} = Density of metal piece to be plated (kg/m^3)
Cp_{CMP} = Specific heat capacity of metal piece to be plated (KJ/kg.K)
$Metal\ Piece_{thick}$ = Thickness of metal piece to be plated (m)
T_{AMB} = Ambient temperature (K)

The energy loss due to the cold plating solution was calculated as follow,

$$E_{CPS} = M_{CPS}*Cp_{CPS}*(T_{L1}-T_{REF}) \quad (31)$$

Where Cp_{CPS} = Specific heat capacity of cold plating solution (KJ/kg.K)
T_{REF} = Reference temperature (K)
T_{L1} = Temperature of plating solution entering the plating bath (K)

The energy lost due to the hot plating solution leaving the plating bath was calculated as follows,

$$E_{HPS} = M_{HPS}*Cp_{HPS}*(T_{L2}-T_{REF}) \quad (32)$$

Where Cp_{HPS} = Specific heat capacity of hot plating solution (KJ/kg.K)
T_{L2} = Temperature of plating solution exiting the plating bath (K)

The conductive and convective energy losses from the sides and the bottom of the plating bath was calculated as follow[27],

$$E_{SIDE\,COND/V} = \frac{T_{PB} - T_{AMB}}{\left(1/\left(h_{HPS}A\right)\right) + \left(PB_{thick}/\left(k_{PB}\,A\right)\right) + \left(1/\left(h_{air}\,A\right)\right)} \quad (33)$$

Where h_{HPS} = Heat transfer co-efficient of plating solution (W/m^2.K)

h_{air} = Heat transfer co-efficient of air (W/m^2.K)

A = Surface area of tank side (m^2)

PB_{thick} = Thickness of plating bath (m)

k_{PB} = Thermal conductivity of plating bath (W/m.K)

The convective energy losses from the top surface of the plating bath was calculated using the following equation[27],

$$E_{CONV} = h_{air} * A * \left(T_{PB} - T_{AMB}\right) \quad (34)$$

The total conductive and convective energy losses are a summation of the losses from the four sides of the tank and the top and bottom surfaces.

$$E_{COND/V} = \sum E_{SIDE\,COND/V} + E_{CONV} \quad (35)$$

The energy loss due to evaporation from the plating bath was calculated using the following equation,

$$E_{EVAP\_PB} = M_{EVAP\_PB} * h_{fg} \quad (36)$$

Where H_{fg} = Latent heat of vapourisation (KJ/kg)

Equations (29), (30), (31), (32), (35) and (36) were substituted into equation (28). Equation (28) was re-arranged to provide the following correlation for the calculation of the plating bath temperature, T_{PB}, after a specified time.

$$T_{PB} = \frac{E_{CPS}\Delta t + E_{ELEC} + E_{CMP} - E_{COND/V}\Delta t - E_{EVAP}\Delta t + \left(M_{HPS}CpT_{REF}\Delta t\right) + \left(M_{PB}CpT_{REF}\right)\Big|_{t=2} + \left(M_{PB}Cp\{T_{PB} - T_{REF}\}\right)\Big|_{t=1}}{M_{PB}Cp + M_{HPS}Cp\Delta t} \quad (37)$$

Equations (21) and (37) were solved iteratively until equilibrium was reached. Equilibrium conditions were defined as no change in temperature of T_{L1} and T_{L2}, but temperature T_{L1} need not be equivalent to temperature T_{L2}.

3.4 Model Development for Region 2: Steady State Temperature

The mass loss in the steady state region was calculated using the following equation given by Kern[25].

$$Mass\ Evap_{\mathrm{Re}gion2} = G\left(X_2 - X_1\right) \tag{38}$$

Where G = Dry air flow rate (kg/m^2.s)

X_1 = Inlet air stream humidity (kg_{H2O}/kg_{air})

X_2 = Exit air stream humidity (kg_{H2O}/kg_{air})

Thus by the solution of equations (26) and (27) for the unsteady state temperature region and equations (27) and (38) for the steady state temperature region, the total mass loss from the CCPS can be calculated. This determines the amount of makeup-water that should be supplied to the CCPS after a specified time, to prevent overflow of the rinse tanks.

3.5 Conclusion

For the solution of the CCPS model, the model was programmed into Matlab. Prior to the programming of the CCPS model in Matlab, experimental methodology was followed to determine plating solution specific input data, which is detailed in Chapter 4. The verification of the CCPS model is detailed in Chapter 5. Single and multiple variable analyses were performed to determine the sensitivity of the model, which is explained in Chapter 6.

CHAPTER 4: EXPERIMENTAL METHODOLOGY FOR THE DETERMINATION OF THE INTERFACIAL PARTIAL PRESSURE OF THE DIFFUSING COMPONENT

4.1 Introduction

The challenge in the development of the CCPS mathematical model was in the determination of the thermodynamic and physical characteristics of the plating solution. This information is solution specific and not readily available.

From Chapter 3, the only unknown solution specific variable was the partial pressure of water at the air-plating solution interface, P_{A1}, in equation (11). The partial pressure of a component is a function of the concentration of the component in the mixture and the system pressure. The system pressure is the summation of all the individual component partial pressures.

The basis of water being the only diffusing component did not negate the effects of the remaining components (acids, salts, etc,) on the rate of water diffusion. Thus the system could not be assumed to be at equilibrium at the air-plating solution interface. As there was no data for the interfacial partial pressure of water in plating solutions, experimental methodology had to be utilised.

For the evaporation of water from the plating bath, the water must move from the bulk plating solution through the gas liquid interface into the bulk air. This movement of water requires the water molecules to undergo phase change, from the liquid to the gas phase. This mass transfer phenomenon is known as gas diffusion thus the gas diffusion experimental methodology was selected for the determination of the water interfacial partial pressure, P_{A1}.

4.2 Gas Diffusion Apparatus

The gas diffusion experiments were based on Fick's law of diffusion which states[32], "The rate of mass transfer is directly proportional to the diffusion area and the concentration gradient in the direction of diffusion." The gas diffusion apparatus was set up to operate under the conditions of component

A (water) diffusing through non-diffusing component B (air). The water from the plating solution will first diffuse through a stagnant air layer and then into the moving bulk air stream.

The gas diffusion experimental methodology followed was based on the Diffusion Coefficient Practical for the subject Heat and Mass Transfer, part of the Bachelor of Technology Chemical Engineering curriculum at the Durban University of Technology (DUT)[32].

The existing gas diffusion apparatus at the Chemical Engineering Department at DUT could only run one plating solution sample at a time, refer to Figure 19. Due to time constraints, larger gas diffusion apparatuses capable of running multiple plating solutions simultaneously were constructed.

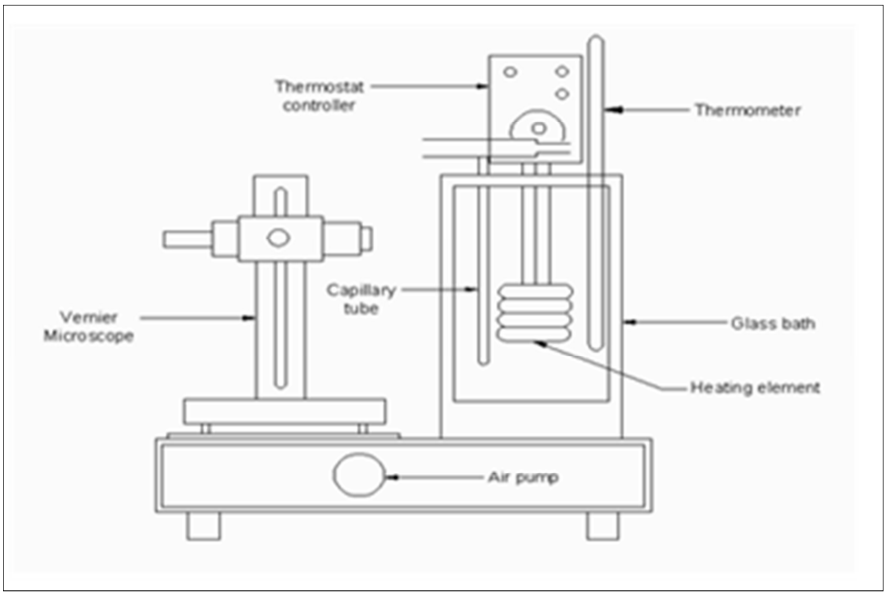

Figure 19: Existing gas diffusion apparatus[32]

4.2.1 Construction of the gas diffusion apparatus

Two gas diffusion apparatuses each capable of handling four plating solutions simultaneously were constructed, refer to Figure 20. Each gas diffusion apparatus consisted of the following components;

- Glass baths
  Fish tanks filled with water for maintaining the plating solution at the required temperature.

- Electrical heaters

  An electrical heater was placed in each glass bath for regulation and maintenance of the water and the plating solution at the required temperature.

- Precision bore capillary tube with a T-piece fitted at the top

  Each bath has a single manifold capable of holding four capillary tubes. The capillary tubes were constructed from 20mm PVC piping. The manifold which was fitted across the length of the glass tank, had four 10mm holes drilled through the pipe such that the capillary tubes could pass through the manifold to be submerged in the water below with the t-piece of the capillary tube resting on top of the manifold. To prevent the movement of the capillary tube as air was being pumped through it, the t-piece was fixed with cable ties to the manifold.

- Air pumps

  A single air pump supplied air to two capillary tubes, such that each gas diffusion apparatus had two air pumps. The pumps had variable speed settings, which were set at the maximum for the experimental work. The air pumps were connected to the t-piece of the capillary tube by 8mm diameter clear flexible piping. Each pump was connected to a petrol filter for the removal of dust and particles from the air stream prior to it passing through the capillary tube. The continuous supply of air facilitated a concentration gradient between the passing air stream and the vapours from the top of the capillary tube[32].

- Vernier microscope

  The glass baths and the vernier microscope were mounted onto a level base to ensure that accurate readings were obtained from the vernier microscope. As there was only one vernier microscope, it was transferred between the two glass baths.

- Thermometer

  It was used to regularly check the temperature of the water in the glass bath.

- Blue stones

  Blue stones were placed in the bath for the circulation of the water and to ensure even temperature distribution.

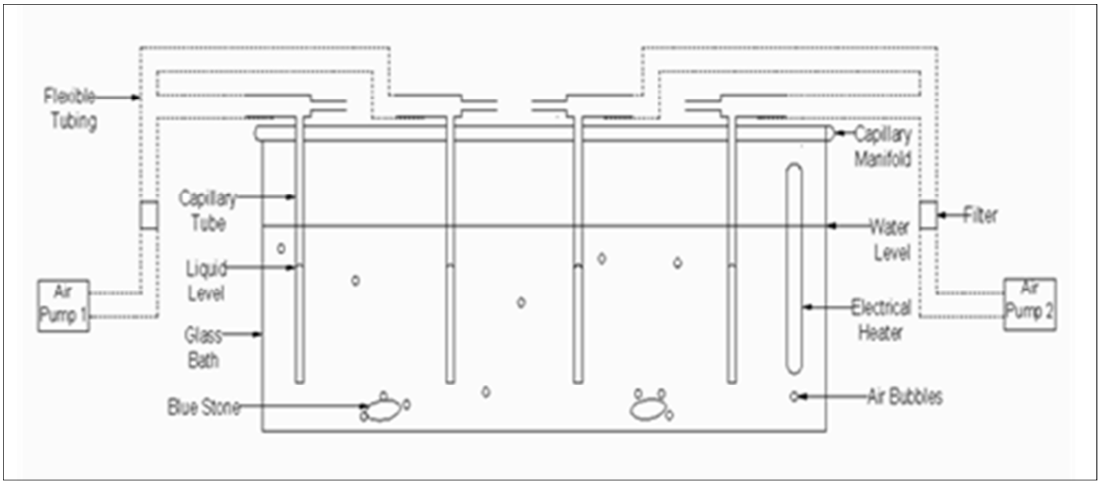

Figure 20: New gas diffusion apparatus

4.2.2 Validation of the gas diffusion apparatus

Prior to using the gas diffusion apparatuses for experimentation, it had to be validated. For validation purposes the Diffusion Coefficient Practical was conducted for the determination of the experimental diffusion coefficient, D_{AB}, which was compared against theoretical results[32]. The diffusing medium selected was acetone due to its affinity to diffuse into air; acetone air diffusion coefficients are readily available and it is the diffusion medium used in the Diffusion Coefficient Practical.

Equation (14) from Chapter 3 was rearranged and used to calculate the experimental diffusion coefficient, where A is acetone and B is air;

$$D_{AB} = -\frac{m_A(x_2 - x_1)}{A*(M_A/RT)*(P_{A2} - P_{A1})} \tag{14}$$

For validation of the experimental results, equation (6) from Chapter 3 was used to determine the theoretical acetone air diffusion coefficient.

$$D_{AB} = \frac{10^{-7} * T_{L2}^{1.75} * \left((1/M_A) + (1/M_B)\right)^{0.5}}{P * \left(v_A^{1/3} + v_B^{1/3}\right)^2} \tag{6}$$

The experimental methodology as discussed in Section 4.5 was followed but with the experimental parameters detailed below;

- Acetone was used as the diffusing medium.
- The validation was run for three temperatures; 24^0C, 27^0C and 30^0C.
- The experimentation was run for a period of two hours.
- Each gas diffusion apparatus utilised two capillary tubes.

The time period was selected due to acetones affinity to diffuse into air. The temperatures selected were based on the operating temperature range of the plating solutions as stated in Sections 4.3.1 and 4.3.2.

From the validation results, the percentage difference between the experimental and theoretical results was approximately equal to or less than five percent. Thus the gas diffusion apparatuses had been validated and could be used for the experimental determination of the interfacial partial pressure, P_{A1}.

4.3 Experimental Design for the Plating Solution

For the gas diffusion experimentation two plating solutions were selected; Ubac 101 copper plating solution and Enthobrite NCZ dimension zinc plating solution. Ubac 101 is a bright acid copper plating process and Enthobrite NCZ is an alkaline non-cyanide zinc plating process. The parameters that would affect the rate of diffusion of water from the plating solution were:

- The plating solution composition.
- The temperature of the plating solution.

Both the zinc and copper plating solutions are composed of four components, excluding water. Assuming that each of the four components and the temperature of the solution are individual factors, the total number of factors affecting the diffusion of water, for each specific plating solution, was five.

Due to the number of experimental factors affecting the rate of diffusion of water, statistical methodology was selected for the development of the experimental design. The statistical software Design Expert 8 was used to

simulate the experimental design parameters. The response surface method (RSM) design was selected to ensure randomness of experimental runs and for the optimization of the experimental design.

Using the RSM design, the central composite design including the axial factors (±2.38), the factorial points (±1) and the centre point (0) was selected. The above values were the default coded values for a five factor design[31]. Based on this design methodology, the software generated 50 randomised standard runs. With randomised standard runs, the individual factor criteria are constant for each run number across all designs but the order of the runs are varied. The standard run experimental design for a five factor system in coded values is tabulated in Table 4. This was used for the diffusion experimentation of the zinc and copper plating solutions. The actual parameter values for the coded factors tabulated in Table 4 are detailed in Sections 4.3.1 and 4.3.2 for zinc and copper plating solutions, respectively.

Table 4: Standard experimental design in coded values[31]

Std	Factor A	Factor B	Factor C	Factor D	Factor E
34	-2,38	0	0	0	0
17	0	-1	-1	-1	1
20	1	1	-1	-1	1
10	1	-1	-1	1	-1
25	-1	-1	-1	1	1
47	0	0	0	0	0
48	0	0	0	0	0
49	0	0	0	0	0
29	-1	-1	1	1	1
3	-1	1	-1	-1	-1
32	1	1	1	1	1
31	-1	1	1	1	1
38	0	0	2,38	0	0
7	-1	1	1	-1	-1
15	-1	1	1	1	-1
30	1	-1	1	1	1
39	0	0	0	-2,38	0
19	-1	1	-1	-1	1
28	1	1	-1	1	1
46	0	0	0	0	0

Std	Factor A	Factor B	Factor C	Factor D	Factor E
33	-2,38	0	0	0	0
14	1	-1	1	1	-1
40	0	0	0	2,38	0
44	0	0	0	0	0
8	1	1	1	-1	-1
1	-1	-1	-1	-1	-1
23	-1	1	1	-1	1
11	-1	1	-1	1	-1
45	0	0	0	0	0
50	0	0	0	0	0
5	-1	-1	1	-1	-1
35	0	-2,38	0	0	0
12	1	1	-1	1	-1
18	1	-1	-1	-1	1
36	0	2,38	0	0	0
9	-1	-1	-1	1	-1
13	-1	-1	1	1	-1
22	1	-1	1	-1	1
41	0	0	0	0	-2,38
37	0	0	-2,38	0	0
43	0	0	0	0	0
2	1	-1	-1	-1	-1
21	-1	-1	1	-1	1
16	1	1	1	1	-1
27	-1	1	-1	1	1
6	1	-1	1	-1	-1
26	1	-1	-1	1	1
42	0	0	0	0	2,38
4	1	1	-1	-1	-1
24	1	1	1	-1	1

4.3.1 Zinc plating solution experimental design parameters

The five diffusion parameters, in terms of actual concentration and temperature, of the zinc plating solution are tabulated in Table 5. The minimum and maximum axial values (±2,38) were obtained from the Enthobrite NCZ dimension alkaline non-cyanide zinc plating solution data sheet[35]. For experimental purposes, Dimensions A, B and C were considered

as a single component due to their low concentrations[35]. Thus the zinc solution was composed of four components excluding water; zinc oxide, sodium hydroxide, dimension and conditioner. The concentration of Dimension A was used as it had the largest concentration of the three[35]. The concentration of the components tabulated in Table 5 is based on a sample size of 25ml. A 25ml sample size was selected due to the small volume of plating solution injected into the diffusion capillary tube. The diffusion parameters and their corresponding factor representation are:

- Zinc oxide – Factor A
- Sodium hydroxide – Factor B
- Dimension A – Factor C
- Conditioner – Factor D
- Temperature – Factor E

Table 5: Actual parameter values for the zinc plating solution diffusion trials[35]

Factor	-2,38	-1	0	1	2,38
Zinc oxide (g/25ml)	0,58	0,65	0,70	0,76	0,83
Sodium hydroxide (g/25ml)	3	3,39	3,68	3,97	4,37
Dimension A (ml/25ml)	0,2	0,25	0,28	0,32	0,37
Dimension B (ml/25ml)	0,006	0,018	0,028	0,037	0,05
Dimension C (ml/25ml)	0,02	0,04	0,05	0,06	0,07
Conditioner (ml/25ml)	0,37	0,44	0,5	0,55	0,62
Temperature (^{o}C)	20	23	26	28	32

4.3.2 Copper plating solution experimental design parameters

The five diffusion parameters, in terms of actual concentration and temperature values, of the copper plating solution are tabulated in Table 6. The minimum and maximum axial values (±2.38) were obtained from the Ubac 101 bright acid copper plating solution data sheet[36]. The concentration of the components tabulated in Table 6, is based on a sample size of 25ml. The diffusion parameters and their corresponding factor representation are:

- Copper sulphate – Factor A
- Sulphuric acid – Factor B
- Sodium chloride – Factor C

- Ubac 101 – Factor D
- Temperature – Factor E

Table 6: Actual parameter values for the copper plating solution diffusion trials[36]

Factor	-2.38	-1	0	1	2.38
Copper sulphate (g/25ml)	1	1,18	1,31	1,43	1,62
Sulphuric acid (g/25ml)	1,25	1,46	1,62	1,78	2
Sodium chloride (g/25ml)	0,0005	0,0008	0,001	0,0012	0,0015
Ubac 101 (ml/25ml)	0,05	0,06	0,07	0,08	0,1
Temperature (deg C)	22	24,8	27	29,1	32

4.4 Plating Solution Preparation

For the purposes of the diffusion experimentation, the solution make-up for barrel plating was considered. The required compositions of the plating solutions were prepared in volumes of 25ml and stored in air tight bottles.

4.4.1 Equipment requirements

The requirements given below are for the zinc and copper plating solutions.

- PVC mixing tank capable of withstanding sodium hydroxide and sulphuric acid
- Mixing rod
- Thermometer
- Electric heater
- Automatic pipette
- 25ml air tight storage bottles
- Mass meter

4.4.2 Zinc plating solution preparation

The Enthobrite NCZ Dimension alkaline non-cyanide zinc plating process was selected for the experimental diffusion trials. The features of the zinc plating solution are[35]:

- Bright deposits
- Even thickness distribution

- Has no chelating agents or complexors
- Coating has a high corrosion resistant

The components of the zinc plating solution are[35]:

- Zinc oxide (ZnO)
- Sodium hydroxide (NaOH)
- Enthobrite NCZ dimension A
- Enthobrite NCZ dimension B
- Enthobrite NCZ dimension C
- Enthobrite NCZ conditioner

For the experimentation, 50 zinc plating solution samples of varying concentration were prepared as specified in Table 4. Based on the coded factor values specified in Table 4, the corresponding actual factor values were determined from Table 5. For the preparation of the fifty 25ml zinc plating solution samples, the following steps were followed[35]:

- The mixing tank was filled with 2/3 of the required 25ml of de-mineralised water.
- Sodium hydroxide was slowly and carefully added to the system until the required amount was dissolved in the de-mineralised water.
- Small amounts of zinc oxide was added to the solution and stirred until the total volume was dissolved in the solution.
- The remaining water was added to solution and stirred.
- Enthobrite NCZ conditioner was added and the solution stirred well.
- Enthobrite NCZ dimension A was added using the automatic pipette and the solution stirred well.
- Enthobrite NCZ dimension B was added using the automatic pipette and the solution stirred well.
- Enthobrite NCZ dimension C was added using the automatic pipette and the solution stirred well.
- The plating solution was then transferred to the 25ml air tight sample bottles.
- The samples were stored in a cool place, away from the sunlight to prevent degradation of the sample.

- The above steps were repeated for the preparation of the 50 samples.

4.4.3 Copper plating solution preparation

For the copper diffusion experimentation, the Ubac 101 bright acid copper plating solution was utilised. The features of the copper plating solution are bright deposits, elimination of copper polishing and high ductility[36].

The components of the copper plating solution are[36]:

- Copper sulphate ($CuSO_4$)
- Sulphuric acid (H_2SO4)
- Sodium chloride (NaCl)
- UBAC 101 brightener

For the experimentation, 50 copper plating solution samples of varying concentrations were prepared as specified in Table 4. Based on the coded factor values specified in Table 4, the corresponding actual factor values were determined from Table 6. For the preparation of the fifty 25ml copper plating solution samples, the following steps were followed[36]:

- The mixing tank was filled with 2/3 of the required 25ml of de-mineralised water.
- Sulphuric acid was slowly added to the de-mineralised water and stirred until the total volume was dissolved.
- The sulphuric acid solution was heated to 60^0C using an electric heater.
- The solution was allowed to stabilise at 60^0C.
- Copper sulphate was added to the solution and stirred well.
- The remaining amount of de-mineralised water was added.
- Sodium chloride was added to the solution and stirred well.
- The solution was allowed to settle overnight.
- UBAC 101 was added to the solution and stirred well.
- The solution was then transferred to the 25ml air tight sample bottles.
- The samples were stored in a cool place, away from the sunlight to prevent degradation of the sample.

4.5 Gas Diffusion Experimental Procedure

The following procedure was used to determine the change in height of the copper and zinc plating solution in the capillary tube for each of the 50 experimental runs and their repeatability, as specified in Table 4. Repeatabilities were performed for verification of the results. The percentage difference between the run and the repeatability had to be equal to or less than five percent.

The gas diffusion experimental procedure followed was[32]:

- The glass bath was filled with cold water.
- The vernier microscope was placed on the same level base as the glass bath.
- The electrical heater was switched on and the thermostat was set to the required temperature. The temperature required was based on the specific standard run temperature factor value, Factor E. The temperature was monitored using the thermometer.
- For each gas diffusion apparatus, two different standard run samples both having the same temperature criteria were selected. Two samples were selected as one capillary tube was used for the run and the other for the repeatability. This was primarily possible at the beginning of the experimentation. Towards the latter part of the experimentation, only one sample and the repeatability was run per apparatus.
- Using a 2,5ml syringe, the required plating solution was extracted from the 25ml sample bottles and injected into the capillary tube.
- The capillary tube was filled to a height of approximately 37mm in each of the capillary tubes.
- The capillary tube was placed in the manifold and the t-piece was secured to the manifold with cable ties.
- The flexible piping from the air pump was fitted to the t-piece of the capillary tube.
- The capillary tube was allowed to stand for a few minutes, to allow the plating solution to stabilise and adjust to the required run temperature.

- The height of the plating solution in the capillary tube and the height of the capillary tube were measured using the vernier microscope and recorded.
- The air pump was switched on and the time recorded.
- After a period of 24 hours the air pump was switched off.
- The level of the plating solution in the capillary tube was measured and recorded.
- The above steps were repeated for the second gas diffusion apparatus.
- The above steps were repeated for the 50 experimental runs and their repeatabilities.

Initially the diffusion trials were run for a time period of 2, 4, 6 and 8 hours respectively, but the rate of diffusion was negligible. A visible change in the plating solution liquid level could not be observed with the use of the vernier microscope. Thus the experimental time period was extended to 24 hours, where a change in liquid height could be measured with the vernier microscope.

The slow rate of diffusion of water from the plating solution for the initial experimental times could be attributed to the following;

- Limited surface area available, the inside diameter of the capillary tube is 2,6mm.
- The height of the fluid in the capillary tube, 37mm, was low as compared to the total height of the tube, 165mm. This possibly resulted in a greater stagnant air film through which the diffusing water vapour had to pass through prior to entering the moving air stream.

4.6 Zinc Plating Solution Gas Diffusion Results

4.6.1 Zinc plating solution experimental results

Table 7 details the experimental conditions in terms of the actual values and the results.

Table 7: Zinc plating solution experimental results

Std	Factor 1	Factor 2	Factor 3	Factor 4	Factor 5	Result	Repeat
	ZnO (g)	NaOH (g)	Dimension (ml)	Conditioner (ml)	Temperature (deg C)	Change in Height (mm)	Change in Height (mm)
31	0,65	3,98	0,32	0,55	28,52	0,047	0,0474
46	0,71	3,69	0,9	0,5	26	0,0126	0,0129
32	0,76	3,98	0,32	0,55	28,52	0,042	0,0418
50	0,71	3,69	0,29	0,5	26	0,022	0,0223
34	0,83	3,69	0,29	0.5	26	0,0132	0,0138
1	0,65	3,4	0,25	0,45	23,48	0,0584	0,0573
29	0,65	3,4	0,32	0,55	28,52	0,0079	0,0076
3	0,65	3,98	0,25	0,45	23,48	0,026	0,0264
11	0,65	3,98	0,25	0,55	23,48	0,0298	0,0294
7	0,65	3,98	0,32	0,45	23,48	0,1266	0,1264
38	0,71	3,69	0,38	0,5	26	0,0184	0,018
10	0,76	3,4	0,25	0,55	23,48	0,0882	0,0885
26	0,76	3,4	0,25	0,55	28,52	0,0266	0,0276
2	0,76	3,4	0,25	0,45	23,48	0,037	0,0373
20	0,76	3,98	0,25	0,45	28,52	0,0075	0,0078
6	0,76	3,4	0,32	0,45	23,48	0,0427	0,0439
8	0,76	3,98	0,32	0,45	23,48	0,0355	0,0349
45	0,71	3,69	0,29	0,5	26	0,0167	0,0161
43	0,71	3,69	0,29	0,5	26	0,0587	0,0572
12	0,76	3,98	0,25	0,55	23,48	0,0423	0,0428
9	0,65	3,4	0,25	0,55	23,4	0,03	0,0311
24	0,76	3,98	0,32	0,45	28,52	0,023	0,0232
44	0,71	3,69	0,29	0,5	26	0,0154	0,0156
36	0,71	4,38	0,29	0,5	26	0,0426	0,0422
21	0,65	3,4	0,32	0,45	28,52	0,0139	0,0146
48	0,71	3,69	0,29	0,5	26	0,0255	0,0248
28	0,76	3,98	0,25	0,55	28,52	0,0302	0,03
25	0,65	3,4	0,25	0,55	28,52	0,0284	0,0286

Std	Factor 1	Factor 2	Factor 3	Factor 4	Factor 5	Result	Repeat
	ZnO (g)	NaOH (g)	Dimension (ml)	Conditioner (ml)	Temperature (deg C)	Change in Height (mm)	Change in Height (mm)
17	0,65	3,4	0,25	0,45	28,52	0,0578	0,0576
22	0,76	3	0,32	0,45	28,52	0,0201	0,0197
47	0,71	3,69	0,29	0,5	26	0,0123	0,0127
37	0,71	3,69	0,2	0,5	26	0,0298	0,0294
42	0,71	3,69	0,29	0,5	32	0,0308	0,0298
33	0,58	3,69	0,29	0,5	26	0,0119	0,0121
15	0,65	3,98	0,32	0,55	23,48	0,0153	0,0156
41	0,71	3,69	0,29	0,5	20	0,0302	0,0293
5	0,65	3,4	0,32	0,45	23,48	0,0283	0,0289
19	0,65	3,98	0,25	0,45	28,52	0,0293	0,0279
14	0,76	3,4	0,32	0,55	23,48	0,0137	0,0144
49	0,71	3,69	0,29	0,5	26	0,0204	0,0205
4	0,76	3,98	0,25	0,45	23,48	0,0251	0,0257
27	0,65	3,98	0,25	0,55	28,52	0,0256	0,0246
16	0,76	3,98	0,32	0,55	23,48	0,0231	0,0235
35	0,71	3	0,29	0,5	26	0,0302	0,0298
39	0,71	3,69	0,29	0,38	26	0,0136	0,0138
40	0,71	3,69	0,29	0,63	26	0,0154	0,015
3	0,76	3,4	0,32	0,55	28,52	0,026	0,0264
13	0,65	3,4	0,32	0,55	23,48	0,0204	0,0201
23	0,65	3,98	0,32	0,45	28,52	0,0296	0,0294
18	0,76	3,4	0,25	0,45	28,52	0,0239	0,0244

4.6.2 Analysis of results

The results from Table 7 were inputted into the statistical software Design Expert 8. A fit summary and analysis of variance of the results was performed. The fit summary determined which mathematical model best described the relationship between the factors and the change in height in the capillary tube. The analysis of variance identified which of the factors had a significant effect on the change in height in the capillary tube. The results are summarised in Table 8.

Table 8: Summary of statistical analysis results of the zinc plating solution[31]

Criteria	Value	Comment
Model selected	Quadratic model	
Significant model factors	Factors AD, BC and B^2	
R –squared	0,483	Preferably should be close to 1
Adeq precision	7,161	Measures the signal to noise ratio. Should be greater than 4

The quadratic equation for predicting the change in height in the capillary tube for a zinc plating solution within the limits specified in Table 5 is as follows[31],

$$\Delta h = \left(\frac{1}{7.08 - (0.021A) - (0.094B) + (0.29C) + (0.04D) + (0.34E) - (0.61AD) - (0.77BC) + (0.47CD) - (0.49DE) - (0.41B^2) - (0.34E^2)} \right)^2 \quad (39)$$

The analysis of variance results, showed three factors as having a significant impact on the change in height in the capillary tube[31]:

- Factor AD – The combined effect of the concentrations of zinc oxide and Enthobrite NCZ conditioner.
- Factor BC - The combined effect of the concentrations of sodium hydroxide and Enthobrite NCZ Dimensiom.
- Factor B – The concentration of sodium hydroxide

Based on the results of the statistical analysis equation (39) was optimised, refer to Appendix C. The final optimised equation for the prediction of the change in height of the zinc plating solution in a capillary tube is as follows,

$$\Delta h = \left(\frac{1}{7.08 + (0.29C) + (0.34E) - (0.61AD) - (0.77BC) - (0.49DE) - (0.41B^2)} \right)^2 \quad (12)$$

The above equation was used to calculate the unknown solution specific interfacial partial pressure, P_{A1}. The use of equation (12) for the calculation of P_{A1} was explained in Chapter 3.

The statistical analysis of the experimental results showed that the results were inaccurate and inconsistent as:

- The R^2 value (0,483) was low.
- Only three model factors were identified to have a significant impact on the change in height in the capillary tube.
- The temperature of the plating solution, Factor E, was not identified as having a significant impact on the change in height in the capillary tube.

The possible reasons for the inaccurate and inconsistent experimental results are:

- Incorrect reading of the vernier microscope.
- Zinc plating solution samples were not prepared correctly.
- The air flow rates through each of the capillary tubes were not equal and consistent.

4.7 Copper Plating Solution Gas Diffusion Results

4.7.1 Copper plating solution experimental results

Table 9 details the experimental conditions in terms of actual values and the experimental results.

Table 9: Copper plating solution experimental results

Std	Factor A	Factor B	Factor C	Factor D	Factor E	Result	Repeat
	$CuSO_4$ (g)	H_2SO_4 (g)	NaCl (g)	Ubac 101 (ml)	Temperature (deg C)	Change in Height (mm)	Change in Height (mm)
32	1,44460	1,78267	0,01080	0,08551	29,10	0,051	0,0053
36	1,31300	2,00000	0,00775	0,07500	27,00	0,0003	0,0003
47	1,31300	1,62500	0,00775	0,07500	27,00	0,0066	0,0068
16	1,44460	1,78267	0,01080	0,08551	24,90	0,0199	0,0201
29	1,18140	1,46733	0,01080	0,08551	29,10	0,0072	0,0074
49	1,31300	1,62500	0,00775	0,07500	27,00	0,007	0,0073
27	1,18140	1,78267	0,00470	0,08551	29,10	0,0125	0,013
6	1,44460	1,46733	0,01080	0,06449	24,90	0,0029	0,0029
42	1,31300	1,62500	0,00775	0,07500	32,00	0,0097	0,0096
46	1,31300	1,62500	0,00775	0,07500	27,00	0,008	0,0081
15	1,18140	1,78267	0,01080	0,08551	24,90	0,0267	0,0273

Std	Factor A	Factor B	Factor C	Factor D	Factor E	Result	Repeat
	$CuSO_4$ (g)	H_2SO_4 (g)	NaCl (g)	Ubac 101 (ml)	Temperature (deg C)	Change in Height (mm)	Change in Height (mm)
23	1,18140	1,78267	0,01080	0,06449	29,10	0,0093	0,0094
33	1,00000	1,62500	0,00775	0,07500	27,00	0,0085	0,0087
3	1,18140	1,78267	0,00470	0,06449	24,90	0,0127	0,0126
11	1,18140	1,78267	0,00470	0,08551	24,90	0,0041	0,0043
18	1,44460	1,46733	0,00470	0,06449	29,10	0,055	0,057
21	1,18140	1,46733	0,01080	0,06449	29,10	0,009	0,0092
48	1,31300	1,62500	0,00775	0,07500	27,00	0,0047	0,0047
44	1,31300	1,62500	0,00775	0,07500	27,00	0,033	0,034
28	1,44460	1,78267	0,00470	0,08551	29,10	0,0059	0,006
14	1,44460	1,46733	0,01080	0,08551	24,90	0,0194	0,0193
20	1,44460	1,78267	0,00470	0,06449	29,10	0,0084	0,0086
13	1,18140	1,46733	0,01080	0,08551	24,90	0,0194	0,0196
9	1,18140	1,46733	0,00470	0,08551	24,90	0,004	0,0041
50	1,31300	1,62500	0,00775	0,07500	27,00	0,0093	0,0054
4	1,44460	1,78267	0,00470	0,06449	24,90	0,008	0,0082
8	1,44460	1,78267	0,01080	0,06449	24,90	0,008	0,0079
34	1,62600	1,62500	0,00775	0,07500	27,00	0,0063	0,006
37	1,31300	1,62500	0,00050	0,07500	27,00	0,0005	0,0006
24	1,44460	1,78267	0,01080	0,06449	29,10	0,0044	0,0045
10	1,44460	1,46733	0,00470	0,08551	24,90	0,0175	0,0177
40	1,31300	1,62500	0,00775	0,10000	27,00	0,0384	0,0386
26	1,44460	1,46733	0,00470	0,08551	29,10	0,0059	0,006
2	1,44460	1,46733	0,00470	0,06449	24,90	0,0162	0,0163
19	1,18140	1,78267	0,00470	0,06449	29,10	0,1615	0,1618
31	1,18140	1,78267	0,01080	0,08551	29,10	0,0054	0,0054
5	1,18140	1,46733	0,01080	0,06449	24,90	0,006	0,0062
45	1,31300	1,62500	0,00775	0,07500	27,00	0,0002	0,0002
38	1,31300	1,62500	0,01500	0,07500	27,00	0,0092	0,0093
41	1,31300	1,62500	0,00775	0,07500	22,00	0,006	0,0001
25	1,18140	1,46733	0,00470	0,08551	29,10	0,0102	0,0104
22	1,44460	1,46733	0,01080	0,06449	29,10	0,0042	0,0044
30	1,44460	1,46733	0,01080	0,08551	29,10	0,0092	0,0093
43	1,31300	1,62500	0,00775	0,07500	27,00	0,0051	0,0052
1	1,18140	1,46733	0,00470	0,06449	24,90	0,0042	0,0042
17	1,18140	1,46733	0,00470	0,06449	29,10	0,0053	0,0053
39	1,31300	1,62500	0,00775	0,05000	27,00	0,0041	0,0043
35	1,31300	1,25000	0,00775	0,07500	27,00	0,0048	0,0049

Std	Factor A	Factor B	Factor C	Factor D	Factor E	Result	Repeat
	$CuSO_4$ (g)	H_2SO_4 (g)	NaCl (g)	Ubac 101 (ml)	Temperature (deg C)	Change in Height (mm)	Change in Height (mm)
12	1,44460	1,78267	0,00470	0,08551	24,90	0,0055	0,0056
7	1,18140	1,78267	0,01080	0,06449	24,90	0,0281	0,0283

4.7.2 Analysis of results

The results from Table 9 were inputted into the statistical software Design Expert 8. A fit summary and analysis of variance of the results was performed. The results are summarised in Table 10.

Table 10: Summary of statistical analysis results of the copper plating solution[31]

Criteria	Value
Model selected	Mean model
Significant model factors	None
R –squared	0
Adeq precision	NA

The mean equation for predicting the change in height in the capillary tube for a copper plating solution within the limits specified in Table 6 is as follows[31],

$$\Delta h_{Cu} = \exp(-4.84) \quad (40)$$

Where Δh_{Cu} = Change in height of the copper solution in the capillary tube (mm)

The statistical analysis of the experimental results showed that the results were inaccurate and inconsistent as:

- None of the five factors were identified to have an impact on the change in height in the capillary tube.
- An R^2 value of zero was calculated.

The inaccurate experimental results could be attributed to the reasons detailed in Section 4.6.2.

From the results summarised in Table 10, it was decided that the copper plating solution results will not be used in the CCPS model developed in Chapter 3.

4.8 Conclusion

Initially, both the zinc and copper plating solutions were to be used to demonstrate the application of the CCPS model developed in Chapter 3. However, the statistical analysis of the experimental results revealed that the copper plating solution results were invalid. Thus, only the optimised results for the zinc plating solution will be utilised in the CCPS model. The use of equation (12) in the development of the CCPS model was detailed in Chapter 3. In Chapter 6, the application of equation (12) for the determination of the optimum operating conditions for the plating bath and cooling tower are discussed.

CHAPTER 5: CLOSED CIRCUIT PLATING SYSTEM MODEL VERIFICATION

5.1 Introduction

Prior to the application of the model developed in Chapter 3 for the determination of the optimum operating parameters of the CCPS, the model had to be verified. As stated in the preceding chapters, due to the scarcity of thermodynamic data for plating solutions and ionic diffusion being slow, the model was developed for an air-water system. The development of the evaluation matrix detailing the verification criteria and acceptable deviation limits are discussed. The results of the Matlab CCPS model was verified against results given by Geankoplis and that of five CCPS models solved in Microsoft Excel for an air-water system.

5.2 Criteria and Limits for Model Verification

For the model verification, key calculated model parameters for comparative analysis with the Geankoplis and Microsoft Excel results were identified. The selection of the key parameters was based on their impact; on the rate of cooling, the amount of water evaporated and the final equilibrium temperatures of the plating bath and the cooling tower. The key parameters identified were:

- Gas phase mass transfer coefficient
- Height of the cooling tower
- Mass evaporated in the unsteady state temperature region
- Mass evaporated in the steady state temperature region
- Equilibrium temperature of the plating bath
- Equilibrium temperature of the cooling tower
- Lowest cooling tower temperature
- Electrical energy
- Energy of cold metal part
- Evaporative energy
- Conduction and convection energy

For the positive verification of the CCPS model, the percentage difference of the Matlab model results to the results from Geankoplis and the five CCPS models solved in Microsoft Excel had to satisfy either the upper or lower limit criteria as detailed in Table 11.

Table 11: Acceptable deviation limits for verification of the CCPS model

Parameter	Lower Limit	Upper Limit
Gas phase mass transfer coefficient, k_G	-5%	+5%
Upper limit of cooling tower height, z	- 10%	+10%
Lower limit of cooling tower height, z	-10%	+10%
Cooling tower exit temperature, T_{L1}.	-5%	+5%
Mass loss in unsteady state temperature region	-5%	+5%
Mass loss in steady state temperature region	-5%	+5%
Electrical energy, E_{ELEC}	-5%	+5%
Energy of cold plating solution, E_{CPS}	-5%	+5%
Conduction and convection energy, $E_{COND+CONV}$	-5%	+5%
Evaporation energy, E_{EVAP}	-5%	+5%
Temperature of plating bath, T_{PB}	-5%	+5%
Minimum cooled plating solution temperature T_{L1}_min	-10%	+10%
Gas phase mass transfer coefficient and packing surface area, k_Ga	-5%	+5%

5.3 Input Data for the Model

The inputs into the model can be broken down into three categories:

- Ambient conditions
- Plating bath data
- Cooling tower data

As the verification of the CCPS model is performed against an air-water system, the physical and thermodynamic characteristics of water were used.

5.3.1 Ambient conditions

The maximum cooling achievable by a cooling tower is dependent on the ambient conditions. The lowest temperature that a system can be cooled to is the wet bulb temperature of the dry air [26]. The following ambient air- data is required:

- Dry bulb temperature of the air
- Air flow rate through the cooling tower
- Humidity of the air
- Saturation humidity of the air
- Heat transfer coefficient of the air
- Density of the air at the dry bulb temperature
- Viscosity of the air at the dry bulb temperature

5.3.2 Plating bath data

The operating conditions and characteristics of the plating bath have a significant affect on the rate of cooling and evaporation in the CCPS. The following plating bath data is required:

- Plating bath operating temperature
- Dimensions of the plating bath; length, width, height and thickness
- Volume of solution in the plating bath
- Thickness and square meter of metal to be plated
- Quantity of metal pieces to be plated
- Thermal conductivity of the material of construction of the plating bath
- Density of metal pieces to be plated
- Specific heat capacity of metal pieces to be plated
- Plating bath voltage and amperage requirements
- Plating time

5.3.3 Cooling tower data

The operational and physical characteristics of the cooling tower affect the rate of water evaporation, the rate of cooling and the plating bath and cooling tower equilibrium temperatures. If the solution being cooled is not water, the properties of water will be replaced by the properties of that solution. The following cooling tower data is required:

- Water re-circulating flow rate
- Water specific heat capacity
- Water density
- Water heat transfer coefficient

- Diameter of cooling tower
- Height of cooling tower
- Packing surface area
- Data for a saturation enthalpy-temperature curve

From above it can be seen that the height of the cooling tower is an input into the system but the model also calculates the height based on the iterative solution of T_{L1}. Also, the input data is information that is readily available and will require minimum time and effort to obtain.

5.4 Model Verification against Five CCPS Models Solved in Microsoft Excel

For the verification of the CCPS model developed in Chapter 3, the CCPS model was set up in Microsoft Excel with one difference. In the CCPS model programmed into Matlab, the exit temperature from the cooling tower, T_{L1}, was the output. In the CCPS model programmed into Microsoft Excel, T_{L1} was an input with the height of the cooling tower, z, as the output. For verification purposes the calculation of the plating bath temperature, T_{PB}, was based on one pass through the CCPS, as depicted in Figure 21. The Microsoft Excel model was first run for the calculation of the cooling tower height required to achieve T_{L1}. The calculated height was then input into the Matlab model to calculate T_{L1}.

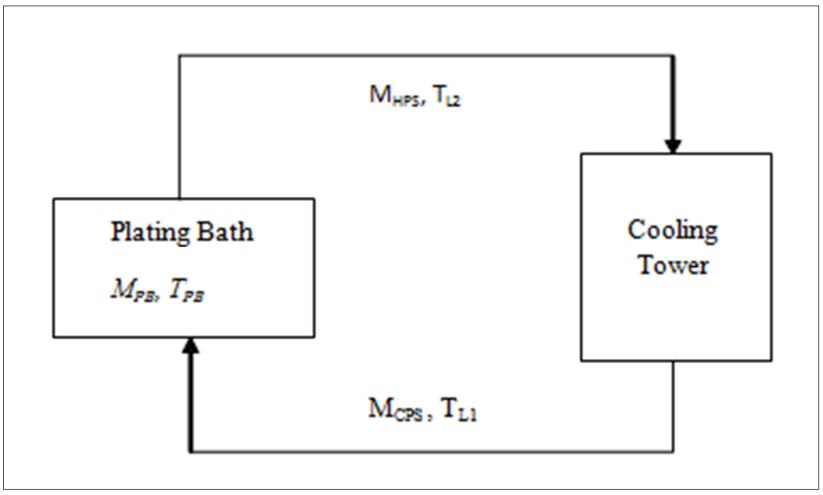

Figure 21: Single pass through the CCPS

5.4.1 Input data for model verification

The input data for the air-water system is tabulated in Table 12.

Table 12: Microsoft Excel verification input data

Parameter	Run 1	Run 2	Run 3	Run 4	Run 5
Water flow rate (kg/s)	1	2	3	4	5
Air flow rate (kg/s)	1,2	2,4	3,6	4,8	6
Cooling tower diameter (m)	0,5	0,5	0,5	0,5	0,5
Inlet temperature, T_{L2} (^{O}C)	20	23	26	29	32
Exit temperature, T_{L1} (^{O}C)	15	15,5	16	14	12
Air heat transfer co-efficient (W/m^2.K)	280	280	280	280	280
Dry bulb temperature (^{O}C)	15	15,5	16	14	12
% Relative humidity	70	70	70	70	60
Mass of water in bath (kg)	3000	3000	3000	3000	3000

The rationale for the selection of the input parameters is detailed below.

- Water and air flow rate

  The air and water flow rates through the cooling tower were selected based on the mass of plating solution in the plating bath. The larger the mass of solution in the plating bath, higher air and water flow rates will be required to see an immediate effect on the CCPS. The air and water flow rates detailed in Table 2 show the effect of the cooling tower on the plating bath temperature after just one pass through the cooling tower.

- Inlet water temperature to cooling tower

  The inlet temperatures were based on the allowable operating temperature range for the zinc plating solution[35].

- Exit water temperature from the cooling tower

  The exit temperatures were selected to show the CCPS model's accuracy over wide cooling ranges, that is from a small cooling range of 5^{0}C to a large cooling range of 20^{0}C.

- Cooling tower diameter

  Due to limited space availability in an electroplating facility, a relatively small cooling tower diameter was selected.

- Mass of water in plating bath

  The mass of water in the plating bath was based on electroplating operational practice.

5.4.2 Results of model verification

The results of the comparative analysis are tabulated in Tables 13 to 17.

Table 13: Comparison of results for verification 1

Criteria	Matlab Model Result	Microsoft Excel Result	% Difference
Gas phase mass transfer coefficient, k_G (kmol/s.m^2.Pa)	8,78E-09	8,78E-09	0,01
Upper limit cooling tower height, z_1, (m)	3,04	2,73	10,22
Lower limit cooling tower height, z_1 (m)	2,23	2,73	18,38
Cooling tower exit temperature, T_{L1} (^{O}C)	14,86	15	0,92
Lowest cooled temperature, T_{L1}_min (^{O}C)	12,94	11,9	8,09
Mass loss in unsteady state temperature region (kg)	4,18	4,07	2,64
Mass loss in steady state temperature region for 1hr (kg)	17,29	17,28	0,00
Electrical energy, E_{ELEC} (KJ)	12,06	12,06	0,04
Energy of cold metal part, E_{CMP} (KJ)	0,46	0,46	0,01
Conduction and convection energy, $E_{COND/V}$ (KJ)	460,54	460,74	0,04
Evaporation energy, E_{EVAP_PB} (KJ)	1,89	1,89	0,05
Temperature of plating bath, T_{PB} (^{O}C)	19,19	19,21	0,10

Table 14: Comparison of results for verification 2

Criteria	Matlab Model Result	Microsoft Excel Result	% Difference
Gas phase mass transfer coefficient, k_G (kmol/s.m^2.Pa)	1,58E-08	1,58E-08	0,0046
Upper limit cooling tower height, z_1, (m)	4,30	4,22	1,96

Criteria	Matlab Model Result	Microsoft Excel Result	% Difference
Lower limit cooling tower height, z_1 (m)	3,20	4,22	24,12
Cooling tower exit temperature, T_{L1} (^{O}C)	15,41	15,5	0,56
Lowest cooled temperature, T_{L1}_min (^{O}C)	13,58	12,2	10,21
Mass loss in unsteady state temperature region (kg)	9,55	9,45	1,04
Mass loss in steady state temperature region for 1hr (kg)	34,57	34,57	9,67E-5
Electrical energy, E_{ELEC} (KJ)	9,32	9,33	0,12
Energy of cold metal part, E_{CMP} (KJ)	0,69	0,69	0,0070
Conduction and convection energy, $E_{COND/V}$ (KJ)	533,93	534,54	0,12
Evaporation energy, E_{EVAP_PB} (KJ)	1,73	1,74	0,12
Temperature of plating bath, T_{PB} (^{O}C)	21,33	21,35	0,080

Table 15: Comparison of results for verification 3

Criteria	Matlab Model Result	Microsoft Excel Result	% Difference
Gas phase mass transfer coefficient, k_G (kmol/s.m^2.Pa)	2,24E-08	2,24E-08	0,00
Upper limit cooling tower height, z_1, (m)	6,44	6,05	6,13
Lower limit cooling tower height, z_1 (m)	4,93	6,05	18,43
Cooling tower exit temperature, T_{L1} (^{O}C)	15,92	16	0,48
Lowest cooled temperature, T_{L1}_min (^{O}C)	14,04	12,7	9,57
Mass loss in unsteady state temperature region (kg)	18,15	18,04	0,64
Mass loss in steady state temperature region for 1hr (kg)	54,44	54,44	0,00
Electrical energy, E_{ELEC} (KJ)	8,89	8,91	0,12
Energy of cold metal part, E_{CMP} (KJ)	0,92	0,92	0,00
Conduction and convection energy, $E_{COND/V}$ (KJ)	679,29	680,12	0,12
Evaporation energy, E_{EVAP_PB} (KJ)	1,97	1,97	0,12
Temperature of plating bath, T_{PB} (^{O}C)	23,14	23,16	0,08

Table 16: Comparison of results for verification 4

Criteria	Matlab Model Result	Microsoft Excel Result	% Difference
Gas phase mass transfer coefficient, k_G (kmol/s.m^2.Pa)	2,91E-08	2,91E-08	0,01
Upper limit cooling tower height, z_1, (m)	11,88	11,23	5,48
Lower limit cooling tower height, z_1 (m)	8,44	11,23	24,85
Cooling tower exit temperature, T_{L1} (^{O}C)	13,97	14	0,20
Lowest cooled temperature, T_{L1}_min (^{O}C)	12,12	10,9	10,03
Mass loss in unsteady state temperature region (kg)	50,34	50,24	0,20
Mass loss in steady state temperature region for 1hr (kg)	63,94	63,94	0,00
Electrical energy, E_{ELEC} (KJ)	12,40	12,40	0,01
Energy of cold metal part, E_{CMP} (KJ)	1,38	1,38	0,00
Conduction and convection energy, $E_{COND/V}$ (KJ)	1420,85	1420,68	0,01
Evaporation energy, E_{EVAP_PB} (KJ)	3,25	3,25	0,01
Temperature of plating bath, T_{PB} (^{O}C)	22,65	22,66	0,05

Table 17: Comparison of results for verification 5

Criteria	Matlab Model Result	Microsoft Excel Result	% Difference
Gas phase mass transfer coefficient, k_G (kmol/s.m^2.Pa)	3,58E-08	3,58E-08	0,01
Upper limit cooling tower height, z_1, (m)	14,65	14,22	2,91
Lower limit cooling tower height, z_1 (m)	10,85	14,22	23,72
Cooling tower exit temperature, T_{L1} (^{O}C)	11,96	12,00	0,37
Lowest cooled temperature, T_{L1}_min (^{O}C)	9,52	8,00	15,97
Mass loss in unsteady state temperature region (kg)	84,90	84,84	0,07
Mass loss in steady state temperature region for 1hr (kg)	88,57	88,57	0,00
Electrical energy, E_{ELEC} (KJ)	12,55	12,57	0,15
Energy of cold metal part, E_{CMP} (KJ)	1,84	1,84	0,00
Conduction and convection energy, $E_{COND/V}$ (KJ)	1916,40	1919,29	0,15

Criteria	Matlab Model Result	Microsoft Excel Result	% Difference
Evaporation energy, E_{EVAP_PB} (KJ)	3,90	3,91	0,15
Temperature of plating bath, T_{PB} (^{O}C)	22,42	22,43	0,06

From Tables 13 to 17, it can be seen that the only factor that does not meet the criteria is the lower limit cooling tower height. The percentage difference in all five runs varies between 18,38% and 24,85%. This large percentage difference could be attributed to the small incremental temperature change of 0,3 between T_{L1_min} and T_{L2} in the iterative calculation of temperature T_{L1}. Refer to Appendix A for the Matlab program.

The remaining verification criteria are within the specified acceptable limits. Thus the CCPS Matlab model can accurately predict the cooling and evaporation that can be achieved by both the cooling tower and the plating bath for specified input conditions. Refer to Appendix D for the Microsoft Excel calculations.

5.5 Model Verification against Results given by Geankoplis

5.5.1 Input data given by Geankoplis

The data given by Geankoplis is for a cooling tower, thus only the cooling tower design could be verified. The input data is tabulated in Table 18. The cooling tower design criteria evaluated were:

- Gas phase mass transfer coefficient and packing surface area , k_Ga
- Upper limit of cooling tower height, z_1
- Lower limit of cooling tower height, z_1
- Cooling tower exit temperature, T_{L1}

Table 18: Input data for model verification against Geankoplis results[26]

Parameter	Value
Water flow rate (kg/s)	1,356
Air flow rate (kg/s)	1,356
Cooling tower cross-sectional area (m^2)	1
Inlet temperature, T_{L2}	43,3
Water heat transfer co-efficient (W/m.K)	280

Parameter	Value
Dry bulb temperature (^{O}C)	29,4
Packing surface area, a (m^2/m^3)	56

5.5.2 Results of model verification

The acceptable limits as detailed in Table 11 were applicable. The results are tabulated in Table 19.

Table 19: Comparison of Matlab and Geankoplis results

Criteria	Matlab Model Result	Geankoplis Result	% Difference
Gas phase mass transfer co-efficient and packing surface area, k_Ga (kmol/s.m^3.Pa)	1,31E-7	1,207 E-7	8,56
Upper limit cooling tower height, z_1 (m)	7,09	6,98	1,54
Lower limit cooling tower height, z_1 (m)	6,93	6,98	0,78
Cooling tower exit temperature, T_{L1} (^{O}C)	28,91	29,4	1,68

From Table 19 it can be seen that the only criteria outside the specified acceptable limit is k_Ga. This can be attributed to the packing surface area not being specified by Geankoplis[26]. In the five CCPS models solved in Microsoft Excel, the percentage difference for k_G was less than one percent. Thus the Matlab model can accurately predict the gas phase mass transfer coefficient, k_G and the cooling tower design has been verified.

5.6 Conclusion

The comparative analysis shows that all the model criteria, except the lower limit cooling tower height, were within the acceptable limits. A possible reason for the lower limit cooling tower height exceeding the acceptable limit is the small incremental temperature change for the calculation of the cooling tower height. Thus the CCPS model has been verified and can be used to determine the optimum operating conditions of the CCPS. The application of the verified CCPS model will be discussed in Chapter 6.

CHAPTER 6: APPLICATION OF THE CLOSED CIRCUIT PLATING SYSTEM MODEL

6.1 Introduction

The aim of this chapter is to show the practical application of the CCPS model. The plating solution characteristics and the model input data were identified. The key variables affecting the performance of the CCPS were identified to illustrate their impact on the final equilibrium conditions. Single and multiple variable sensitivity analyses were performed using Matlab to determine the optimum operational status of the key variables, for the recovery of the rinse system water.

6.2 Plating Solution Physical Characteristics

For the practical application of the CCPS model, only the data for the zinc plating solution was utilised as the copper plating solution experimental results were invalid. The zinc plating solution composition data specified in Table 5 in Chapter 4 indicated that the plating solution is composed primarily of water. The water concentration was approximately 88 to 90 percent by volume based on solution composition.

Due to the scarcity of plating solution specific information and water being the largest component in the zinc plating solution, it was assumed that the physical and thermodynamic properties of the plating solution would be that of water. However, the effects of the remaining components (acids, salts, bases, etc) of the plating solution were not neglected. Experimental methodology was used to determine the concentration dependant interfacial partial pressure, P_{A1}, as detailed in Chapter 4. The CCPS model can be customised to alternate systems provided the relevant thermodynamic data is available.

6.3 Identification of Factors that Affect the Performance of the CCPS

The key factors affecting the performance of the CCPS based on cooling tower operational performance and plating bath characteristics are:

- Plating solution composition and operational temperature

  The Enthobrite NCZ alkaline non-cyanide zinc plating solution data sheet provides a range of concentrations for each of the components and an operational temperature range[35]. By varying the concentrations of each of the components and the operational temperature, the optimum component concentration and temperature for maximum cooling and water evaporation was determined.

- Ambient air temperature

  The ambient air temperature determines the lowest temperature that the plating bath and cooling tower can achieve. The lowest cooled temperature that can be achieved by both the cooling tower and the plating bath is the wet bulb temperature[26]. The greater the temperature difference between the wet bulb temperature and the plating solution temperature, the greater the potential for cooling.

- Air flow rate

  The flow rate of air through the cooling tower is critical as it determines the contact time between the "hot" plating solution and the "cool" air stream. The contact time needs to be sufficient such that heat and mass transfer can occur but must not be long enough to promote negative heat transfer. This is especially critical at high ambient air temperatures.

- Packing Area

  The purpose of the packing is to provide a lager surface area for mass and heat transfer to occur. The larger the packing surface area, the greater the area available for heat and mass transfer to occur. There are basically two types of packing, random and structured packing.

6.4 Universal Input Data

To determine the effects of the parameters identified in Section 6.3, various sensitivity analyses were conducted in Matlab. For the comparative analysis of these simulations, a basis of universal input data had to be established. The universal input data for the simulations are tabulated in Table 20.

Table 20: Universal input data

Input Parameter	Value
Height of cooling tower	2,5m
Diameter of cooling tower	0,5m
Air heat transfer co-efficient	11W/m^2.K
Water heat transfer co-efficient	280W/m^2.K
Packing surface area[a]	500m^2/m^3
Initial mass of plating bath	3000kg
Plating bath length	1,5m
Plating bath width	1,5m
Plating bath height	2m
Thickness of mild steel plate to be plated	1mm
Area of mild steel metal plate to be plated	0,0025m^2
Number of mild steel metal pieces to be plated	10
Density of mild steel	7801kg/m^3
Specific heat capacity of mild steel	0,473KJ/kg.K
Current density	150A/m^2
Voltage	6V
Thermal conductivity of plating bath - PVC	0,19W/m.K

a – Is not applicable when the effects of packing area is being determined.

6.5 Effect of Plating Solution Composition and Plating Bath Temperature on the CCPS

The Enthobrite NCZ Dimension alkaline non-cyanide zinc plating solution data sheet, stipulates the allowable component concentrations and the operational temperature ranges[35]. Based on these ranges, five input data sets, with varying plating solution compositions and operational temperatures, were developed in Chapter 4 using the statistical analysis software Design Expert 8.

These five data sets were the basis for the analysis of the effect of plating solution composition and plating bath operational temperature on the performance of the CCPS. The compositions and temperatures of the five data sets and the input data for the model are tabulated in Table 21.

Table 21: Input data for plating composition and operational temperature sensitivity analysis

Factor	Minimum	-1	Mean	1	Maximum
Zinc oxide (g/25ml)	0,58	0,65	0,70	0,76	0,83
Sodium hydroxide (g/25ml)	3	3,39	3,68	3,97	4,37
Dimension A (ml/25ml)	0,2	0,25	0,28	0,324	0,37
Dimension B (ml/25ml)	0,006	0,019	0,028	0,037	0,05
Dimension C (ml/25ml)	0,025	0,039	0,05	0,060	0,075
Conditioner (ml/25ml)	0,37	0,44	0,5	0,55	0,62
Plating solution temperature (^{o}C)	20	23,5	26	28,5	32
Ambient air temperature (^{0}C)	12	12	12	12	12
Plating solution flow rate (kg/s)	1	1	1	1	1
Air flow rate (kg/s)	1,2	1,2	1,2	1,2	1,2

6.5.1 Results of matlab simulations

The data from Table 21 was programmed into Matlab and the results obtained are illustrated in Figures 22 to 25.

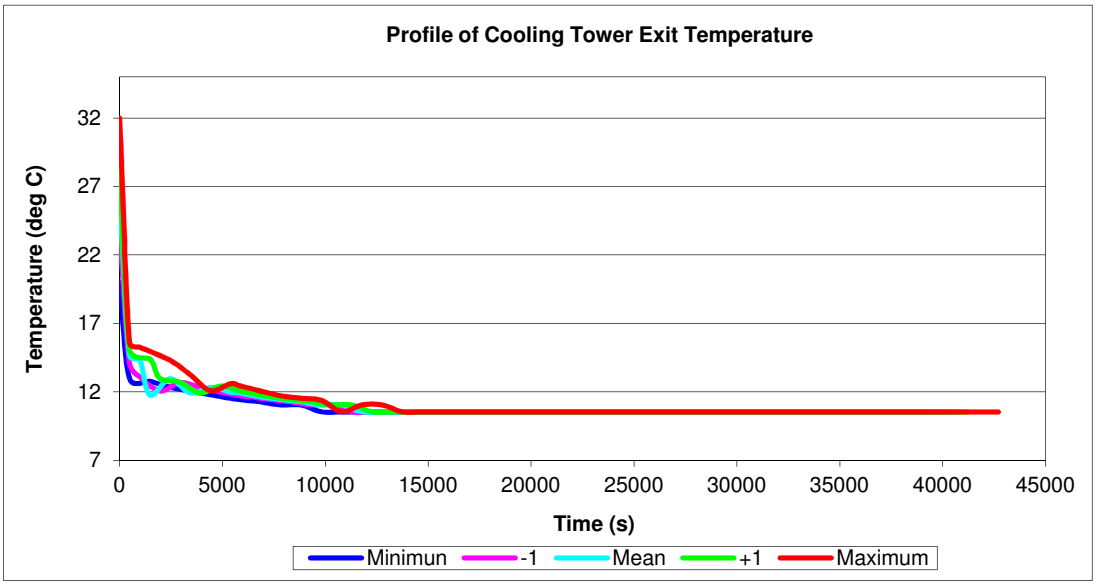

Figure 22: Effect of plating solution composition and operational temperature on the plating solution exit temperature from the cooling tower

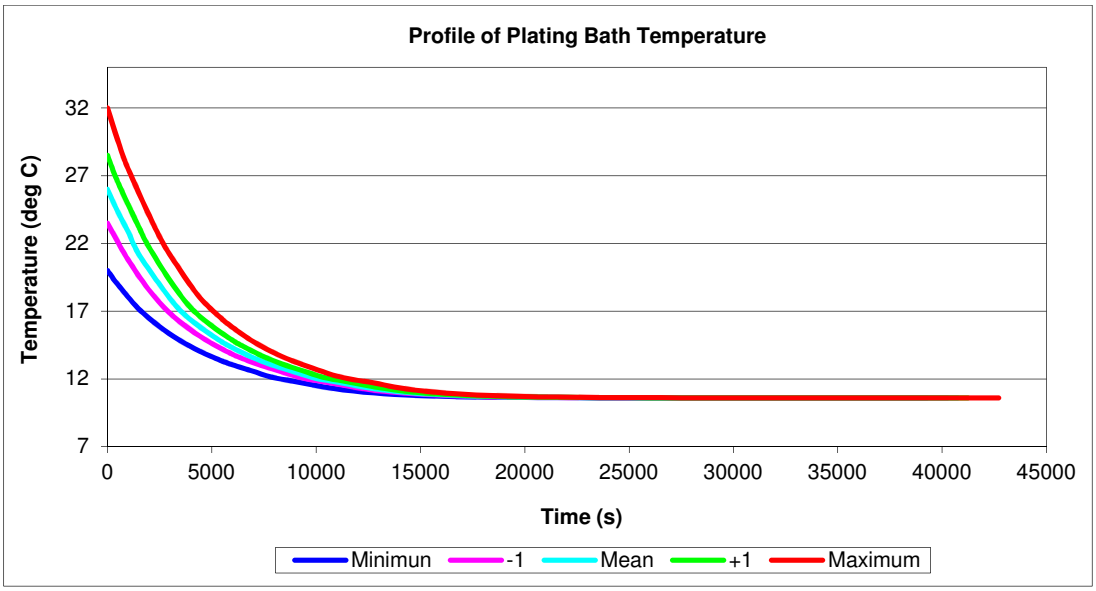

Figure 23: Effect of plating solution composition and operational temperature on the plating bath temperature

Figures 22 and 23 illustrate that the plating solution composition and operational temperature has minimal impact on the final equilibrium temperature achieved by the CCPS. The equilibrium temperature of the stream exiting the cooling tower and the plating bath is approximately 10,5^{0}C and 10,6^{0}C, respectively. This indicates that the CCPS equilibrium temperatures are significantly impacted by the ambient air temperature. Based on the input ambient air conditions of 12^{0}C and a 70 percent relative humidity, the wet bulb temperature is 9^{0}C. Thus the equilibrium temperatures of 10,5^{0}C and 10,6^{0}C are valid. The temperature of the plating bath is slightly higher than the plating solution stream exiting the cooling tower. This was expected, as the surface area available for heat transfer in the cooling tower is larger than that of the plating bath and in the plating bath there is continuous supply of electrical energy for the electrochemical reactions.

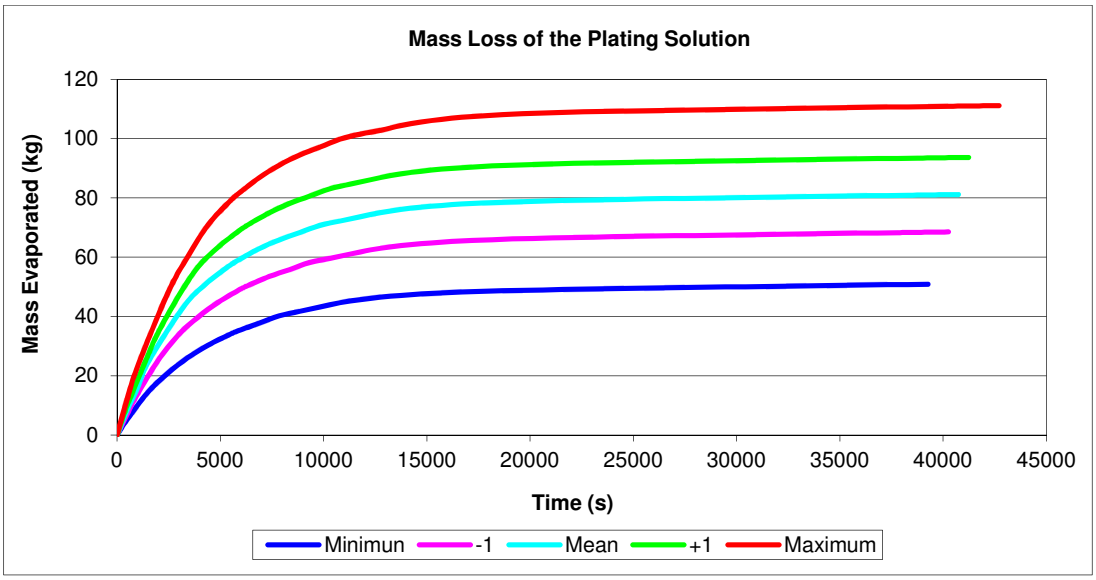

Figure 24: Effect of plating solution composition and operational temperature on the mass of water evaporated in the unsteady state temperature region

Figure 24 illustrates that the higher the plating bath operational temperature, the greater the rate of water evaporation in both the plating bath and the cooling tower in the unsteady state temperature region.

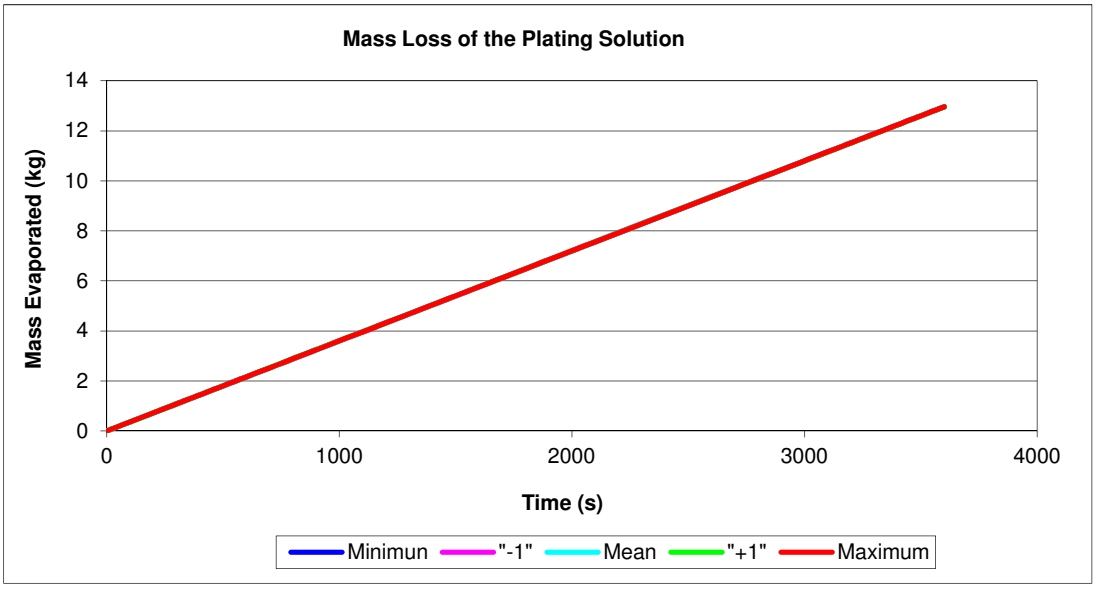

Figure 25: Effect of plating solution composition and operational temperature on the mass of water evaporated in the steady state temperature region

From Figure 25 it can be seen that the plating solution composition and operational temperature has minimal impact on the rate of water evaporation in the steady state temperature region. Equation (38) shows that the rate of evaporation in the steady state temperature region is governed by the air flow

rate and air saturation humidity. As these parameters are identical for the varying plating solution compositions and operational temperatures, the mass loss in the steady state temperature region is identical for all five data sets.

6.6 Effects of Air Flow Rate on the CCPS

To analyse the effects of air flow rate on the CCPS, the air flow rate was varied while the remaining input data was kept constant. The air flow rate was varied from five percent to forty five percent greater than that of the plating solution flow rate through the cooling tower. Refer to Table 22 for the CCPS model input data.

Table 22: Input data for air flow rate sensitivity analysis

Factor	5% Air	15% Air	30% Air	45% Air
Zinc oxide (g/25ml)	0,76	0,76	0,76	0,76
Sodium hydroxide (g/25ml)	3,97	3,97	3,97	3,97
Dimension A (ml/25ml)	0,32	0,32	0,32	0,32
Dimension B (ml/25ml)	0,037	0,037	0,037	0,037
Dimension C (ml/25ml)	0,06	0,06	0,06	0,06
Conditioner (ml/25ml)	0,55	0,55	0,55	0,55
Plating solution flow rate (kg/s)	1	1	1	1
Air flow rate (kg/s)	1,05	1,15	1,3	1,45
Plating solution temperature (^{o}C)	28,5	28,5	28,5	28,5
Ambient air temperature (^{0}C)	12	12	12	12

6.6.1 Results

Figures 26 to 29 illustrate the results obtained from Matlab.

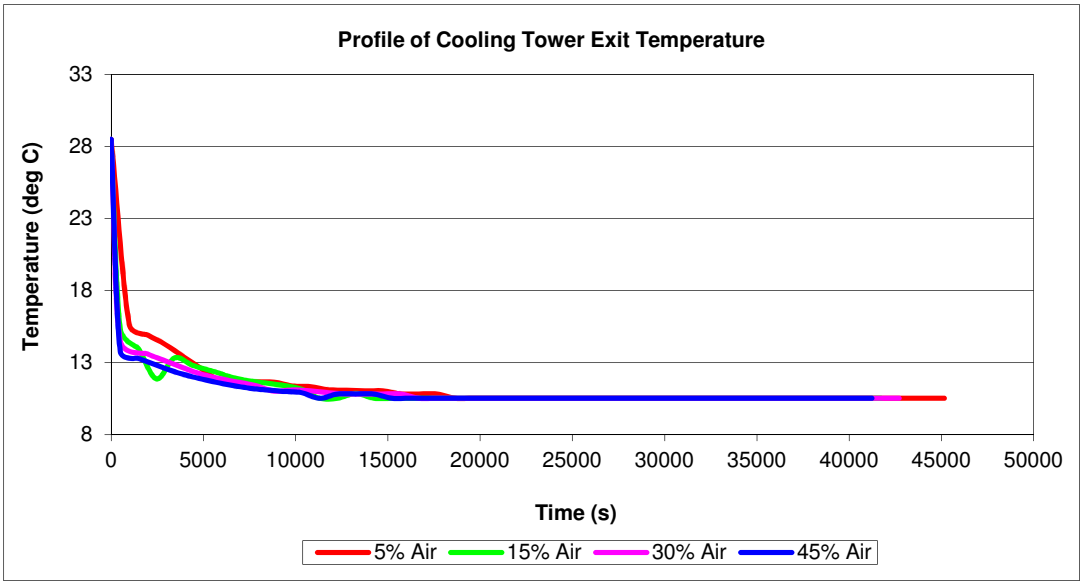

Figure 26: Effect of air flow rate on the plating solution exit temperature from the cooling tower.

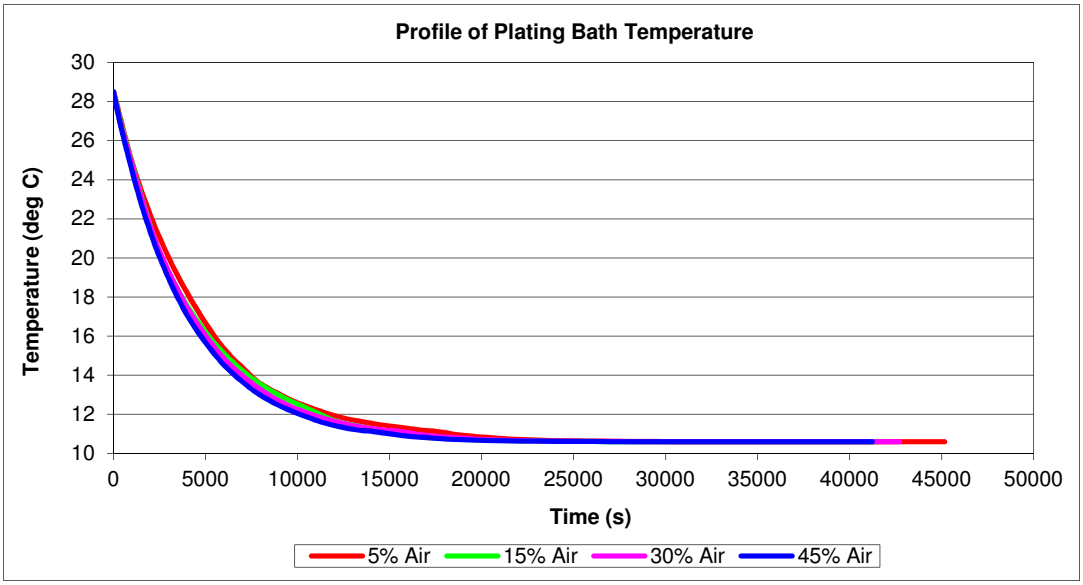

Figure 27: Effect of air flow rate on the plating bath temperature

Figures 26 and 27 illustrate that the higher the air flow rate, the greater the temperature drop across the height of the cooling tower and the lower the plating bath temperature until equilibrium is reached, respectively. This was expected, as the higher the air flow rate the greater the volume of air available, per square meter of cooling tower, for heat and mass transfer to occur. However, the final equilibrium temperatures for the varying air flow

rates are identical as it is dependant on the ambient air conditions specified in Table 22.

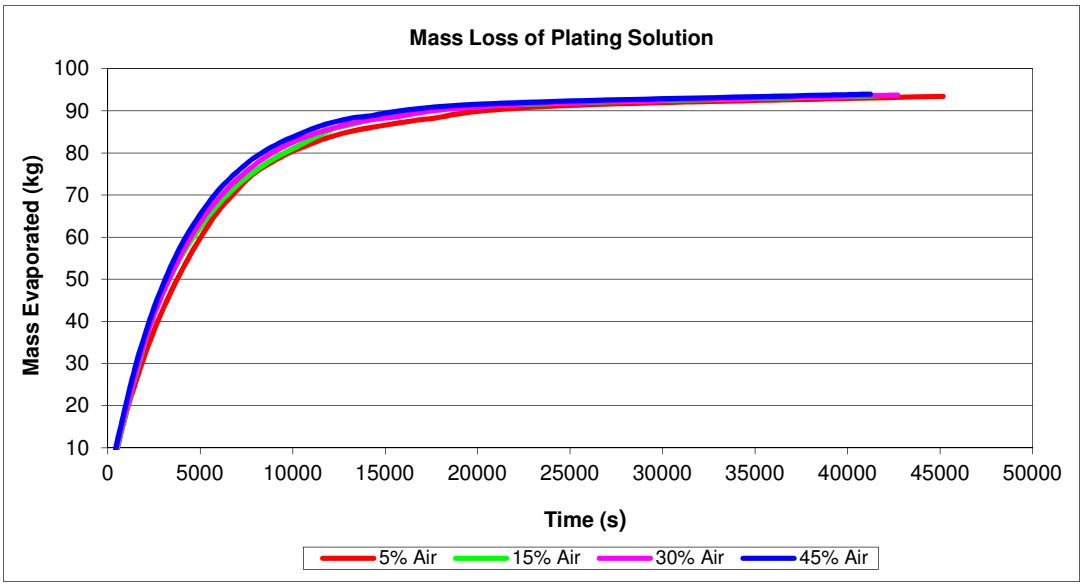

Figure 28: Effect of air flow rate on the mass of water evaporated in the unsteady state temperature region

Table 23: Results for varying air flow rate from Matlab

Parameter	5% Air	15% Air	30% Air	45% Air
Final exit temperature from cooling tower (^{0}C)	10,53	10,53	10,53	10,53
Final plating bath temperature (^{0}C)	10,59	10,59	10,59	10,59
Total mass evaporated from the unsteady state temperature region (kg)	93,43	93,54	93,75	93,95
Total mass evaporated from the steady state temperature region (kg)	11,34	12,42	14,04	5,66

Figure 28 and Table 23 show that higher rates of evaporation are achieved at higher air flow rates until equilibrium is reached for the unsteady state temperature region. In the unsteady state temperature region evaporation occurs in the plating bath and the cooling tower, with significantly greater rates of evaporation occurring in the cooling tower. The rate of evaporation in the cooling tower is governed by the re-circulating plating solution flow rate and the entering and exiting temperatures of the plating solution, as detailed in equation (26).

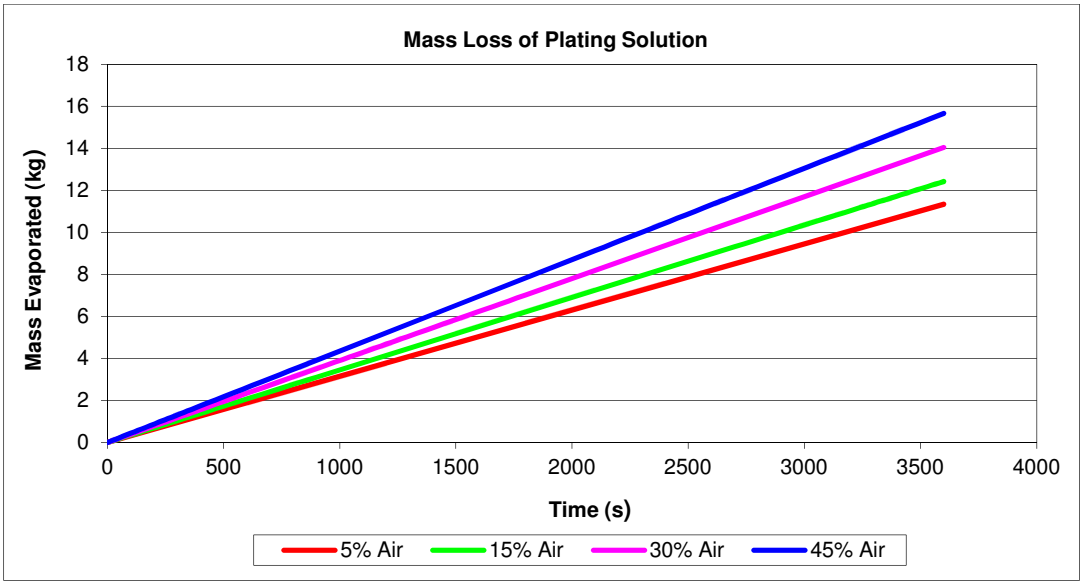

Figure 29: Effect of air flow rate on mass of water evaporated in the steady state temperature region

The higher the air flow rate the greater the rate of evaporation in the steady state temperature region as illustrated in Figure 29.

6.7 Effects of Ambient Air Temperature on the CCPS

To determine the effects of the ambient air temperature on the CCPS, weather data for the city of Durban in Kwa-Zulu Natal was used. The temperature data was monthly averages and was obtained from the BBC weather site[37]. The air temperature ranges and input data for the Matlab simulations are tabulated in Table 24.

Table 24: Input data for ambient air temperature sensitivity analysis

Factor	Run 1	Run 2	Run 3	Run 4
Zinc oxide (g/25ml)	0,83	0,83	0,83	0,83
Sodium hydroxide (g/25ml)	4,37	4,37	4,37	4,37
Dimension A (ml/25ml)	0,37	0,37	0,37	0,37
Dimension B (ml/25ml)	0,05	0,05	0,05	0,05
Dimension C (ml/25ml)	0,075	0,075	0,075	0,075
Conditioner (ml/25ml)	0,625	0,625	0,625	0,625
Plating solution flow rate (kg/s)	1	1	1	1
Air flow rate (kg/s)	1,2	1,2	1,2	1,2
Plating solution temperature (^{o}C)	32	32	32	32
Ambient air temperature (^{0}C)	11	15	19	23
% Relative humidity	70	70	70	70

6.7.1 Results

The results of the Matlab simulations are illustrated in Figures 30 to 33.

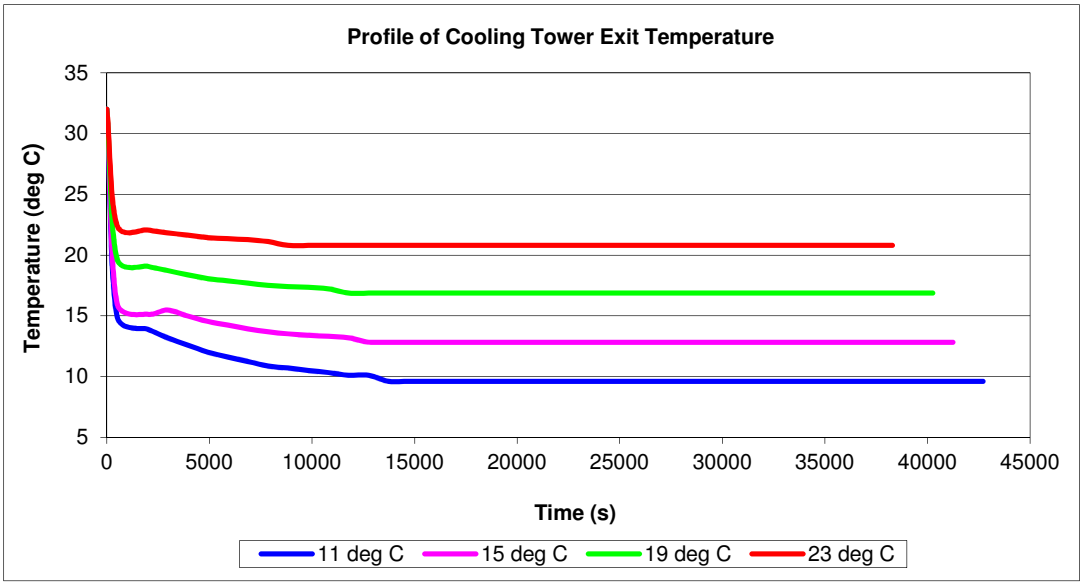

Figure 30: Effect of ambient air temperature on the plating solution exit temperature from the cooling tower.

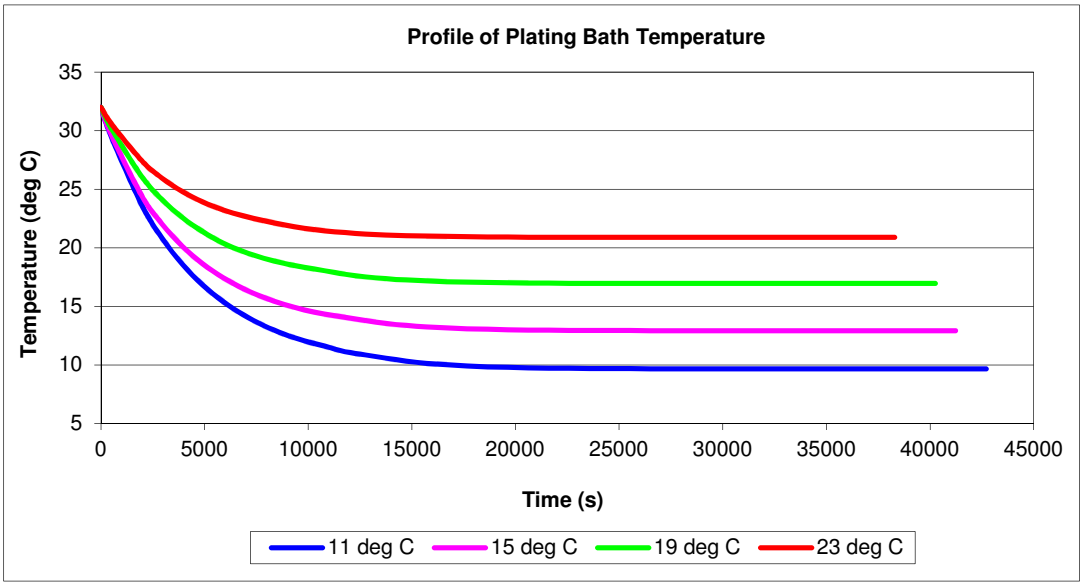

Figure 31: Effect of ambient air temperature on the plating bath temperature

Figures 30 and 31 shows that the lower the ambient air temperature the lower the equilibrium output temperatures from the cooling tower, T_{L2}, and the plating bath, T_{PB}, respectively. This was expected, as the lower the ambient air temperature the lower the wet bulb temperature. This results in a larger temperature gradient between the plating solution and the wet bulb temperature, thus facilitating heat transfer.

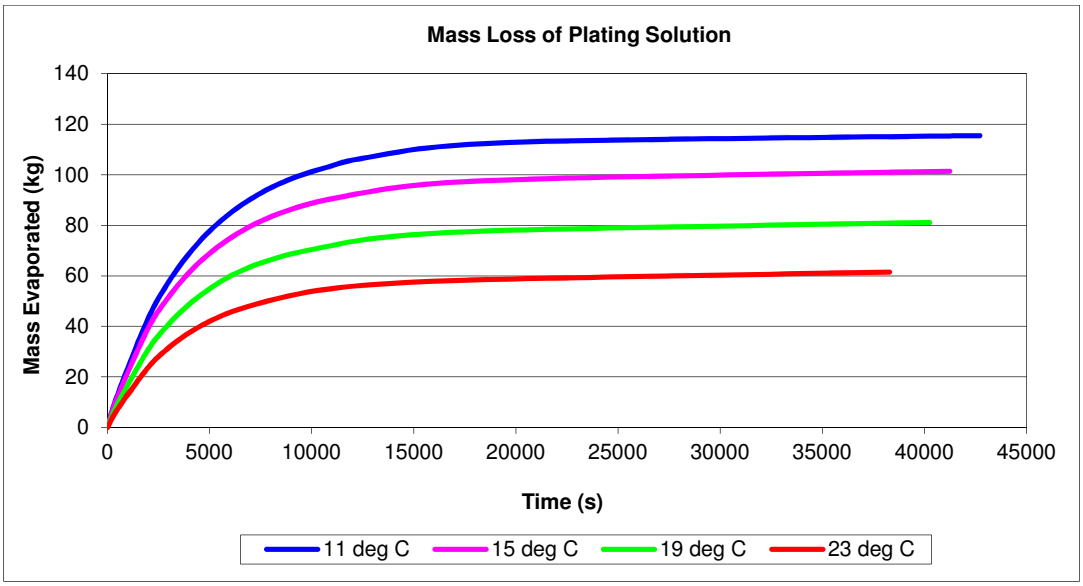

Figure 32: Effect of ambient air temperature on mass of water evaporated in the unsteady state temperature region

The lower the ambient air temperature, the greater the mass of water evaporated in the unsteady state temperature region as shown in Figure 32. The initial mass loss in the unsteady state temperature region is large but as the system reaches equilibrium the mass loss reduces. This is due to the minimisation of the plating solution temperature differential in the cooling tower, T_{L2}-T_{L1}, as shown in equation (26).

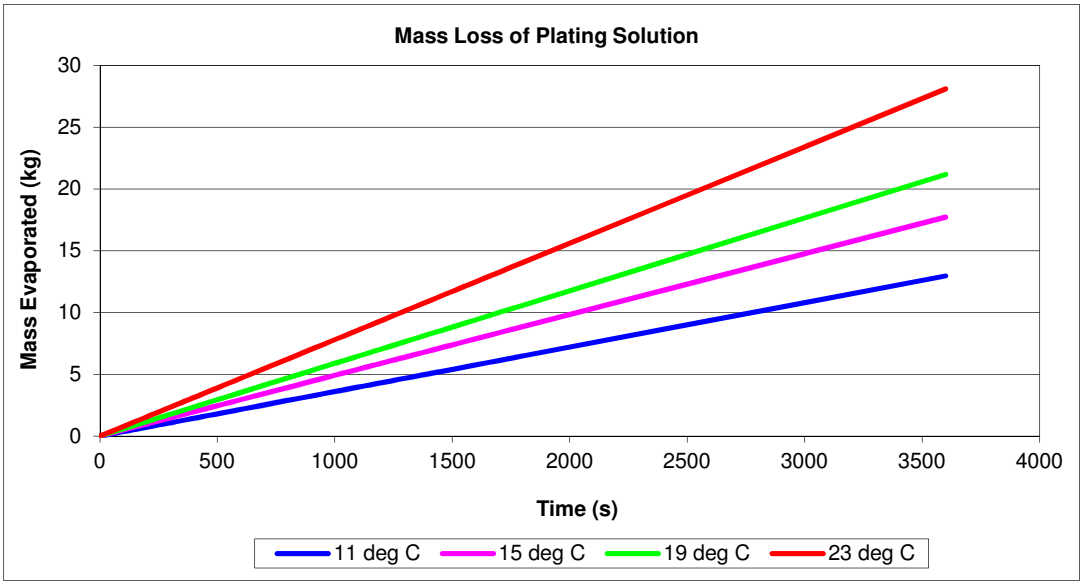

Figure 33: Effect of ambient air temperature on mass of water evaporated in the steady state temperature region

Figure 33 illustrates that the higher the ambient air temperature, the greater the evaporative loss in the steady state temperature region. This is due to the fact that the higher the ambient air temperature for a constant relative humidity, the greater the concentration gradient between the actual humidity and saturation humidity.

If temperatures lower than the actual ambient temperatures are required, air pre-cooling should be considered. The possible methods for air pre-cooling and their application are outside the scope of this study.

6.8 Effect of Packing Surface Area on the CCPS

To analyse the effects of packing surface area on the performance of a cooling tower, a range of packing surface areas valid for both structured and random packing were selected[33]. The packing surface area ranges and the CCPS model input conditions are tabulated in Table 25.

Table 25: Input data for packing surface area sensitivity analysis

Factor	Run 1	Run 2	Run 3	Run 4
Zinc oxide (g/25ml)	0,83	0,83	0,83	0,83
Sodium hydroxide (g/25ml)	4,37	4,37	4,37	4,37
Dimension A (ml/25ml)	0,37	0,37	0,37	0,37
Dimension B (ml/25ml)	0,05	0,05	0,05	0,05
Dimension C (ml/25ml)	0,075	0,075	0,075	0,075
Conditioner (ml/25ml)	0,625	0,625	0,625	0,625
Plating solution flow rate (kg/s)	1	1	1	1
Air flow rate (kg/s)	1,2	1,2	1,2	1,2
Packing surface area (m^2/m^3)	150	300	500	700
Plating solution temperature (^oC)	32	32	32	32
Ambient air temperature (^0C)	19	19	19	19

6.8.1 Results

The results of the Matlab analysis are illustrated in Figures 34 to 37.

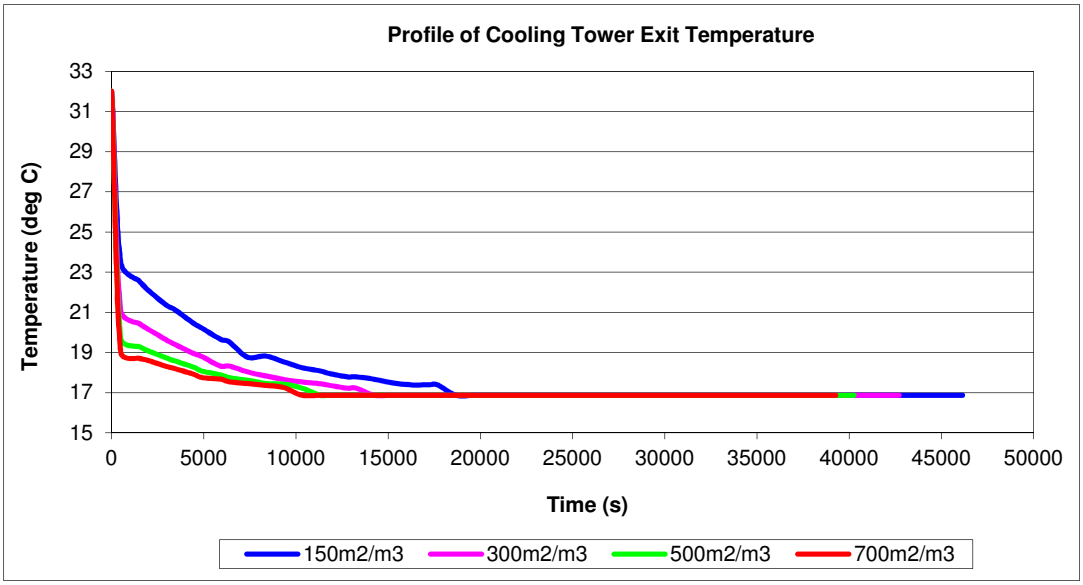

Figure 34: Effect of packing surface area on the plating solution exit temperature from the cooling tower.

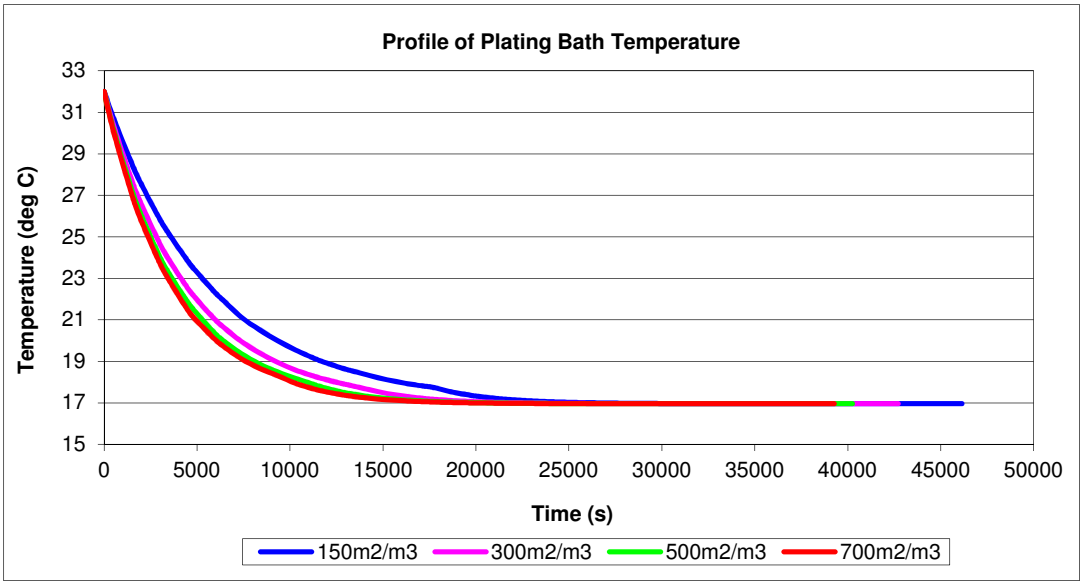

Figure 35: Effect of packing surface area on the plating bath temperature

Figures 34 and 35 show that the larger the packing surface area, the greater the temperature drop across the height of the cooling tower and the lower the plating bath temperature until equilibrium is reached, respectively.

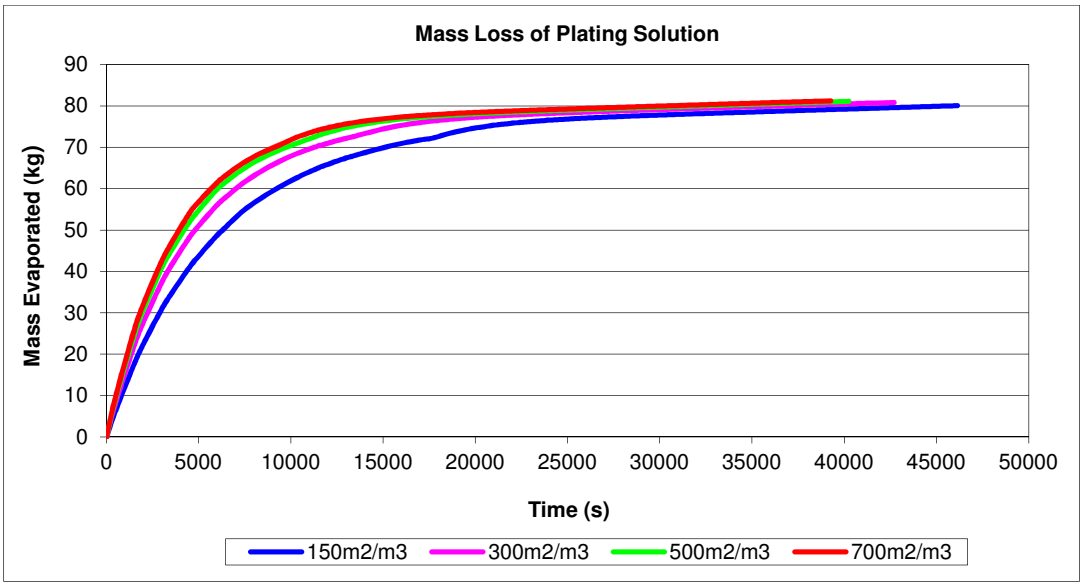

Figure 36: Effect of packing surface area on the mass of water evaporated from the unsteady state temperature region

From Figure 36 it can be seen that the larger the packing surface area, the greater the mass of water evaporated in the unsteady state region.

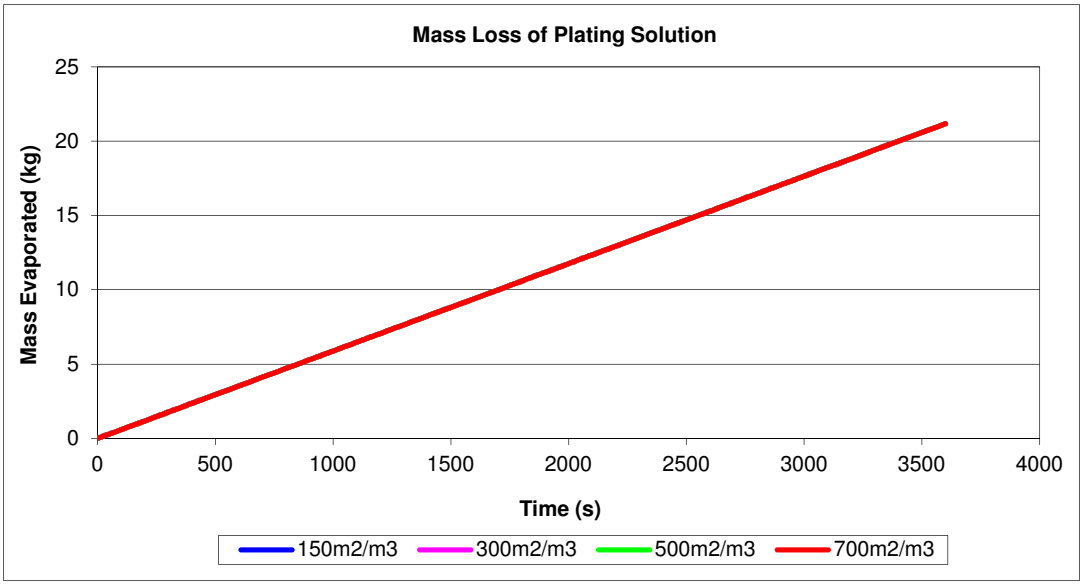

Figure 37: Effect of packing surface area on the mass evaporated from the steady state temperature region

Figure 37 illustrates that the packing surface area has no impact on the rate of evaporation in the steady state temperature region. In this region, the evaporation rates are governed by the humidity concentration gradient and air flow rate in the cooling tower.

Larger packing surface areas also reduce the required height and diameter of the cooling tower, which is especially significant in plating processes where space is limited. Thus the selection of the packing type should be based on the performance of the cooling tower, the cost of the packing and the space available.

6.9 Multiple Variable Analysis on the CCPS

In Sections 6.5 to 6.8 the effect of the individual key parameters on the CCPS was determined. In the practical application of the CCPS model, all the individual parameters will simultaneously have an effect on the CCPS. Thus the combined effect of the parameters on the CCPS was analysed. Table 26 details the input data for the Matlab simulations.

Table 26: Input data for multiple variable sensitivity analysis

Factor	Minimum	Mean	Maximum
Zinc oxide (g/25ml)	0,58	0,705	0,83
Sodium hydroxide (g/25ml)	3	3,68	4,37
Dimension A (ml/25ml)	0,2	0,28	0,37
Dimension B (ml/25ml)	0,006	0,028	0,05
Dimension C (ml/25ml)	0,025	0,05	0,075
Conditioner (ml/25ml)	0,37	0,5	0,62
Plating solution flow rate (kg/s)	3	3	3
Air flow rate (kg/s)	3,15	3,3	3,45
Temperature of plating bath (^{0}C)	32	32	32
Ambient air temperature (^{0}C)	19	15	11
Packing surface area (m^2/m^3)	250	500	700
% Relative humidity	70	70	70

6.9.1 Results

The results from the Matlab simulations are illustrated in Figures 38 to 41.

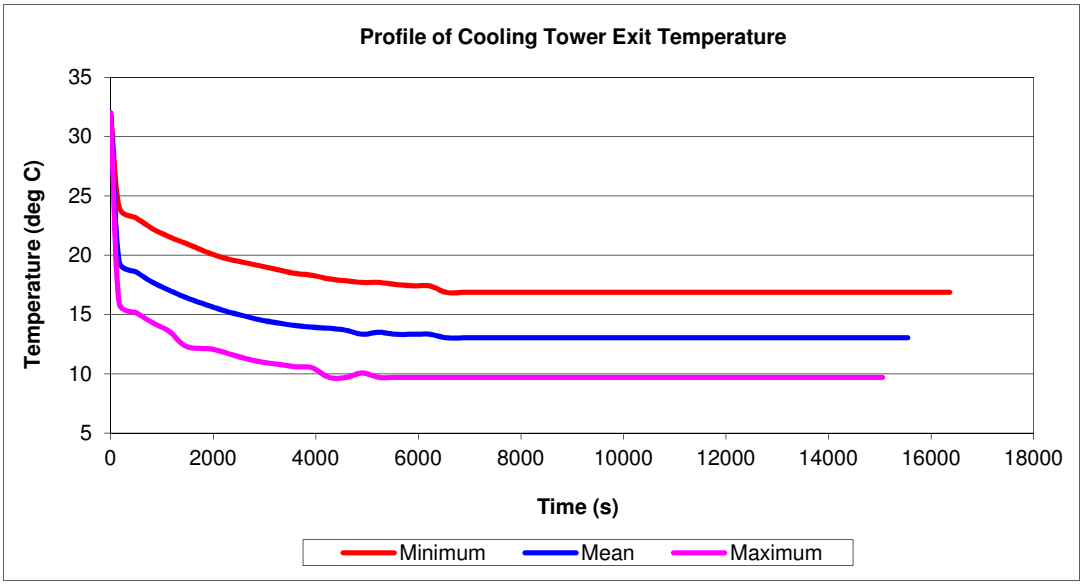

Figure 38: Effect of the combined parameters on the plating solution exit temperature from the cooling tower

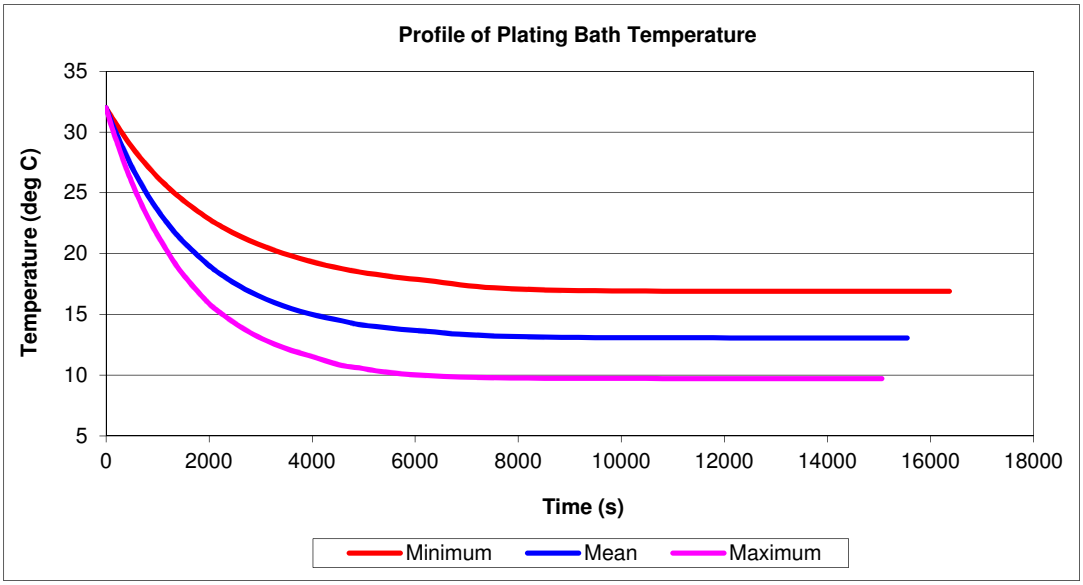

Figure 39: Effect of the combined parameters on the plating bath temperature

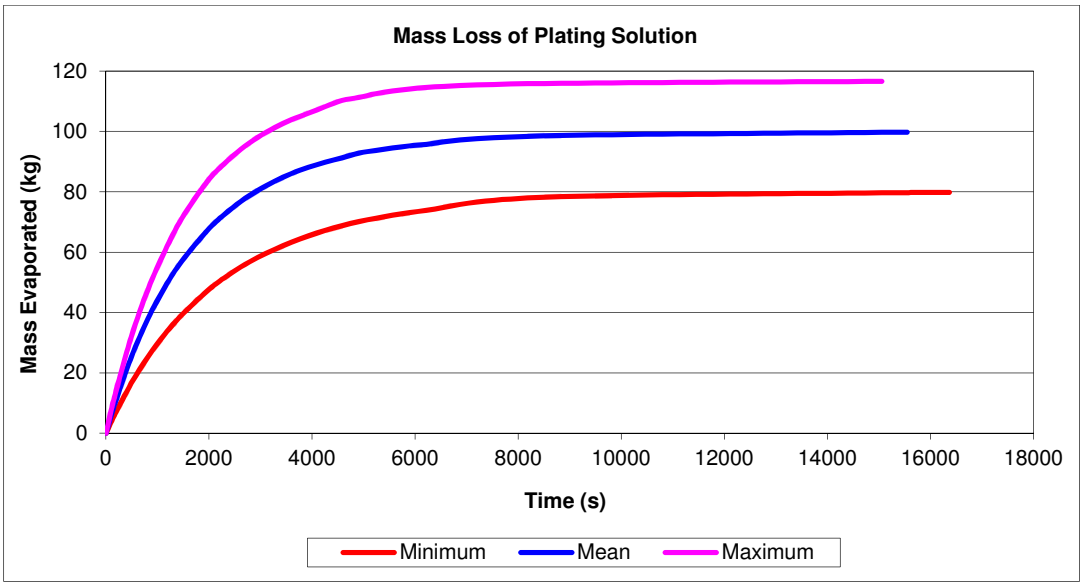

Figure 40: Effect of the combined parameters on the mass of water evaporated in the unsteady state temperature region.

From Figures 38 to 40 it can be seen that the maximum input conditions, as tabulated in Table 26 provide the optimum operating conditions for the CCPS. It provided the largest temperature drop across the height of the cooling tower, the minimum plating bath temperature and the maximum amount of water evaporation in the unsteady state temperature region.

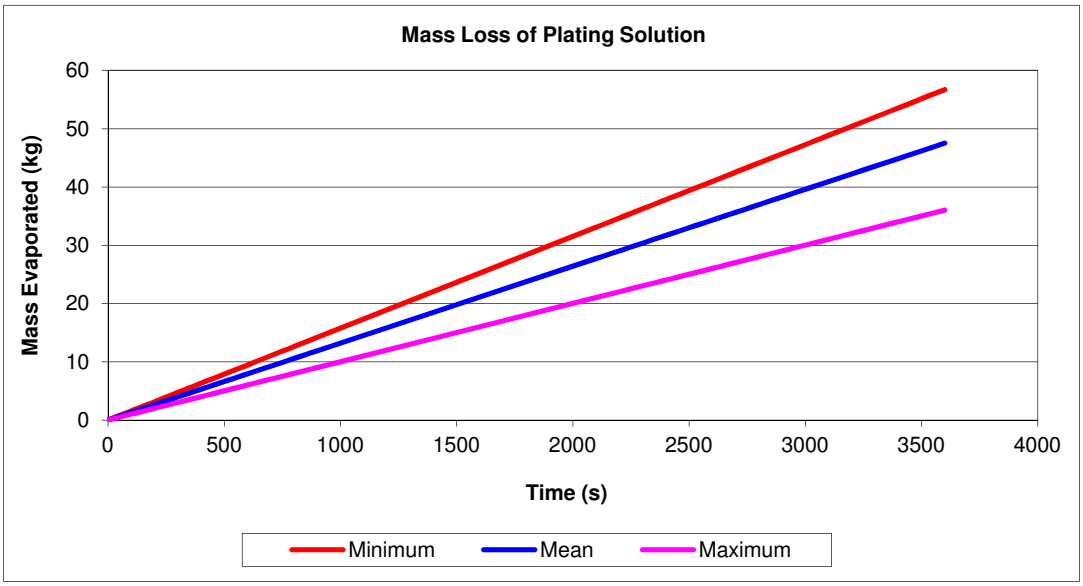

Figure 41: Effect of the combined parameters on the mass of water evaporated in the steady state temperature region.

In the steady state temperature region the minimum input conditions provided the maximum amount of water evaporation, as shown in Figure 41. This was

expected as the minimum operating conditions have the highest ambient air temperature, thus the largest humidity gradient, which facilitates greater rates of water evaporation in the steady state temperature region. However, the rates of water evaporation are significantly greater in the unsteady state temperature region as compared to the steady state temperature region. Thus, the maximum input conditions represent the ideal operational state of each of the parameters and are the optimum operating conditions of the CCPS.

6.10 Conclusion

The results of the sensitivity analysis performed on Matlab showed that the following conditions provided low cooling tower and plating bath temperatures and high rates of water evaporation in the unsteady state temperature region:

- Upper operational temperature limit of the plating solution
- High air flow rates
- Low ambient air temperatures
- Large packing surface areas

The only exception is that at low ambient air temperatures the rate of evaporation from the steady state temperature region is lower than that at higher ambient temperatures. However, as the rate of evaporation in the steady state temperature region is lower than that of the unsteady state temperature region and that the ambient temperature is the key factor in determining the final equilibrium temperatures of the plating bath and the cooling tower, lower ambient air temperatures are recommended.

CHAPTER 7: CONCLUSION AND RECOMMENDATIONS

7.1 Introduction

This master's study proposed the use of an induced draft evaporative cooling tower for close circuiting the three stage low flow counter current rinse electroplating process and reducing the rinse system waste water generation to almost zero. However, for the reduction of the rinse waste water generation to almost zero, the rate of water evaporation from the cooling tower and the plating bath had to be optimised to be equivalent to the rinse tank/s make-up water requirements.

For the optimisation of the operating conditions of the cooling tower and the plating bath, a CCPS mathematical model was developed. The CCPS mathematical model predicts the equilibrium temperatures and rate of water evaporation for both the cooling tower and plating bath. The CCPS model was programmed into Matlab and a sensitivity analysis was performed. The results of the sensitivity analysis identified the optimum operating conditions of the plating bath and cooling tower for the recovery of the rinse tank water in the plating bath, based on user specified input data.

7.2 CCPS Model Characteristics

The CCPS model was developed based on evaporative cooling theory and the mechanisms of heat and mass transfer from an open tank. The design basis of the CCPS model was:

- Water is the only diffusing component as ionic diffusion is very slow[30].
- Radiation heat transfer from the plating bath is negligible.
- Minimum plating solution specific input data.

The outputs from the model are:

- Equilibrium temperature of the cooling tower and plating bath
- Mass of water evaporated in the unsteady state and steady state temperature region

From literature and electroplating operational practices, the following were identified as key parameters affecting the performance of the CCPS.

- Plating solution composition and operational temperature
- Air flow rate through the cooling tower
- Ambient air temperature
- Cooling tower packing surface area

The effects of the key parameters on the CCPS were determined by:

- Individually varying each parameter
- Simultaneously varying all the parameters.

Thus based on user specific input data, the current operational status of the electroplating process can be identified and optimised to achieve the required evaporation rates for recovery of the rinse tank water in the plating bath. The electroplater can either individually and/or simultaneously vary all the key parameters to identify its operational status to achieve the required evaporation rates.

7.3 Model Results

The results of the sensitivity analysis of the CCPS model showed:

- The plating solution composition has a negligible effect on the final equilibrium temperatures of the plating bath and the cooling tower.
- The upper limit operational temperatures of the plating bath facilitates greater rates of evaporation from both the cooling tower and the plating bath.
- Higher air flow rates facilitate greater rates of water evaporation in the cooling tower and the plating bath for both the unsteady state and steady state temperature regions.
- Higher air flow rates result in a greater temperature drop across the height of the cooling tower until equilibrium is reached.
- Higher air flow rates result in a lower plating bath temperature until equilibrium is reached.

- The ambient air conditions are the controlling factor in the final equilibrium temperature of the plating bath and the cooling tower. The lower the ambient air temperature, the lower the equilibrium temperatures of the cooling tower and the plating bath.
- The lower the ambient air temperature, the greater the rate of evaporation in the unsteady state temperature region. In the steady state temperature region the higher the ambient air temperature, the higher the rate of evaporation for a constant relative humidity.
- Larger packing surface areas results in a greater temperature drop and evaporation rate across the height of the cooling tower until equilibrium is reached.

The above are the generic operational status of the key parameters for the recovery of the rinse system water in the plating bath. Based on user specific input data, the electroplater can identify specific operating points or ranges for the optimisation of the CCPS.

7.4 CCPS Model Limitation

The primary limitation of the CCPS model is that it is based on an air-water system. For the use of alternate cooling mediums, alternate saturation enthalpy-temperature data obtained either from literature or experimental methodology has to be inputted into the model.

7.5 Recommendation

The CCPS model was developed based on theoretical and experimental data and verified. It is recommended that the CCPS model be validated, either by the construction of a laboratory scale induced draft evaporative cooling tower or by the application of an induced draft evaporative cooling tower in an electroplating facility. For the validation, the experimental equilibrium temperatures and rates of evaporation have to be compared against that of the CCPS model and meet the pre-determined validation criteria.

REFERENCE

1. Reeve, J. D. 2006, Environmental improvements in the metal finishing industry in Australasia. *Journal of Cleaner Production* (online), 15(8-9):756-763. Available WWW": http://www.sciencedirect.com (Accessed June 2009).
2. Szafnicki, K., Bourgois, J., Graillot, D., Benedetto, D. D., Breuil, P. and Poyet, J. P. 1997, Real-time supervision of industrial waste water treatment plants applied to the surface treatment industries, Water Research, 32(8):2480-2490. Available WWW: http://www.sciencedirect.com (Accessed June 2009).
3. Qin, J-J., Wai, M-N., Oo, M-H. and Wong, F-S. 2002, A feasibility study on the treatment and recycling of a wastewater from metal plating. *Journal of Membrane Science* (online), 208(1-2):213-221. Available WWW: http://www.sciencedirect.com (Accessed June 2009).
4. Telukdarie, A., Buckley, C. and Koefoed, M. 2006. The importance of assessment tools in promoting cleaner production in the metal finishing industry. *Journal of Cleaner Production* (online), 14(18):1612-1621. Available WWW: http://www.sciencedirect.com (Accessed June 2009).
5. Fresner, J. 1998, Cleaner production as a means for effective environmental management. *Journal of Cleaner Production* (online) 6(3-4): Available WWW: http://www.sciencedirect.com (Accessed June 2009).
6. Katsumata, H., Kaneco, S., Inomata, K., Itoh, K., Funasaka, K., Masuyama, K., Suzuki, T and Ohta, K. 2003. Removal of heavy metals in rinsing waste water from plating factory by adsorption with economical viable material. *Journal of Environmental Management* (online), 69(2):187-191. Available WWW": http://www.sciencedirect.com (Accessed June 2009).
7. United States of America. U.S. Environmental Protection Agency, 1995. Profile of the Fabricated Metal Products Industry. Pittsburgh: U.S. Government Printing Office.
8. Hamid, N. H. AB and Idris, A. 1996. Towards a sludgeless heavy metal finishing industry for a cleaner environment. *Desalination* (online),106(1-3):411-413. Available WWW": http://www.sciencedirect.com (Accessed June 2009).
9. Fresner, J., Schnitzer, H., Gwehenberger, G., Planasch, M., Brunner, C., Taferner, K. and Mair, J. 2007. Practical experiences with the implementation of the concept of zero emissions in the surface treatment industry in Austria. *Journal of Cleaner Production* (online), 15(13-14):1228-1239. Available WWW: http://www.sciencedirect.com (Accessed June 2009).

10. Koefoed, M. and Buckley, C. 2008. Clean technology transfer: A case study from the South African metal finishing industry, 2002-2005. *Journal of Cleaner Production* (online), 16(1):S78-S84. Available WWW: http://www.sciencedirect.com (Accessed June 2009).
11. Telukdarie, A. 2007. Development of a hybrid fuzzy-mathematical cleaner production evaluation tool or surface finishing. D.Tech.:Chemical Engineering,, Durban University of Technology.
12. Viguri J. R., Andrés, A. and Irabien, A. 2002. Waste minimisation in a hard chromium plating small medium enterprise (SME). *Waste Management* (online), 22(28):931-936. Available WWW": http://www.sciencedirect.com (Accessed June 2009).
13. Alvarez-Aayuso, E., Garcia-Sanchez, A. and Querol, X. 2003. Purification of metal electroplating waste waters using zeolites. *Water Research* (online), 37(20):4855-4862. Available WWW: http://www.sciencedirect.com (Accessed June 2009).
14. Chai, X., Chen, G., Yue, P-L., and Mi, Y. 1997. Pilot scale membrane separation of electroplating wastewater by reverse osmosis. *Journal of Membrane Science* (online), 123(2):235-242. Available WWW: http://www.sciencedirect.com (Accessed June 2009).
15. Fu, F. and Wang, Q. 2011. Removal of heavy metal ions from wastewaters: A review. *Journal of Environmental Management* (online), 92(3): 407-418. Available WWW: http://www.sciencedirect.com (Accessed March 2011).
16. Christensen, E.R., and Delwiche, J.T. 1982. Removal of heavy metals from electroplating rinsewaters by precipitation, flocculation and ultrafiltration. *Water Research* (online), 16(5):729-737. Available WWW: http://www.sciencedirect.com (Accessed February 2011).
17. *Environmental Guidelines for Electroplating Industry* (online). Available WWW: http://www.miga.org/documents/ElectroplatingIndustry.pdf (Accessed January 2011)
18. *Conventional Treatment Technologies* (online). Available WWW: http://www.nmfrc.org/bluebook/sec622.htm (Accessed January 2011)
19. *Chapter 8 Wastewater Treatment Technologies* (online). Available WWW. http://water.epa.gov/scitech/wastetech/guide/treatment/upload/2000_12_19_cwt_final_develop_ch8.pdf (Accessed January 2011)
20. Morgan, S. M. and Lee, C .M. 1997. Metal and acid recovery options for the plating industry. *Resources, Conservation and Recycling*, 19(1):55-71. Available WWW: http://www.sciencedirect.com (Accessed June 2009).

21. Milosavljevic, N. and Heikkilä, P. 2001. A comprehensive approach to cooling tower design. *Applied Thermal Engineering* (online), 21(9): 899-915. Available WWW: http://www.sciencedirect.com (Accessed June 2009).
22. Qureshi, B. A. and Zubair, S. M. 2006. A complete model of wet cooling towers with fouling in fills. *Applied Thermal Engineering* (online), 26(16):1982-2989. Available WWW: http://www.sciencedirect.com (Accessed June 2009).
23. 2005. Electroplating Theory and Practice Manual. South African Metal Finishing Association, March 2007
24. Mohiuddin, A. K. M. and Kant, K. 1996. Knowledge base for the systematic design of wet cooling towers. Part I: Selection and tower characteristics. *International Journal of Refrigeration* (online), 19(1):43-51. Available WWW: http://www.sciencedirect.com (Accessed June 2009).
25. Kern, D. Q. 1999. *Process Heat Transfer*. 3RD Edition. New Delhi: Tata McGraw-Hill Publishing Company Limited.
26. Geankoplis, C. J. 1993. *Transport Processes and Unit Operations*. 3rd Edition. New Delhi: Prentice Hall Incorporation.
27. Welty, J. R., Wilson, R.E. and Wicks, C. E. 1976. *Fundamentals of Momentum, Heat and Mass Transfer*. 2nd Edition. United States of America:John Wiley and Sons.
28. Qi, X., Liu, Z. and Li, D. 2007. Performance characteristics of a shower cooling tower. *Energy Conversion and Management* (online), 48(1):193-203. Available WWW: http://www.sciencedirect.com (Accessed June 2009).
29. Jain, S., Dhar, P. L. and Kaushik, S. C. 2000. Experimental studies on the dehumidifier and regenerator of a liquid desiccant cooling system. *Applied Thermal Engineering* (online), 20(3): 253-267. Available WWW: http://www.sciencedirect.com (Accessed June 2009).
30. King, J. E. 1959. *Qualitative Analysis and Electrolytic Solutions*. Harcourt Brace Jovanovich.
31. Design Expert 8 Software, Available WWW: http://www.statease.com
32. Vallabh, S. 2005. Diffusion Coefficient Practical. Durban University of Technology: Department of Chemical Engineering. March 2005.
33. Perry, R. H. and Green, D. W. 1999. *Perry's Chemical Engineers' Handbook*. 7th Edition. United States of America: McGraw Hill.
34. Telukdarie, A. and Overcash, M. 2008. Heuristic based life cycle inventory for electroplating systems. *Journal of Applied Surface Finishing*. (Accessed October 2009).

35. Enthobrite NCZ dimension alkaline non-cyanide zinc plating process product data sheet. Chemserve Systems: Applied Metal Sciences Division. February 2007.
36. UBAC 101 bright acid copper plating process product data sheet. Chemserve Systems: Applied metal Sciences Division. February 2007.
37. BBC Weather Center (online). Available WWW: http://www.bbc.com (Accessed June 2010).

ANNEXURE A: MATLAB PROGRAM

Annexure A1: Construction of the saturation enthalpy-temperature curve

```
Temp = [8.33 9.00 10.00 11.00 12.00 13.00 14.00 15.00 16.00 17 18 19 20
21 22 23 24 25 26 27 28 29 30 31 32 33 34 35 36 37 38 39 40 41 42 43 44
45 46 47 48 49 50];
Hy = [25818.6 27214.2 29540.2 31866.2 34424.8 36983.4 39774.6 42333.2
45357 48380.8 51404.6 54661 57917.4 61406.4 65128 69082.2 73036.4
76990.6 81410 86062 90714 95598.6 100715.8 106065.6 111880.6
117695.6 123975.8 130488.6 137234 144444.6 151887.8 159796.2
167937.2 176776 185847.4 195616.6 205618.4 216318 227250.2 239578
251208 265164 279120];


p=polyfit(Temp,Hy,3);
A1=num2str(p(1));
B1=num2str(p(2));
C1=num2str(p(3));
D1=num2str(p(4));
fun01=strcat ('(',A1,')*x^3 + (',B1,')*x^2 +(',C1,')*x + (',D1,')');
Equilibrium=inline(char(fun01));
```

Annexure A2: Calculation of the gas phase mass transfer co-efficient

```
 TL2=32;
Ttank=32;
Ttank_K=Ttank+273.15;
Temperature_o=0;
T_output=[ ];
Time_run=[ ];
Ttankdata=[ ];
Mass_evaporated=[ ];
Time_run_2=[ ];
Initial_tank =3000;
```

```
time_20=2400;
total_mevp=0;
Temperature_change =1;
Mass_loss2=[ ];

for k=1:100
if abs(Temperature_change)>0.00001
P=101325.000;
TL2_K=TL2+273.15;
TL2_F=(1.8*TL2)+32;
Humidity=0.0074;
PA2=0.000; % Pa
MA_water = 18;
MB_air   = 29;
VA_water = 12.7;
VB_air  = 20.1;
P_atm = 1;
Diffusivity=
((1*10^(7))*(TL2_K^1.75)*(((1/MA_water)+(1/MB_air))^(1/2)))/(P_atm*(((VA_
water^(1/3))+( VB_air^(1/3)))^2));

A=+2.38;
B=+2.38;
C=+2.38;
D=+2.38;
 E=+2.38;
Change_height_capillary_tube_mm =((1/(7.08+(0.29*C)+(0.34*E)+(
0.61*A*D)+(0.77*B*C)+(-0.49*D*E)+(-0.41*(B^2))))^2);
Change_height_capillary_tube = Change_height_capillary_tube_mm /1000;

 PA0= exp(73.649+(-7258.2/TL2_K)+(
7.3037*log(TL2_K))+(0.00000416536*(TL2_K^2)));
MA_diff = 18;
R = 8314;
```

```
ID_cappillary_tube = 0.0026;
c_s_Area_cappillary =pi*(ID_cappillary_tube^2)/4;
x1 = 37/1000;
x2 = 16.5/100;
Diff_time = 24*3600;
PA1=PA2+((((MA_diff*PA0)/(R*TL2_K))*(c_s_Area_cappillary*Change_heigh
t_capillary_tube)*(x2x1))/(Diff_time*c_s_Area_cappillary*Diffusivity*(MA_diff/(
R*TL2_K))));
PB1=P-PA1;
PB2=P-PA2;
PBM=(PB2-PB1)/log(PB2/PB1);

Diameter=0.5;
c_s_Area=(pi*(Diameter^2))/4;
Gas_massflow rate=1.2;
G=Gas_massflowrate/c_s_Area;
TG1=12;
Density_air=1.238158273;
Viscosity=0.00001789;
Volumetric_flowrate=Gas_massflowrate/Density_air;
Velocity=Volumetric_flowrate/c_s_Area;
Reeynolds_number=Density_air*Velocity*Diameter/Viscosity;
Schmidt_number=Viscosity/(Density_air*Diffusivity);
Sherwood_number=0.023*(((Diameter*Velocity*Density_air)/Viscosity)^0.83)
*((Viscosity/(Density_air*Diffusivity))^0.33);
kc=(Sherwood_number*Diffusivity)/Diameter;
R=8314.000;
kg=(kc*P)/(R*(TG1+273.15)*PBM);
```

Annexure A3: Calculation of the wet bulb temperature

```
Water_massflowrate =1;
L=Water_massflowrate/c_s_Area;
Hy1=(1.005+1.88*Humidity)*10^3*(TG1-0)+2.501*10^6*Humidity;
min=A1*x^3 + B1*x^2 + C1*x + D1 - Hy1;
```

```
roots1=solve(min,x);
if isreal(roots1(1))==1
TL1_min=double(roots1(1));
elseif isreal(roots1(2))==1
TL1_min=double(roots1(2));
else
TL1_min=double(roots1(3));
end
```

Annexure A4: Calculation of cooling tower height from assumed T_{L1}

```
if TL1_min<TL2
A_1=[ ];
B_1=[ ];
C_1=[ ];
D_1=[ ];
Height=2.5;
for j=TL1_min:0.3:TL2
TL1=j;
cL=4187;
Slope_o=L*cL/G;
B=double(Hy1-Slope_o*TL1);
Slope_o_s=num2str(Slope_o);
B_s=num2str(B);
fun02=strcat('(',Slope_o_s,')*x+(',B_s,')');
Hy=inline(char(fun02));
a=500.000;
Mb=29.000;
hL=280.00;
Slope_i=-hL*a/(kg*a*Mb*P);
E_1=[ ];
F_1=[ ];
for i=TL1:0.3:TL2
T=i;
HY=double(Hy(T));
```

```
C=HY-Slope_i*T;
Slope_i_s=num2str(Slope_i);
C_s=num2str(C);
cross=A1*x^3+B1*x^2+C1*x+D1-(Slope_i_s*x+C_s);
roots2=solve(cross,x);
if isreal(roots2(1))==1
Hyi=double(Equilibrium(roots2(1)));
elseif isreal(roots2(2))==1
Hyi=double(Equilibrium(roots2(2)));
else
Hyi=double(Equilibrium(roots2(3)));
end
E_1=[E_1 HY];F_1=[F_1 1/(Hyi-HY)];
end
 [row col]=size(E_1);
if col>1
integ=trapz(E_1,F_1);
z=G/(Mb*kg*a*P)*integ;
else
z=0
end
if z<=Height & z>0
A_1=[A_1 TL1];B_1=[B_1 z];
elseif z>=Height & z>0
C_1=[C_1 TL1];D_1=[D_1 z];
end
end
[row1 col1]=size(A_1);
[row2 col2]=size(C_1);
if col2==0 | col1==0
Temperature_o=TL1_min
else
```

```
Temperature_o=((Height-D_1(col2))*A_1(1)+(B_1(1)-
Height)*C_1(col2))/(B_1(1)-D_1(col2));
end
else
Temperature_o=TL2;
end
T_output=[T_output Temperature_o]
T_output_K = Temperature_o+273.15;
```

Annexure A5: Calculation of plating bath temperature

```
Density_water=1000.000; % kg/m3
Volumetric_flowrate_water =Water_massflowrate /Density_water ;
Cooling_Time=(c_s_Area*Height)/Volumetric_flowrate_water;
Time_run=[Time_run k*Cooling_Time];
time_20=time_20+Cooling_Time;
Temperature_o_F=Temperature_o*1.8+32;

Water_massflow_gal_min=( Water_massflowrate*264.17*60)/Density_water;
Rate_of_EvapCT =0.00085*Water_massflow_gal_min*(TL2_F-
Temperature_o_F);
EvapCT= (Rate_of_EvapCT*3.758412)/60;
Mass_EvapCT=EvapCT*Cooling_Time;

T_amb= 12;
T_amb_K=T_amb+273.15 ;
T_ref=12;
T_ref_K =  T_ref+273.15
Tank_length =1.5;
Tank_width = 1.5;
Tank_height = 2;

Mass_Flowrate_hot_plating_soln =  Water_massflowrate
Surface_area_top_tank =  Tank_length*Tank_width;
```

```
Rate_of_Mass_EvapPT = 0.352*exp(-(7.2-0.032*((Ttank*(9/5))+32)));
EvapPT=(Rate_of_Mass_EvapPT*Surface_area_top_tank)/3600;
Mass_EvapPT=EvapPT*Cooling_Time;

Mass_Flowrate_Cold_Plating_Soln=Mass_Flowrate_hot_plating_soln-
(EvapCT);
Mass_Cold_Plating_Soln=Mass_Flowrate_Cold_Plating_Soln*Cooling_Time;
Mass_hot_plating_soln=Mass_Flowrate_hot_plating_soln*Cooling_Time;
Mass_time_2 =Mass_Cold_Plating_Soln - Mass_hot_plating_soln -
Mass_EvapPT + Initial_tank;

Thickness_metal_plate = 0.001;
Square_meter_metal_plate = 0.0025;
No_of_metal_pieces = 10;
Amperage_per_meter = 150;
Volts = 6;
Plating_time = 2400;
EELEC = ((( Amperage_per_meter*
Volts)*Square_meter_metal_plate*No_of_metal_pieces)*Cooling_Time)/100;

CP_plating_soln_leaving = 4.18;
ECPS =(Mass_Cold_Plating_Soln*CP_plating_soln_leaving*(T_output_K-
T_ref_K));

k_mild_steel = 0.19; %W/m.K
h_water = hL; %W/m2.K
h_air = 11.3;  %W/m2.K
Thickness_of_tank = 0.001; %m
Area_side_1 =Tank_length*Tank_height;       %m2
Q_side_1_W = ((Ttank-T_amb)/((1/(h_water* Area_side_1))+(
Thickness_of_tank /( k_mild_steel*Area_side_1 ))+(1/(
h_air*Area_side_1))))*2;
Q_side_1_KW =Q_side_1_W /1000;          % KW
```

```
k_mild_steel = 0.19; %W/m.K
h_water = hL; %W/m2.K
h_air = 11.3;  %W/m2.K
Thickness_of_tank = 0.001; %m
Area_side_2 = Tank_width*Tank_height;       %m2
Q_side_2_W = ((Ttank-T_amb)/((1/(h_water* Area_side_2))+(
Thickness_of_tank /( k_mild_steel*Area_side_2 ))+(1/(
h_air*Area_side_2))))*2;
Q_side_2_KW =Q_side_2_W /1000;  % KW

k_mild_steel = 0.19; %W/m.K
h_water = hL; %W/m2.K
h_air = 11.3;  %W/m2.K
Area_side_3 = Tank_width*Tank_length;       %m2
Q_side_3_W = (Ttank-T_amb)/((1/(h_water* Area_side_3))+(
Thickness_of_tank /( k_mild_steel*Area_side_3 ))+(1/(  h_air*Area_side_3)));
Q_side_3_KW = Q_side_3_W/1000; %KW

Area_side_4 = Tank_width*Tank_length; %m2
h_air = 11.3;  %W/m2.K
Q_side_4_W =  h_air*Area_side_4*(Ttank-T_amb);
Q_side_4_KW = Q_side_4_W/1000;  %KW

ECONDCONV=(Q_side_1_KW+Q_side_2_KW+Q_side_3_KW+Q_side_4_K
W)*Coolin_Time;

T_Critical=647.3;
TR = Ttank_K/T_Critical;
W1= 52053000;
W2=0.3199;
W3=-0.212;
W4=0.25795;
Heat_vapourisation_Jkmol= W1*((1-TR)^( W2+(W3*TR)+(W4*(TR^2))));
Heat_vapourisation_KJkg=(Heat_vapourisation_Jkmol)/(18*1000);
```

```
EEVAP=Mass_EvapPT* Heat_vapourisation_KJkg;
 CP_plating_tank_soln = 4.18;
CP_hot_plating_soln = 4.18;

if time_20<2400
T_plating_tank_K = (ECPS + EELEC - ECONDCONV - EEVAP +
(Mass_hot_plating_soln*CP_plating_tank_soln*T_ref_K)+(Mass_time_2*CP_
plating_tank_soln*T_ref_K)+(Initial_tank*CP_plating_tank_soln*(Ttank_KT_r
ef_K)))/((Mass_time_2*CP_plating_tank_soln)+(Mass_hot_plating_soln*CP_
plating_tank_soln))

else
Density_metal_piece= 7801;
CP_metal_piece = 0.473;      %KJ/kg.K
ECMP = ((Density_metal_piece*CP_metal_piece*Thickness_metal_plate*
Square_meter_metal_plate*(Ttank_K- T_amb_K)))*No_of_metal_pieces;
T_plating_tank_K = (ECPS + EELEC + ECMP -EEVAP - ECONDCONV +
(Mass_hot_plating_soln*CP_plating_tank_soln*T_ref_K)+(Mass_time_2*CP_
plating_tank_soln*T_ref_K)+(Initial_tank*CP_plating_tank_soln*(Ttank_K-
T_ref_K)))/((Mass_time_2*CP_plating_tank_soln)+(Mass_hot_plating_soln*C
P_plating_tank_soln))
time_20=0;
end

T_plating_tank_degC = T_plating_tank_K -273.15 ;
Temperature_change=Ttank-T_plating_tank_degC
Ttank =  T_plating_tank_degC;
Ttank_K=   T_plating_tank_degC+273.15;
Ttankdata=[Ttankdata Ttank];
TL2 = T_plating_tank_degC;
total_mevp=total_mevp+ Mass_EvapPT+ Mass_EvapCT;
Mass_evaporated=[Mass_evaporated total_mevp];
Initial_tank=Mass_time_2
```

```
end
end
```

Annexure A6: Calculation of mass evaporated in the steady state temperature region

```
Lo_1=[ ];
Lo_T=0;
 X1= 0.0074;
X2=0.0104;
for t=300:300:3600
Time_run_2=[Time_run_2 t];
Gas_massflowrate=1.2;
Diameter =0.5;
c_s_Area=(pi*(Diameter^2))/4;
G=Gas_massflowrate/c_s_Area;
Steady_mass=G*(X2-X1)*c_s_Area*300;
Tank_length =1.5;
Tank_width = 1.5;
Tank_height = 2;
Surface_area_top_tank2 =  Tank_length*Tank_width;
Rate_of_Mass_EvapPT2 = 0.352*exp(-(7.2-0.032*((Ttank*(9/5))+32)));
EvapPT2=(Rate_of_Mass_EvapPT2*Surface_area_top_tank)/3600;
Mass_EvapPT2=EvapPT2*300;
Mass_total=Mass_EvapPT2+Steady_mass;
Lo_1=[Lo_1 Mass_total];
Lo_T=Lo_T+Mass_total;
Mass_loss2=[Mass_loss2 Lo_T];
end
```

ANNEXURE B: GAS DIFFUSION EXPERIMENTAL RESULTS

Annexure B1: Zinc plating solution gas diffusion experimental results

Table 27: Diffusion experimental results for the zinc plating solution

Run No	Run Type	Initial Height	Final Height	Run No	Run Type	Initial Height	Final Height
Run 1	Actual	36.7511	36.7379	Run 2	Actual	37.2666	37.2088
	Repeat	36.595	36.5812		Repeat	36.6183	36.5607
Run 3	Actual	36.9244	36.9169	Run 4	Actual	36.8551	36.7669
	Repeat	36.7284	36.7206		Repeat	36.4449	36.3564
Run 5	Actual	36.6756	36.6472	Run 6	Actual	36.5486	36.5363
	Repeat	36.7325	36.7039		Repeat	36.6794	36.6667
Run 7	Actual	36.7822	36.7567	Run 8	Actual	36.8031	36.7827
	Repeat	37.4333	37.4085		Repeat	36.5411	36.5206
Run 9	Actual	36.7891	36.7812	Run 10	Actual	37.6153	37.5893
	Repeat	36.8571	36.8495		Repeat	36.7551	36.7287
Run 11	Actual	37.6414	37.5994	Run 12	Actual	36.897	36.85
	Repeat	37.0082	36.9664		Repeat	36.6438	36.5964
Run 13	Actual	36.8564	36.838	Run 14	Actual	36.6659	36.5393
	Repeat	36.7469	36.7289		Repeat	37.3309	37.2045
Run 15	Actual	36.8325	36.8172	Run 16	Actual	37,6415	37,5989
	Repeat	36.8595	36.8439		Repeat	37,0094	36,9654
Run 17	Actual	36.5492	36.5356	Run 18	Actual	36.7854	36.7561
	Repeat	37.2599	37.2461		Repeat	36.64	36.6121
Run 19	Actual	37.7063	37.6761	Run 20	Actual	36.7461	36.7335
	Repeat	36.9426	36.9126		Repeat	36.5993	36.5864
Run 21	Actual	37.5348	37.5229	Run 22	Actual	36.5992	36.5855
	Repeat	36.7016	36.6895		Repeat	37.343	37.3286
Run 23	Actual	36.7688	36.7534	Run 24	Actual	36.6038	36.5884
	Repeat	36.6592	36.6442		Repeat	37.2954	37.2798
Run 25	Actual	36.6542	36.6187	Run 26	Actual	37.2669	37.2085
	Repeat	36.8664	36.8315		Repeat	36.6182	36.5609
Run 27	Actual	36.7554	36.7258	Run 28	Actual	36.8865	36.8567
	Repeat	37.0129	36.9835		Repeat	36.5653	36.5359

Run No	Run Type	Initial Height	Final Height	Run No	Run Type	Initial Height	Final Height
Run 29	Actual	37.5311	37.5144	Run 30	Actual	36.7679	36.7459
	Repeat	36.937	36.9209		Repeat	36.6091	36.5868
Run 31	Actual	36.5759	36.5476	Run 32	Actual	36.684	36.6538
	Repeat	36.4329	36.404		Repeat	37.333	37.3032
Run 33	Actual	37.3319	37.2896	Run 34	Actual	36.7896	36.7657
	Repeat	37.1082	37.0654		Repeat	36.8283	36.8039
Run 35	Actual	37.6428	37.6002	Run 36	Actual	36.484	36.454
	Repeat	36.9096	36.8674		Repeat	37.339	37.3079
Run 37	Actual	37.4931	37.4727	Run 38	Actual	37.6931	37.673
	Repeat	36.5305	36.5104		Repeat	36.7303	36.7106
Run 39	Actual	36.394	36.3638	Run 40	Actual	36.8885	36.8587
	Repeat	37.1328	37.1035		Repeat	36.5673	36.5379
Run 41	Actual	37.1672	37.1085	Run 42	Actual	36.4968	36.4598
	Repeat	36.3179	36.2607		Repeat	36.6438	36.6065
Run 43	Actual	36.7633	36.7494	Run 44	Actual	36.3603	36.3372
	Repeat	36.5461	36.5315		Repeat	36.4452	36.4217
Run 45	Actual	36.8358	36.8102	Run 46	Actual	37.5412	37.4985
	Repeat	36.629	36.6044		Repeat	37.0089	36.965
Run 47	Actual	37.442	37.4154	Run 48	Actual	36.284	36.2532
	Repeat	36.789	36.7614		Repeat	37.3327	37.3029
Run 49	Actual	37.4149	37.3898	Run 50	Actual	36.7705	36.7475
	Repeat	36.7549	36.7292		Repeat	36,7451	36,7219

Annexure B2: Copper plating solution gas diffusion experimental results

Table 28: Diffusion experimental results for the copper plating solution

Run No	Run Type	Initial Height	Final Height	Run No	Run Type	Initial Height	Final Height
Run 1	Actual	36.0193	36.013	Run 2	Actual	36.7278	36.7225
	Repeat	36.6961	36.6901		Repeat	36.3523	36.347
Run 3	Actual	35.8688	35.8604	Run 4	Actual	36.5293	36.5118
	Repeat	36.6071	36.5985		Repeat	36.6925	36.6748
Run 5	Actual	37.4298	37.4196	Run 6	Actual	36.5862	36.5796

Run No	Run Type	Initial Height	Final Height	Run No	Run Type	Initial Height	Final Height
	Repeat	36.3529	36.3425		Repeat	36.3333	36.3265
Run 7	Actual	35.8135	35.8088	Run 8	Actual	36.6189	36.6119
	Repeat	37.52	37.5153		Repeat	36.7813	36.774
Run 9	Actual	37.1851	37.1779	Run 10	Actual	35.6464	35.6337
	Repeat	36.5364	36.529		Repeat	36.3842	36.3716
Run 11	Actual	36.5646	36.5595	Run 12	Actual	36.4479	36.4425
	Repeat	36.5437	36.5384		Repeat	35.8415	35.8361
Run 13	Actual	36.8801	36.8709	Run 14	Actual	35.7219	35.6938
	Repeat	36.7237	36.7144		Repeat	36.5123	36.484
Run 15	Actual	35.8377	35.811	Run 16	Actual	36.8091	36.7999
	Repeat	36.6754	36.6481		Repeat	36.1528	36.1435
Run 17	Actual	35.865	35.8609	Run 18	Actual	36.6675	36.506
	Repeat	36.7052	36.7009		Repeat	36.7997	36.6379
Run 19	Actual	35.9483	35.9424	Run 20	Actual	36.8987	36.8907
	Repeat	36.7293	36.7233		Repeat	36.233	36.2249
Run 21	Actual	36.7489	36.7404	Run 22	Actual	36.6317	36.6123
	Repeat	36.6991	36.6904		Repeat	36.5022	36.4829
Run 23	Actual	36.7079	36.6695	Run 24	Actual	36.4962	36.4632
	Repeat	36.1943	36.1557		Repeat	36.8097	36.7757
Run 25	Actual	36.4444	36.4364	Run 26	Actual	37.1529	37.1487
	Repeat	35.9677	35.9598		Repeat	36.8432	36.839
Run 27	Actual	35.8533	35.844	Run 28	Actual	37.2831	37.279
	Repeat	36.5417	36.5323		Repeat	36.5236	36.5193
Run 29	Actual	36.5919	36.5917	Run 30	Actual	36.4915	36.4863
	Repeat	36.5041	36.5039		Repeat	36.8686	36.8632
Run 31	Actual	37.5199	37.5139	Run 32	Actual	36.5072	36.5024
	Repeat	36.7343	36.7281		Repeat	36.4414	36.4365
Run 33	Actual	36.5249	36.5194	Run 34	Actual	36.7088	36.6538
	Repeat	36.4753	36.4697		Repeat	36.756	36.699
Run 35	Actual	36.8953	36.895	Run 36	Actual	37.8943	37.8903
	Repeat	36.7964	36.7961		Repeat	35.869	35.8649
Run 37	Actual	36.5192	36.4998	Run 38	Actual	37.1737	37.1695
	Repeat	37.6493	37.6297		Repeat	37.4646	37.4602

Run No	Run Type	Initial Height	Final Height	Run No	Run Type	Initial Height	Final Height
Run 39	Actual	36.6552	36.6492	Run 40	Actual	37.1969	37.1964
	Repeat	36.5223	36.5222		Repeat	36.694	36.6934
Run 41	Actual	35.5754	35.5703	Run 42	Actual	36.6645	36.6483
	Repeat	35.8509	35.8457		Repeat	35.6596	35.6433
Run 43	Actual	36.6	36.591	Run 44	Actual	36.8724	36.8525
	Repeat	36.6609	36.6517		Repeat	36.8485	36.8284
Run 45	Actual	36.8439	36.8314	Run 46	Actual	35.8922	35.8893
	Repeat	36.6652	36.6522		Repeat	36.7375	36.7346
Run 47	Actual	36.8065	36.8006	Run 48	Actual	35.8738	35.8641
	Repeat	35.9313	35.9253		Repeat	36.6653	36.6557
Run 49	Actual	35.6949	35.6869	Run 50	Actual	36.6592	36.6548
	Repeat	37.5702	37.562		Repeat	36.8345	36.83

ANNEXURE C: OPTIMISATION OF THE QUADRATIC EQUATION FOR THE PREDICTION OF WATER DIFFUSION FROM A ZINC PLATING SOLUTION

Table 29: Results of the optimisation of the quadratic equation for the prediction of water diffusion from a zinc plating solution

Std Run	Actual Result	Original Model	% Difference between Original Model and Actual Result	Model 1	% Difference between Model 1 and Actual Result	Model 2	% Difference between Model 2 and Actual Result	Model 3	% Difference between Model 3 and Actual Result	Model 4	% Difference between Model 4 and Actual Result
1	0.0584	0.0522	10.54	0.0541	7.39	0.0357	38.81	0.0551	5.64	0.0575	1.53
2	0.0370	0.0324	12.35	0.0328	11.30	0.0236	36.23	0.0333	10.00	0.0344	6.97
3	0.0260	0.0305	14.72	0.0293	11.33	0.0214	17.55	0.0297	12.54	0.0307	15.23
4	0.0251	0.0210	16.44	0.0201	20.07	0.0154	38.52	0.0203	19.16	0.0208	17.04
5	0.0283	0.0324	12.67	0.0333	15.01	0.0214	24.25	0.0338	16.25	0.0253	10.69
6	0.0427	0.0221	48.34	0.0223	47.83	0.0154	63.86	0.0225	47.20	0.0177	58.48
7	0.1266	0.0683	46.07	0.0644	49.12	0.0357	71.77	0.0657	48.07	0.0443	64.99
8	0.0355	0.0399	11.07	0.0376	5.48	0.0236	33.53	0.0381	6.94	0.0281	20.96
9	0.0300	0.0306	2.02	0.0323	7.26	0.0236	21.35	0.0319	5.92	0.0246	17.85
10	0.0882	0.0504	42.82	0.0531	39.81	0.0357	59.48	0.0521	40.90	0.0377	57.25
11	0.0298	0.0000	100.00	0.0000	100.00	0.0154	48.22	0.0000	100.00	0.0556	46.43
12	0.0423	0.0297	29.85	0.0289	31.62	0.0214	49.32	0.0285	32.54	0.0223	47.18

Std Run	Actual Result	Original Model	% Difference between Original Model and Actual Result	Model 1	% Difference between Model 1 and Actual Result	Model 2	% Difference between Model 2 and Actual Result	Model 3	% Difference between Model 3 and Actual Result	Model 4	% Difference between Model 4 and Actual Result
13	0.0204	0.0130	36.34	0.0135	34.03	0.0154	24.36	0.0133	34.64	0.0139	31.99
14	0.0137	0.0177	22.67	0.0183	24.98	0.0214	36.09	0.0181	24.17	0.0189	27.59
15	0.0153	0.0201	24.02	0.0199	23.31	0.0236	35.16	0.0197	22.44	0.0207	26.10
16	0.0231	0.0299	22.69	0.0291	20.68	0.0357	35.36	0.0287	19.59	0.0305	24.16
17	0.0578	0.0228	60.57	0.0232	59.92	0.0287	50.30	0.0235	59.43	0.0241	58.28
18	0.0239	0.0192	19.58	0.0194	18.84	0.0236	1.27	0.0196	17.93	0.0201	15.82
19	0.0293	0.0183	37.45	0.0178	39.32	0.0214	26.84	0.0180	38.67	0.0184	37.17
20	0.0075	0.0136	44.98	0.0132	42.97	0.0154	51.40	0.0133	43.49	0.0136	44.66
21	0.0139	0.0192	27.64	0.0196	29.14	0.0214	35.16	0.0198	29.93	0.0158	12.15
22	0.0201	0.0142	29.37	0.0143	28.81	0.0154	23.23	0.0144	28.13	0.0119	40.83
23	0.0296	0.0332	10.88	0.0319	7.17	0.0357	17.17	0.0323	8.50	0.0243	17.78
24	0.0230	0.0225	2.12	0.0215	6.52	0.0236	2.53	0.0218	5.42	0.0172	25.32
25	0.0284	0.0341	16.72	0.0361	21.42	0.0236	16.92	0.0356	20.22	0.0271	4.43
26	0.0266	0.0580	54.12	0.0613	56.58	0.0357	25.56	0.0601	55.72	0.0425	37.43
27	0.0256	0.0218	14.70	0.0216	15.52	0.0154	39.72	0.0214	16.51	0.0173	32.55
28	0.0302	0.0330	8.48	0.0321	5.97	0.0214	29.02	0.0317	4.62	0.0245	18.91

Std Run	Actual Result	Original Model	% Difference between Original Model and Actual Result	Model 1	% Difference between Model 1 and Actual Result	Model 2	% Difference between Model 2 and Actual Result	Model 3	% Difference between Model 3 and Actual Result	Model 4	% Difference between Model 4 and Actual Result
29	0.0079	0.0139	43.26	0.0144	45.31	0.0154	48.81	0.0143	44.79	0.0149	47.01
30	0.0426	0.0192	54.88	0.0198	53.43	0.0214	49.68	0.0196	53.95	0.0206	51.68
31	0.0470	0.0220	53.26	0.0218	53.71	0.0236	49.80	0.0215	54.26	0.0226	51.89
32	0.0420	0.0332	20.86	0.0323	22.98	0.0357	14.92	0.0319	24.08	0.0339	19.25
33	0.0119	0.0197	39.50	0.0199	40.35	0.0199	40.35	0.0199	40.35	0.0199	40.35
34	0.0132	0.0197	32.90	0.0199	33.83	0.0199	33.83	0.0199	33.83	0.0199	33.83
35	0.0302	0.0403	25.06	0.0442	31.64	0.0442	31.64	0.0442	31.64	0.0442	31.64
36	0.0426	0.0486	12.43	0.0442	3.58	0.0442	3.58	0.0442	3.58	0.0442	3.58
37	0.0298	0.0245	17.81	0.0245	17.81	0.0199	33.06	0.0245	17.81	0.0245	17.81
38	0.0184	0.0166	9.98	0.0166	9.98	0.0199	7.77	0.0166	9.98	0.0166	9.98
39	0.0136	0.0205	33.65	0.0199	31.83	0.0199	31.83	0.0205	33.65	0.0199	31.83
40	0.0154	0.0194	20.72	0.0199	22.81	0.0199	22.81	0.0194	20.72	0.0199	22.81
41	0.0302	0.0530	42.99	0.0530	42.99	0.0199	33.94	0.0530	42.99	0.0254	15.79
42	0.0308	0.0281	8.70	0.0281	8.70	0.0199	35.23	0.0281	8.70	0.0161	47.83
43	0.0587	0.0199	66.01	0.0199	66.01	0.0199	66.01	0.0199	66.01	0.0199	66.01
44	0.0154	0.0199	22.81	0.0199	22.81	0.0199	22.81	0.0199	22.81	0.0199	22.81

Std Run	Actual Result	Original Model	% Difference between Original Model and Actual Result	Model 1	% Difference between Model 1 and Actual Result	Model 2	% Difference between Model 2 and Actual Result	Model 3	% Difference between Model 3 and Actual Result	Model 4	% Difference between Model 4 and Actual Result
45	0.0167	0.0199	16.29	0.0199	16.29	0.0199	16.29	0.0199	16.29	0.0199	16.29
46	0.0126	0.0199	36.84	0.0199	36.84	0.0199	36.84	0.0199	36.84	0.0199	36.84
47	0.0123	0.0199	38.34	0.0199	38.34	0.0199	38.34	0.0199	38.34	0.0199	38.34
48	0.0255	0.0199	21.77	0.0199	21.77	0.0199	21.77	0.0199	21.77	0.0199	21.77
49	0.0204	0.0199	2.21	0.0199	2.21	0.0199	2.21	0.0199	2.21	0.0199	2.21
50	0.0220	0.0199	9.32	0.0199	9.32	0.0199	9.32	0.0199	9.32	0.0199	9.32
Average % Difference			**28.18**		**28.28**		**32.08**		**28.17**		**29.17**
Max % Difference			**100.00**		**100.00**		**71.77**		**100.00**		**66.01**
Min % Difference			**2.02**		**2.21**		**1.27**		**2.21**		**1.53**

Table 30: Results of the optimisation of the quadratic equation for the prediction of water diffusion from a zinc plating solution continued

Std Run	Actual Result	Model 5	% Difference between Model 5 and Actual Result	Model 6	% Difference between Model 6 and Actual Result	Model 7	% Difference between Model 7 and Actual Result	Model 8	% Difference between Model 8 and Actual Result	Model 9	% Difference between Model 9 and Actual Result
1	0.0584	0.0656	10.95	0.0491	16.00	0.0528	9.67	0.0546	6.57	0.0460	21.32
2	0.0370	0.0387	4.40	0.0500	25.97	0.1233	69.99	0.0336	9.31	0.0293	20.84
3	0.0260	0.0362	28.15	0.0291	10.50	0.0567	54.14	0.0295	11.90	0.0276	5.87
4	0.0251	0.0241	3.79	0.0295	14.83	0.0324	22.63	0.0204	18.67	0.0193	23.04
5	0.0283	0.0275	2.66	0.0227	19.73	0.0345	18.09	0.0335	15.60	0.0361	21.55
6	0.0427	0.0193	54.86	0.0230	46.12	0.0369	13.66	0.0227	46.87	0.0241	43.58
7	0.1266	0.0542	57.22	0.0415	67.20	0.0826	34.78	0.0650	48.62	0.0799	36.86
8	0.0355	0.0334	6.03	0.0423	15.98	0.3258	89.10	0.0385	7.70	0.0450	21.08
9	0.0300	0.0261	12.86	0.0322	6.76	0.0755	60.25	0.0316	5.21	0.0277	7.56
10	0.0882	0.0413	53.22	0.0327	62.97	0.1049	15.89	0.0526	40.33	0.0445	49.60
11	0.0298	0.0000	100.00	0.0000	100.00	0.0000	100.00	0.0000	100.00	0.0000	100.00
12	0.0423	0.0254	39.96	0.0211	50.13	0.0000	100.00	0.0287	32.06	0.0269	36.36
13	0.0204	0.0145	28.93	0.0169	17.21	0.0178	12.85	0.0133	34.95	0.0139	31.91
14	0.0137	0.0202	32.04	0.0171	19.76	0.0118	13.91	0.0182	24.59	0.0192	28.52
15	0.0153	0.0231	33.82	0.0281	45.52	0.0179	14.40	0.0196	21.98	0.0219	30.14

Std Run	Actual Result	Model 5	% Difference between Model 5 and Actual Result	Model 6	% Difference between Model 6 and Actual Result	Model 7	% Difference between Model 7 and Actual Result	Model 8	% Difference between Model 8 and Actual Result	Model 9	% Difference between Model 9 and Actual Result
16	0.0231	0.0354	34.74	0.0285	18.91	0.0302	23.57	0.0289	20.16	0.0331	30.25
17	0.0578	0.0264	54.32	0.0264	54.32	0.0349	39.55	0.0235	59.43	0.0209	63.81
18	0.0239	0.0220	7.98	0.0266	10.10	0.0218	8.93	0.0197	17.44	0.0178	25.68
19	0.0293	0.0209	28.67	0.0177	39.76	0.0177	39.65	0.0179	39.02	0.0170	42.09
20	0.0075	0.0153	50.85	0.0178	57.98	0.0127	40.97	0.0133	43.77	0.0128	41.19
21	0.0139	0.0169	17.91	0.0145	4.36	0.0132	4.95	0.0197	29.51	0.0209	33.34
22	0.0201	0.0127	36.67	0.0147	26.96	0.0138	31.59	0.0145	27.76	0.0152	24.23
23	0.0296	0.0282	4.80	0.0232	21.66	0.0216	26.94	0.0321	7.80	0.0370	20.05
24	0.0230	0.0196	14.59	0.0235	2.08	0.0389	40.83	0.0219	4.83	0.0246	6.53
25	0.0284	0.0289	1.64	0.0359	20.98	0.0400	29.00	0.0353	19.59	0.0307	7.57
26	0.0266	0.0468	43.15	0.0365	27.16	0.1615	83.53	0.0607	56.18	0.0507	47.49
27	0.0256	0.0191	25.42	0.0228	11.05	0.0678	62.25	0.0212	17.02	0.0201	21.56
28	0.0302	0.0280	7.25	0.0231	23.64	0.0371	18.59	0.0319	5.33	0.0298	1.40
29	0.0079	0.0156	49.38	0.0183	56.80	0.0210	62.39	0.0142	44.51	0.0149	47.07
30	0.0426	0.0220	48.37	0.0185	56.58	0.0135	68.32	0.0197	53.68	0.0209	51.02
31	0.0470	0.0254	46.00	0.0311	33.75	0.0211	55.05	0.0214	54.54	0.0240	48.97

Std Run	Actual Result	Model 5	% Difference between Model 5 and Actual Result	Model 6	% Difference between Model 6 and Actual Result	Model 7	% Difference between Model 7 and Actual Result	Model 8	% Difference between Model 8 and Actual Result	Model 9	% Difference between Model 9 and Actual Result
32	0.0420	0.0398	5.33	0.0316	24.75	0.0377	10.30	0.0321	23.50	0.0371	11.78
33	0.0119	0.0197	39.50	0.0197	39.50	0.0330	63.92	0.0197	39.50	0.0197	39.50
34	0.0132	0.0197	32.90	0.0197	32.90	0.0199	33.83	0.0197	32.90	0.0197	32.90
35	0.0302	0.0403	25.06	0.0403	25.06	0.0403	25.06	0.0442	31.64	0.0403	25.06
36	0.0426	0.0486	12.43	0.0486	12.43	0.1686	74.74	0.0442	3.58	0.0486	12.43
37	0.0298	0.0245	17.81	0.0245	17.81	0.0677	55.97	0.0245	17.81	0.0199	33.06
38	0.0184	0.0166	9.98	0.0166	9.98	0.0199	7.77	0.0166	9.98	0.0199	7.77
39	0.0136	0.0205	33.65	0.0205	33.65	0.0170	19.89	0.0205	33.65	0.0205	33.65
40	0.0154	0.0194	20.72	0.0194	20.72	0.0199	22.81	0.0194	20.72	0.0194	20.72
41	0.0302	0.0530	42.99	0.0530	42.99	0.0507	40.46	0.0530	42.99	0.0530	42.99
42	0.0308	0.0281	8.70	0.0281	8.70	0.0960	67.90	0.0281	8.70	0.0281	8.70
43	0.0587	0.0199	66.01	0.0199	66.01	0.0281	52.09	0.0199	66.01	0.0199	66.01
44	0.0154	0.0199	22.81	0.0199	22.81	0.0199	22.81	0.0199	22.81	0.0199	22.81
45	0.0167	0.0199	16.29	0.0199	16.29	0.0199	16.29	0.0199	16.29	0.0199	16.29
46	0.0126	0.0199	36.84	0.0199	36.84	0.0199	36.84	0.0199	36.84	0.0199	36.84
47	0.0123	0.0199	38.34	0.0199	38.34	0.0199	38.34	0.0199	38.34	0.0199	38.34

Std Run	Actual Result	Model 5	% Difference between Model 5 and Actual Result	Model 6	% Difference between Model 6 and Actual Result	Model 7	% Difference between Model 7 and Actual Result	Model 8	% Difference between Model 8 and Actual Result	Model 9	% Difference between Model 9 and Actual Result
48	0.0255	0.0199	21.77	0.0199	21.77	0.0199	21.77	0.0199	21.77	0.0199	21.77
49	0.0204	0.0199	2.21	0.0199	2.21	0.0199	2.21	0.0199	2.21	0.0199	2.21
50	0.0220	0.0199	9.32	0.0199	9.32	0.0199	9.32	0.0199	9.32	0.0199	9.32
Average % Difference			**28.07**		**29.34**		**37.76**		**28.07**		**29.45**
Max % Difference			**100.00**		**100.00**		**100.00**		**100.00**		**100.00**
Min % Difference			**1.64**		**2.08**		**2.21**		**2.21**		**1.40**

Table 31: Results of the optimisation of the quadratic equation for the prediction of water diffusion from a zinc plating solution continued

Std Run	Actual Result	Model 10	% Difference between Model 10 and Actual Result	Model 11	% Difference between Model 11 and Actual Result	Model 12	% Difference between Model 12 and Actual Result	Model 13	% Difference between Model 13 and Actual Result
1	0.0584	0.0546	10.54	0.0586	0.39	0.0575	1.53	0.0503	13.92
2	0.0370	0.0331	12.35	0.0349	5.57	0.0344	6.97	0.0310	16.23
3	0.0260	0.0295	14.72	0.0311	16.41	0.0307	15.23	0.0278	6.40
4	0.0251	0.0202	16.44	0.0211	16.08	0.0208	17.04	0.0192	23.57
5	0.0283	0.0244	12.67	0.0256	9.54	0.0253	10.69	0.0278	1.85
6	0.0427	0.0172	48.34	0.0179	58.03	0.0177	58.48	0.0192	55.07
7	0.1266	0.0423	46.07	0.0451	64.39	0.0443	64.99	0.0503	60.29
8	0.0355	0.0271	11.07	0.0284	19.89	0.0281	20.96	0.0310	12.69
9	0.0300	0.0321	2.02	0.0243	18.87	0.0246	17.85	0.0225	24.85
10	0.0882	0.0526	42.82	0.0371	57.91	0.0377	57.25	0.0338	61.69
11	0.0298	0.0000	100.00	0.0000	100.00	0.0000	100.00	0.0000	100.00
12	0.0423	0.0287	29.85	0.0221	47.80	0.0223	47.18	0.0205	51.48
13	0.0204	0.0169	36.34	0.0137	32.63	0.0139	31.99	0.0149	27.10
14	0.0137	0.0238	22.67	0.0187	26.79	0.0189	27.59	0.0205	33.25
15	0.0153	0.0264	24.02	0.0205	25.24	0.0207	26.10	0.0225	32.14
16	0.0231	0.0410	22.69	0.0300	23.09	0.0305	24.16	0.0338	31.64
17	0.0578	0.0322	60.57	0.0306	47.12	0.0301	47.85	0.0273	52.73

Std Run	Actual Result	Model 10	% Difference between Model 10 and Actual Result	Model 11	% Difference between Model 11 and Actual Result	Model 12	% Difference between Model 12 and Actual Result	Model 13	% Difference between Model 13 and Actual Result
18	0.0239	0.0262	19.58	0.0250	4.24	0.0246	3.02	0.0225	5.67
19	0.0293	0.0237	37.45	0.0226	22.82	0.0223	23.74	0.0205	29.95
20	0.0075	0.0168	44.98	0.0161	53.55	0.0160	53.07	0.0149	49.57
21	0.0139	0.0199	27.64	0.0191	27.34	0.0189	26.53	0.0205	32.28
22	0.0201	0.0145	29.37	0.0140	30.32	0.0139	30.98	0.0149	26.01
23	0.0296	0.0326	10.88	0.0309	4.17	0.0305	2.81	0.0338	12.40
24	0.0230	0.0219	2.12	0.0209	8.94	0.0207	9.99	0.0225	1.98
25	0.0284	0.0255	16.72	0.0339	16.26	0.0344	17.49	0.0310	8.37
26	0.0266	0.0394	54.12	0.0564	52.85	0.0575	53.75	0.0503	47.09
27	0.0256	0.0164	14.70	0.0206	19.59	0.0208	18.66	0.0192	25.06
28	0.0302	0.0231	8.48	0.0302	0.15	0.0307	1.54	0.0278	8.02
29	0.0079	0.0142	43.26	0.0175	54.97	0.0177	55.44	0.0192	58.82
30	0.0426	0.0195	54.88	0.0250	41.42	0.0253	40.67	0.0278	34.79
31	0.0470	0.0214	53.26	0.0277	41.09	0.0281	40.30	0.0310	34.05
32	0.0420	0.0317	20.86	0.0436	3.63	0.0443	5.24	0.0503	16.46
33	0.0119	0.0199	39.50	0.0199	40.35	0.0199	40.35	0.0199	40.35
34	0.0132	0.0199	32.90	0.0199	33.83	0.0199	33.83	0.0199	33.83
35	0.0302	0.0442	25.06	0.0442	31.64	0.0442	31.64	0.0442	31.64

Std Run	Actual Result	Model 10	% Difference between Model 10 and Actual Result	Model 11	% Difference between Model 11 and Actual Result	Model 12	% Difference between Model 12 and Actual Result	Model 13	% Difference between Model 13 and Actual Result
36	0.0426	0.0442	12.43	0.0442	3.58	0.0442	3.58	0.0442	3.58
37	0.0298	0.0245	17.81	0.0245	17.81	0.0245	17.81	0.0199	33.06
38	0.0184	0.0166	9.98	0.0166	9.98	0.0166	9.98	0.0199	7.77
39	0.0136	0.0205	33.65	0.0205	33.65	0.0199	31.83	0.0199	31.83
40	0.0154	0.0194	20.72	0.0194	20.72	0.0199	22.81	0.0199	22.81
41	0.0302	0.0530	42.99	0.0376	19.77	0.0376	19.77	0.0376	19.77
42	0.0308	0.0281	8.70	0.0376	18.18	0.0376	18.18	0.0376	18.18
43	0.0587	0.0199	66.01	0.0199	66.01	0.0199	66.01	0.0199	66.01
44	0.0154	0.0199	22.81	0.0199	22.81	0.0199	22.81	0.0199	22.81
45	0.0167	0.0199	16.29	0.0199	16.29	0.0199	16.29	0.0199	16.29
46	0.0126	0.0199	36.84	0.0199	36.84	0.0199	36.84	0.0199	36.84
47	0.0123	0.0199	38.34	0.0199	38.34	0.0199	38.34	0.0199	38.34
48	0.0255	0.0199	21.77	0.0199	21.77	0.0199	21.77	0.0199	21.77
49	0.0204	0.0199	2.21	0.0199	2.21	0.0199	2.21	0.0199	2.21
50	0.0220	0.0199	9.32	0.0199	9.32	0.0199	9.32	0.0199	9.32
Average % Difference			**28.18**		**27.88**		**28.05**		**29.04**
Max % Difference			**100.00**		**100.00**		**100.00**		**100.00**
Min % Difference			**2.02**		**0.15**		**1.53**		**1.85**

ANNEXURE D: MICROSOFT EXCEL MODEL VERIFICATION

Annexure D1: Microsoft excel results for verification 1

Table 32: Calculation of cooling tower height for verification 1

Calculation of diffusivity coefficient	**Value**	**Unit**
Molecular mass of diffusing component, M_A	18	kg/kmol
Molecular mass of non diffusing component, M_B	29	kg/kmol
Va	12.7	
Vb	20.1	
Pressure of system, P	1	atm
Temperature of water	293.15	K
D_{AB}	2.44E-05	m^2/s
Calculation of gas phase mass transfer coefficient	**Value**	**Unit**
Pressure of the system	101325	Pa
Temperature of the entering water, T_{L2}	20	oC
	293.150	K
Humidity of the air stream	0.0088	kg H_2O/kg air
Partial pressure of water in the bulk air stream - P_{A2}	0	Pa
Partial pressure at the interface - P_{A1}	2339.30	Pa
Log mean partial pressure, P_{BM}	100150.80	Pa
Diameter of cooling tower	0.50	m
Cross sectional area of cooling tower	0.20	m^2
Air mass flow rate	1.20	kg/s
G	6.11	$kg/s.m^2$
Temperature of air	15.00	^oC
	288.15	K
Density of air	1.23	kg/m^3
Viscosity of air	1.80E-05	Pa.s
Volumetric flow rate	0.98	m^3/s
Velocity	4.98	m/s
Reynolds number	169616.13	>2100 - turbulent flow
Schmidt number	0.60	range is 0.5 - 3
Sherwood number	425.96	
kc'	2.08E-02	m/s
R	8314	m^3.Pa/kmol.K
k_G	8.78E-09	$kmol/s.m^2$.Pa
a	500.000	m^2/m^3
k_Ga	4.39E-06	$kmol/s.m^3$.Pa
Calculation of slope of operating line	**Value**	**Unit**
Water mass flow rate	1.00	kg/s
L	5.09	$kg/s.m^2$
Specific heat capacity of water, C_L	4187.00	KJ/kg.K

Slope	3489.17	
H_{Y1}	37331.96	J/kg.K
H_{Y2}	54777.79	J/kg.K
Calculation of slope of locus	**Value**	**Unit**
Heat transfer co-efficient of water - h_L	280	$W/m^2.K$
Molecular mass of air -M_B	29	kg/kmol
Slope	-10847.41	
Calculation of cooling tower height	**Value**	**Unit**
Integral	5.77	
Height, z	2.73	m

Table 33: Calculation of plating bath temperature for verification 1

Unsteady state temperature region	**Value**	**Unit**
Inlet temperature to cooling tower - T_{L2}	68	^oF
	20.00	^oC
Exit temperature from cooling tower - T_{L1}	59	^oF
	15.00	^oC
Ambient Temperature - T_{AMB}	15	^oC
	288.15	K
Reference Temperature - T_{REF}	15	^oC
	288.15	K
Length of tank	1.5	m
Height of tank	2	m
Width of tank	1.5	m
Volume of plating soln tank	4.5	m^3
Volume of plating soln in tank	3	m^3
Initial Mass of plating tank $M_{PT\|t=0}$	3000	kg
Initial Temperature of tank $T_{PT\|t=0}$	20	^oC
Volumetric flow rate of water	0.001	m^3/s
Time to pass through cooling tower - $Time_{CT}$	536.27	s
	8.94	min
Surface area of top of tank	2.25	m^2
Rate of Mass $Evap_{PT}$	0.0023	$L/m^2.hr$
Mass $Evap_{PT}$	0.000001	kg/s
	0.00078	kg
Re-circulating flow rate of water	0.26	gal/s
	15.85	gal/min
Rate of Mass $Evap_{CT}$	0.12	gal/min
Mass $Evap_{CT}$	0.01	kg/s
	4.07	kg
Mass flow rate of H_{PS}	1	kg/s
Mass H_{PS}	536.27	kg
Mass flow rate of C_{PS}	0.99	kg/s
Mass C_{PS}	532.20	kg

Mass of plating tank at time 2 - $M_{PT\|t=2}$	2996.08	kg
Thickness of metal plate	0.001	m
Length of metal piece	0.05	m
Width of metal piece	0.05	m
Square meter of metal plate	0.0025	m^2
No. of metal pieces	10	
CD	150	A/m^2
V	6	V
E_{ELEC}	12.07	KJ
Density of metal piece - mild steel	7801	kg/m^3
Cp of mild steel	0.473	$KJ/kg.^oC$
E_{CMP}	4.61E-01	KJ
M_{CPS}	0.99	kg/s
Cp of C_{PS}	4.18	KJ/kg.K
E_{CPS}	0.00	KJ
Conduction and Convection Losses from Side 1 = L*H		
Plating bath material of construction	mild steel	
Thermal conductivity of mild steel	0.19	W/m.K
Heat transfer co-efficient of water	280	$W/m^2.K$
Thickness of steel - Δx	0.001	m
Heat transfer co-efficient of air	11.3	$W/m^2.K$
Area for heat transfer	3	m^2
Q	308.23	W
	0.31	KW
Conduction and Convection Losses from Side 2 = W*H		
Plating bath material of construction	mild steel	
Thermal conductivity of mild steel	0.19	W/m.K
Heat transfer co-efficient of water	280	$W/m^2.K$
Thickness of steel - Δx	0.001	m
Heat transfer co-efficient of air	11.3	$W/m^2.K$
Area for heat transfer	3	m^2
Q	308.23	W
	0.31	KW
Conduction and Convection Losses from Bottom of Tank = W*L		
Plating bath material of construction	mild steel	
Thermal conductivity of mild steel	0.19	W/m.K
Heat transfer co-efficient of water	280	$W/m^2.K$
Thickness of steel - Δx	0.001	m
Heat transfer co-efficient of air	11.3	$W/m^2.K$
Area for heat transfer	2.25	m^2
Q	115.59	W

	0.12	KW
Convection Losses from Top of Tank = W*L		
Plating bath material of construction	mild steel	
Heat transfer co-efficient of air	11.3	$W/m^2.K$
Area for heat transfer	2.25	m^2
Q	127.13	W
	0.13	KW
Total conduction and convection losses	460.75	KJ
Mass Evaporated from plating tank	0.000001	kg/s
Critical temperature for water - T_C	647.3	K
Reduced temperature - T_R	0.45	
C_1	52053000	
C_2	0.3199	
C_3	-0.212	
C4	0.25795	
Latent heat of vapourisation	44050216.68	J/kmol
	2447234.26	J/kg
	2447.23	KJ/kg
E_{EVAP}	1.90	KJ
Temperature of plating bath - T_{PB}	292.37	K
	19.216	^oC
Steady State Temperature Region	**Value**	**Unit**
Humidity - X_1	0.0088	kg H_2O/kg air
Saturation humidity - X_2	0.0128	kg H_2O/kg air
Mass of water evaporated in cooling tower for 1 hour	17.28	kg
Surface area of top of tank	2.25	m^2
Rate of Mass $Evap_{PT}$	0.0022	$L/m^2.hr$
Mass $Evap_{PT}$	0.000001	kg/s
	0.0050	kg
Total mass evaporated	17.28	kg

Table 34: Data for operating line and loci for verification 1

Operating Line					
Slope	3489.17		Temperature (^0C)	15	20
Y-intercept	-15005.54		Enthalpy (J/kg)	37331.96	54777.79
Enthalpy of entering air (J/kg)	37331.96				
Point 1					
Temperature (^0C)	15	15	15	15	
Enthalpy (J/kg)	28377.20	29075.00	29772.80	37331.96	
Locus Point					
Slope	-10847.41		Temperature (^0C)	15	14.63
Y-intercept	200043.09		Enthalpy (J/kg)	37331.96	41399.74

Point 2					
Temperature (^{0}C)	15.5	15.5	15.5	15.5	
Enthalpy (J/kg)	28377.20	29075.00	29772.80	39076.80	
Locus Point					
Slope	-10847.41		Temperature (^{0}C)	15.5	15.15
Y-intercept	207211.64		Enthalpy (J/kg)	39076.80	42873.39
Point 3					
Temperature (^{0}C)	16	16	16	16	
Enthalpy (J/kg)	28377.2	29075	29772.8	40705	
Locus Point					
Slope	-10847.41		Temperature (^{0}C)	16	15.67
Y-intercept	214263.54		Enthalpy (J/kg)	40705	44284.64
Point 4					
Temperature (^{0}C)	16.5	16.5	16.5	16.5	
Enthalpy (J/kg)	28377.2	29075	29772.8	42333.2	
Locus Point					
Slope	-10847.41		Temperature (^{0}C)	16.5	16.19
Y-intercept	221315.45		Enthalpy (J/kg)	42333.2	45695.90
Point 5					
Temperature (^{0}C)	17	17	17	17	
Enthalpy (J/kg)	28377.2	29075	29772.8	44194	
Locus Point					
Slope	-10847.41		Temperature (^{0}C)	17	16.72
Y-intercept	228599.95		Enthalpy (J/kg)	44194	47231.27
Point 6					
Temperature (^{0}C)	17.5	17.5	17.5	17.5	17.5
Enthalpy (J/kg)	28377.2	29075	29772.8	44194	46054.8
Locus Point					
Slope	-10847.41		Temperature (^{0}C)	17.5	17.23
Y-intercept	235884.46		Enthalpy (J/kg)	46054.8	48983.6004
Point 7					
Temperature (^{0}C)	18	18	18	18	18
Enthalpy (J/kg)	28377.2	29075	29772.8	44194	47683
Locus Point					
Slope	-10847.41		Temperature (^{0}C)	18	17.75
Y-intercept	242936.36		Enthalpy (J/kg)	47683	50394.85
Point 8					
Temperature (^{0}C)	18.5	18.5	18.5	18.5	18.5
Enthalpy (J/kg)	28377.2	29075	29772.8	44194	49311.2

Locus Point					
Slope	-10847.41		Temperature (^{0}C)	18.5	18.24
Y-intercept	249988.26		Enthalpy (J/kg)	49311.2	52131.53
Point 9					
Temperature (^{0}C)	19	19	19	19	19
Enthalpy (J/kg)	28377.2	29075	29772.8	44194	51172
Locus Point					
Slope	-10847.41		Temperature (^{0}C)	19	18.77
Y-intercept	257272.77		Enthalpy (J/kg)	51172	53666.90
Point 10					
Temperature (^{0}C)	19.5	19.5	19.5	19.5	19.5
Enthalpy (J/kg)	28377.2	29075	29772.8	44194	52800.2
Locus Point					
Slope	-10847.41		Temperature (^{0}C)	19.5	19.26
Y-intercept	264324.67		Enthalpy (J/kg)	52800.2	55403.58
Point 11					
Temperature (^{0}C)	20	20	20	20	20
Enthalpy (J/kg)	28377.2	29075	29772.8	44194	54777.79
Locus Point					
Slope	-10847.41		Temperature (^{0}C)	20	19.78
Y-intercept	271725.97		Enthalpy (J/kg)	54777.79	57164.22

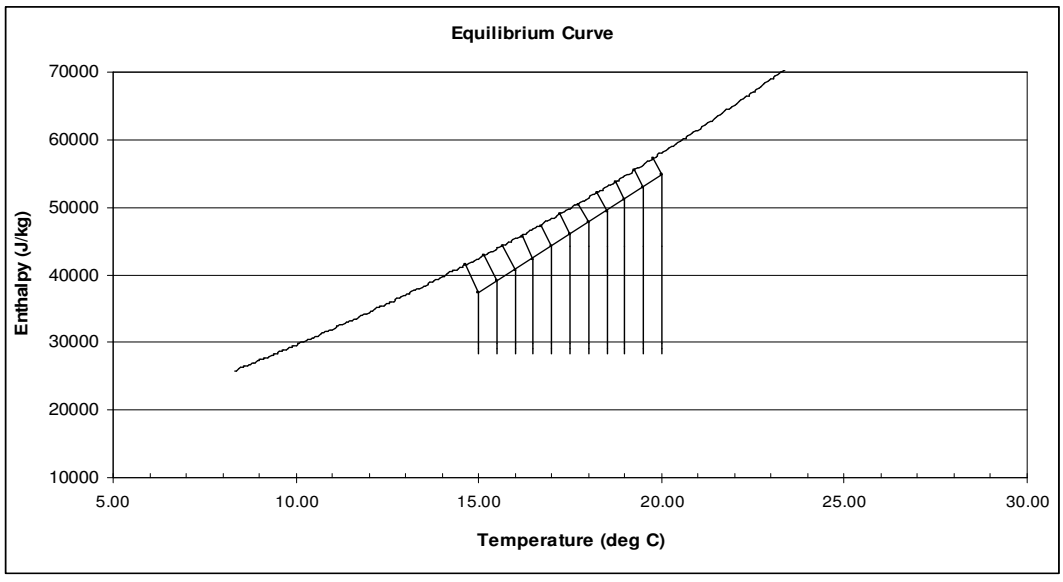

Figure 42: Equilibrium curve with operating line and loci for verification 1

Table 35: Data for construction of area under the curve graph for verification 1

Temperature (^{0}C)	Hy (J/kg)	Hyi (J/kg)	Hyi – Hy (J/kg)	1/Hyi - Hy
15	37331.96	41399.74	4067.78	2.46E-04
15.5	39076.80	42873.39	3796.59	2.63E-04
16	40705.00	44284.64	3579.64	2.79E-04
16.5	42333.20	45695.90	3362.70	2.97E-04
17	44194.00	47231.27	3037.27	3.29E-04
17.5	46054.80	48983.60	2928.80	3.41E-04
18	47683.00	50394.85	2711.85	3.69E-04
18.5	49311.20	52131.53	2820.33	3.55E-04
19	51172.00	53666.90	2494.90	4.01E-04
19.5	52800.20	55403.58	2603.38	3.84E-04
20	54777.79	57164.22	2386.43	4.19E-04

Figure 43: Area under the curve for verification 1

Table 36: Results of graphical solution of integral for verification 1

Area	ΔX	ΔY	ΔX * ΔY
Area 1	1000	2.46E-04	2.46E-01
Area 2	1000	2.55E-04	2.55E-01
Area 3	1000	2.66E-04	2.66E-01
Area 4	1000	2.75E-04	2.75E-01
Area 5	1000	2.85E-04	2.85E-01
Area 6	1000	2.97E-04	2.97E-01
Area 7	1000	3.15E-04	3.15E-01
Area 8	1000	3.30E-04	3.30E-01
Area 9	1000	3.36E-04	3.36E-01
Area 10	1000	3.45E-04	3.45E-01
Area 11	1000	3.65E-04	3.65E-01
Area 12	1000	3.65E-04	3.65E-01
Area 13	1000	3.55E-04	3.55E-01

Area	ΔX	ΔY	ΔX * ΔY
Area 14	1000	3.80E-04	3.80E-01
Area 15	1000	4.02E-04	4.02E-01
Area 16	1000	3.87E-04	3.87E-01
Area 17	1445.83	3.90E-04	5.64E-01
Total			**5.77E+00**

Annexure D2: Microsoft excel results for verification 2

Table 37: Calculation of cooling tower height for verification 2

Calculation of diffusivity coefficient	**Value**	**Unit**
Molecular mass of diffusing component, M_A	18	kg/kmol
Molecular mass of non diffusing component, M_B	29	kg/kmol
va	12.7	
vb	20.1	
Pressure of system, P	1	atm
Temperature of water	296.15	K
D_{AB}	2.49E-05	m^2/s
Calculation of gas phase mass transfer coefficient	**Value**	**Unit**
Pressure of the system	101325	Pa
Temperature of the entering water, T_{L2}	23	^oC
	296.15	K
Humidity of the air stream	0.0093	kg H_2O/kg air
Partial pressure of water in the bulk air stream - P_{A2}	0.000	Pa
Partial pressure at the interface - P_{A1}	2811.34	Pa
Log mean partial pressure, P_{BM}	99912.74	Pa
Diameter of cooling tower	0.50	m
Cross sectional area of cooling tower	0.20	m^2
Air mass flow rate	2.40	kg/s
G	12.22	$kg/s.m^2$
Temperature of air	15.50	^oC
	288.65	K
Density of air	1.22	kg/m^3
Viscosity of air	1.80E-05	Pa.s
Volumetric flow rate	1.96	m^3/s
Velocity	9.98	m/s
Reynolds number	338826.35	>2100 - turbulent flow
Schmidt number	0.59	range is 0.5 - 3
Sherwood number	752.73	
kc'	3.74E-02	m/s
R	8314.000	m^3.Pa/kmol.K
k_G	1.58E-08	$kmol/s.m^2$.Pa
a	700	m^2/m^3

k_Ga	1.11E-05	kmol/s.m^3.Pa
Calculation of slope of operating line	**Value**	**Unit**
Water mass flow rate	2	kg/s
L	10.19	kg/s.m^2
Specific heat capacity of water, C_L	4187	KJ/kg.K
Slope	3489.17	
H_{Y1}	39107.80	J/kg.K
H_{Y2}	65276.55	J/kg.K
Calculation of slope of locus	**Value**	**Unit**
Heat transfer co-efficient of water - h_L	280	W/m^2.K
Molecular mass of air -M_B	29	kg/kmol
Slope	-6026.10	
Calculation of cooling tower height	**Value**	**Unit**
integral	11.24	
Height, z	4.22	m

Table 38: Calculation of plating bath temperature for verification 2

Unsteady state temperature region	**Value**	**Unit**
Inlet temperature to cooling tower - T_{L2}	73.4	^{o}F
	23	^{o}C
Exit temperature from cooling tower - T_{L1}	59.9	^{o}F
	15.50	^{o}C
Ambient Temperature - T_{AMB}	15.5	^{o}C
	288.65	K
Reference Temperature - T_{REF}	15.5	^{o}C
	288.65	K
Length of tank	1.5	m
Height of tank	2	m
Width of tank	1.5	m
Volume of plating soln tank	4.5	m^3
Volume of plating soln in tank	3	m^3
Initial Mass of plating tank $M_{PT\|t=0}$	3000	kg
Initial Temperature of tank $T_{PT\|t=0}$	23	^{o}C
Volumetric flow rate of water	0.002	m^3/s
Time to pass through cooling tower - $Time_{CT}$	414.78	s
	6.91	min
Surface area of top of tank	2.25	m^2
Rate of Mass $Evap_{PT}$	0.0028	L/m^2.hr
Mass $Evap_{PT}$	1.72E-06	kg/s
	0.00071	kg
Re-circulating flow rate of water	0.53	gal/s
	31.70	gal/min
Rate of Mass $Evap_{CT}$	0.36	gal/min

Mass $Evap_{CT}$	0.02	kg/s
	9.45	kg
Mass flow rate of H_{PS}	2	kg/s
Mass H_{PS}	829.56	kg
Mass flow rate of C_{PS}	1.98	kg/s
Mass C_{PS}	820.11	kg
Mass of plating tank at time 2 - $M_{PT\|t=2}$	2990.55	kg
Thickness of metal plate	0.001	m
Length of metal piece	0.05	m
Width of metal piece	0.05	m
Square meter of metal plate	0.0025	m^2
No. of metal pieces	10	
CD	150	A/m^2
V	6	V
E_{ELEC}	9.33	KJ
Density of metal piece - mild steel	7801	kg/m^3
Cp of mild steel	0.47	$KJ/kg.^oC$
E_{CMP}	6.92E-01	KJ
M_{CPS}	1.98	kg/s
Cp of C_{PS}	4.18	KJ/kg.K
E_{CPS}	0.00	KJ
Conduction and Convection Losses from Side 1 = L*H		
Plating bath material of construction	mild steel	
Thermal conductivity of mild steel	0.19	W/m.K
Heat transfer co-efficient of water	280	$W/m^2.K$
Thickness of steel - Δx	0.001	m
Heat transfer co-efficient of air	11.3	$W/m^2.K$
Area for heat transfer	3	m^2
Q	462.34	W
	0.46	KW
Conduction and Convection Losses from Side 2 = W*H		
Plating bath material of construction	mild steel	
Thermal conductivity of mild steel	0.19	W/m.K
Heat transfer co-efficient of water	280	$W/m^2.K$
Thickness of steel - Δx	0.001	m
Heat transfer co-efficient of air	11.3	$W/m^2.K$
Area for heat transfer	3	m^2
Q	462.34	W
	0.46	KW
Conduction and Convection Losses from Bottom of Tank = W*L		

Plating bath material of construction	mild steel	
Thermal conductivity of mild steel	0.19	W/m.K
Heat transfer co-efficient of water	280	$W/m^2.K$
Thickness of steel - Δx	0.001	m
Heat transfer co-efficient of air	11.3	$W/m^2.K$
Area for heat transfer	2.25	m^2
Q	173.38	W
	0.17	KW
Convection Losses from Top of Tank = W*L		
Plating bath material of construction	mild steel	
Heat transfer co-efficient of air	11.3	$W/m^2.K$
Area for heat transfer	2.25	m^2
Q	190.69	W
	0.19	KW
Total conduction and convection losses	534.55	KJ
Mass Evaporated from plating tank	1.72E-06	kg/s
Critical temperature for water - T_C	647.3	K
Reduced temperature - T_R	0.46	
C_1	52053000	
C_2	0.3199	
C_3	-0.212	
C4	0.25795	
Latent heat of vapourisation	43943768.35	J/kmol
	2441320.46	J/kg
	2441.32	KJ/kg
E_{EVAP}	1.74	KJ
Temperature of plating bath - T_{PB}	294.51	K
	21.36	^oC
Steady State Temperature Region	**Value**	**Unit**
Humidity - X_1	0.0093	kg H_2O/kg air
Saturation humidity - X_2	0.0133	kg H_2O/kg air
Mass of water evaporated in cooling tower for 1 hour	34.56	kg
Surface area of top of tank	2.25	m^2
Rate of Mass $Evap_{PT}$	0.0025	$L/m^2.hr$
Mass $Evap_{PT}$	0.000002	kg/s
	0.0056	kg
Total mass evaporated	34.57	kg

Table 39: Data for operating line and loci for verification 2

Operating Line					
Slope	3489.17		Temperature (^{0}C)	15.5	23
Y-intercept	-14974.28		Enthalpy (J/kg)	39107.80	65276.55
Enthalpy of entering air (J/kg)	39107.80				
Point 1					
Temperature (^{0}C)	15.5	15.5	15.5	15.5	
Enthalpy (J/kg)	28377.2	30238	32098.8	39107.80	
Locus Point					
Slope	-6026.10		Temperature (^{0}C)	15.5	14.97
Y-intercept	132512.41		Enthalpy (J/kg)	39107.80	42301.64
Point 2					
Temperature (^{0}C)	16	16	16	16	
Enthalpy (J/kg)	28377.2	30238	39107.802	40705	
Locus Point					
Slope	-6026.10		Temperature (^{0}C)	16	15.49
Y-intercept	137122.66		Enthalpy (J/kg)	40705	43778.31
Point 3					
Temperature (^{0}C)	16.5	16.5	16.5	16.5	
Enthalpy (J/kg)	28377.2	30238	39107.80	42565.8	
Locus Point					
Slope	-6026.10		Temperature (^{0}C)	16.5	16.03
Y-intercept	141996.51		Enthalpy (J/kg)	42565.8	45398.07
Point 4					
Temperature (^{0}C)	17	17	17	17	
Enthalpy (J/kg)	28377.2	30238	39107.80	44426.6	
Locus Point					
Slope	-6026.10		Temperature (^{0}C)	17	16.57
Y-intercept	146870.36		Enthalpy (J/kg)	44426.6	47017.82
Point 5					
Temperature (^{0}C)	17.5	17.5	17.5	17.5	
Enthalpy (J/kg)	28377.2	30238	39107.80	46054.8	
Locus Point					
Slope	-6026.10		Temperature (^{0}C)	17.5	17.1
Y-intercept	151511.61		Enthalpy (J/kg)	46054.8	48465.24
Point 6					
Temperature (^{0}C)	18	18	18	18	18
Enthalpy (J/kg)	28377.2	30238	39107.80	46054.8	47683
Locus Point					
Slope	-6026.10		Temperature (^{0}C)	18	17.6

Y-intercept	156152.86		Enthalpy (J/kg)	47683	50093.44
Point 7					
Temperature (^{0}C)	18.5	18.5	18.5	18.5	18.5
Enthalpy (J/kg)	28377.2	30238	39107.802	46054.8	49543.8
Locus Point					
Slope	-6026.10		Temperature (^{0}C)	18.5	18.12
Y-intercept	161026.72		Enthalpy (J/kg)	49543.8	51833.72
Point 8					
Temperature (^{0}C)	19	19	19	19	19
Enthalpy (J/kg)	28377.2	30238	39107.80	46054.8	51172
Locus Point					
Slope	-6026.10		Temperature (^{0}C)	19	18.63
Y-intercept	165667.97		Enthalpy (J/kg)	51172	53401.66
Point 9					
Temperature (^{0}C)	19.5	19.5	19.5	19.5	19.5
Enthalpy (J/kg)	28377.2	30238	39107.80	46054.8	53032.8
Locus Point					
Slope	-6026.10		Temperature (^{0}C)	19.5	19.16
Y-intercept	170541.82		Enthalpy (J/kg)	53032.8	55081.68
Point 10					
Temperature (^{0}C)	20	20	20	20	20
Enthalpy (J/kg)	28377.2	30238	39107.802	46054.8	54661
Locus Point					
Slope	-6026.10		Temperature (^{0}C)	20	19.65
Y-intercept	175183.07		Enthalpy (J/kg)	54661	56770.14
Point 11					
Temperature (^{0}C)	20.5	20.5	20.5	20.5	20.5
Enthalpy (J/kg)	28377.2	30238	39107.80	46054.8	56521.8
Locus Point					
Slope	-6026.10		Temperature (^{0}C)	20.5	20.16
Y-intercept	180056.92		Enthalpy (J/kg)	56521.8	58570.68
Point 12					
Temperature (^{0}C)	21	21	21	21	21
Enthalpy (J/kg)	28377.2	30238	39107.80	46054.8	58150
Locus Point					
Slope	-6026.10		Temperature (^{0}C)	21	20.65
Y-intercept	184698.17		Enthalpy (J/kg)	58150	60259.14
Point 13					
Temperature (^{0}C)	21.5	21.5	21.5	21.5	21.5

Enthalpy (J/kg)	28377.2	30238	39107.80	46054.8	60010.8
Locus Point					
Slope	-6026.10		Temperature (^{0}C)	21.5	21.16
Y-intercept	189572.03		Enthalpy (J/kg)	60010.8	62059.68
Point 14					
Temperature (^{0}C)	22	22	22	22	22
Enthalpy (J/kg)	28377.2	30238	39107.80	46054.8	61660
Locus Point					
Slope	-6026.10		Temperature (^{0}C)	22	21.65
Y-intercept	194234.28		Enthalpy (J/kg)	61660	63769.14
Point 15					
Temperature (^{0}C)	22.5	22.5	22.5	22.5	22.5
Enthalpy (J/kg)	28377.2	30238	39107.80	46054.8	63499.8
Locus Point					
Slope	-6026.10		Temperature (^{0}C)	22.5	22.15
Y-intercept	199087.13		Enthalpy (J/kg)	63499.8	65608.94
Point 16					
Temperature (^{0}C)	23	23	23	23	23
Enthalpy (J/kg)	28377.2	30238	39107.80	46054.8	65276.55
Locus Point					
Slope	-6026.10		Temperature (^{0}C)	23	22.64
Y-intercept	203876.93		Enthalpy (J/kg)	65276.55	67445.95

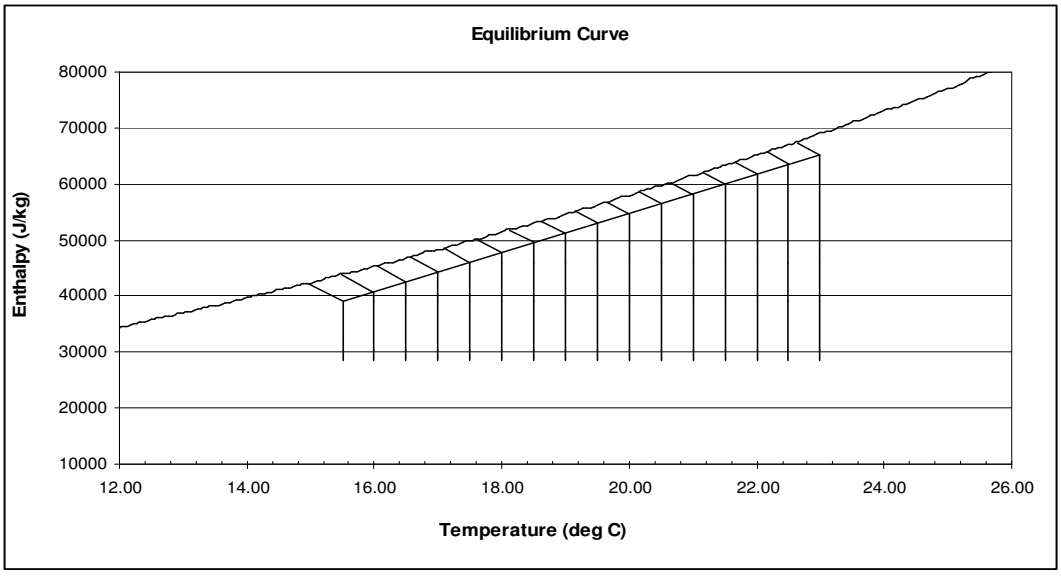

Figure 44: Equilibrium curve with operating line and loci for verification 2

Table 40: Data for construction of area under the curve graph for verification 2

Temperature (^{0}C)	Hy (J/kg)	Hyi (J/kg)	Hyi – Hy (J/kg)	1/Hyi - Hy
15.5	39107.80	42301.64	3193.83	3.13E-04
16	40705.00	43778.31	3073.31	3.25E-04
16.5	42565.80	45398.07	2832.27	3.53E-04
17	44426.60	47017.82	2591.22	3.86E-04
17.5	46054.80	48465.24	2410.44	4.15E-04
18	47683.00	50093.44	2410.44	4.15E-04
18.5	49543.80	51833.72	2289.92	4.37E-04
19	51172.00	53401.66	2229.66	4.48E-04
19.5	53032.80	55081.68	2048.88	4.88E-04
20	54661.00	56770.14	2109.14	4.74E-04
20.5	56521.80	58570.68	2048.88	4.88E-04
21	58150.00	60259.14	2109.14	4.74E-04
21.5	60010.80	62059.68	2048.88	4.88E-04
22	61660.00	63769.14	2109.14	4.74E-04
22.5	63499.80	65608.94	2109.14	4.74E-04
23	65276.55	67445.95	2169.40	4.61E-04

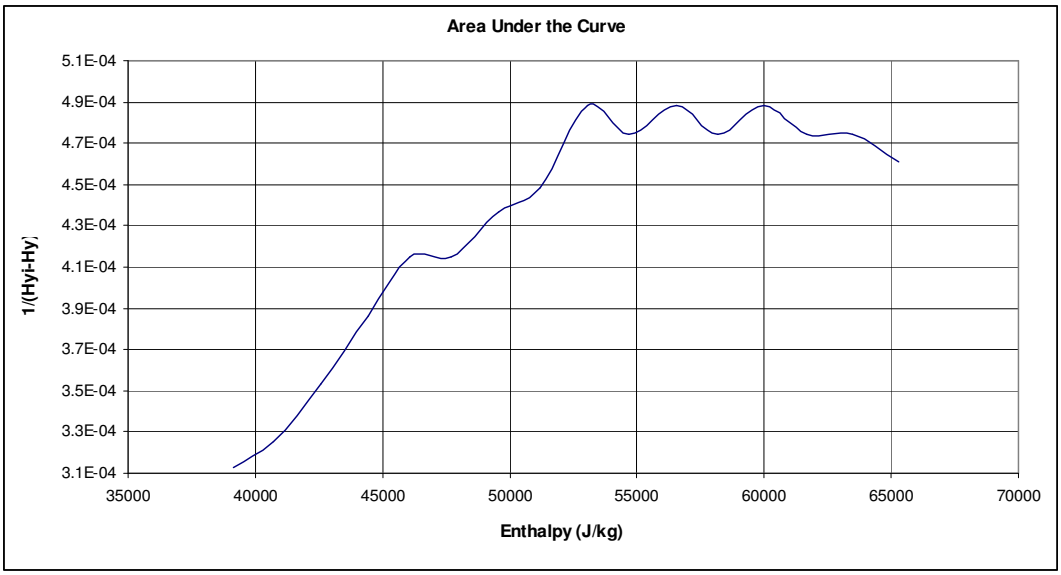

Figure 45: Area under the curve for verification 2

Table 41: Results of graphical solution of integral for verification 2

Area	ΔX	ΔY	ΔX * ΔY
Area 1	2000	3.13E-04	6.26E-01
Area 2	2000	3.31E-04	6.61E-01
Area 3	2000	3.62E-04	7.24E-01
Area 4	2000	3.99E-04	7.98E-01
Area 5	2000	4.15E-04	8.29E-01
Area 6	2000	4.32E-04	8.63E-01
Area 7	2000	4.48E-04	8.95E-01
Area 8	2000	4.89E-04	9.77E-01

Area	ΔX	ΔY	ΔX * ΔY
Area 9	2000	4.76E-04	9.52E-01
Area 10	2000	4.84E-04	9.68E-01
Area 11	2000	4.81E-04	9.63E-01
Area 12	2000	4.79E-04	9.57E-01
Area 13	2168.75	4.75E-04	1.03E+00
Total			**11.24**

Annexure D3: Microsoft excel results for verification 3

Table 42: Calculation of cooling tower height for verification 3

Calculation of diffusivity coefficient	**Value**	**Unit**
Molecular mass of diffusing component, M_A	18	kg/kmol
Molecular mass of non diffusing component, M_B	29	kg/kmol
va	12.7	
vb	20.1	
Pressure of system, P	1	atm
Temperature of water	299.15	K
D_{AB}	2.53E-05	m^2/s
Calculation of gas phase mass transfer coefficient	**Value**	**Unit**
Pressure of the system	101325	Pa
Temperature of the entering water, T_{L2}	26	oC
	299.15	K
Humidity of the air stream	0.0096	kg H_2O/kg air
Partial pressure of water in the bulk air stream - P_{A2}	0.000	Pa
Partial pressure at the interface - P_{A1}	3364.46	Pa
Log mean partial pressure, P_{BM}	99633.30	Pa
Diameter of cooling tower	0.50	m
Cross sectional area of cooling tower	0.20	m^2
Air mass flow rate	3.60	kg/s
G	18.33	$kg/s.m^2$
Temperature of air	16	^oC
	289.15	K
Density of air	1.22	kg/m^3
Viscosity of air	1.81E-05	Pa.s
Volumetric flow rate	2.94	m^3/s
Velocity	15	m/s
Reynolds number	507632.12	>2100 - turbulent flow
Schmidt number	0.58	range is 0.5 - 3
Sherwood number	1047.70	
kc'	5.30E-02	m/s
R	8314	m^3.Pa/kmol.K
k_G	2.24E-08	$kmol/s.m^2$.Pa

a	700.000	m^2/m^3
k_Ga	1.57E-05	$kmol/s.m^3.Pa$
Calculation of slope of operating line	**Value**	**Unit**
Water mass flow rate	3	kg/s
L	15.28	$kg/s.m^2$
Specific heat capacity of water, C_L	4187	KJ/kg.K
Slope	3489.17	
H_{Y1}	40378.37	J/kg.K
H_{Y2}	75270.03	J/kg.K
Calculation of slope of locus	**Value**	**Unit**
Heat transfer co-efficient of water - h_L	280	$W/m^2.K$
Molecular mass of air -M_B	29	kg/kmol
Slope	-4249.27	
Calculation of cooling tower height	**Value**	**Unit**
integral	15.21	
Height, z	6.05	m

Table 43: Calculation of plating bath temperature for verification 3

Unsteady state temperature region	**Value**	**Unit**
Inlet temperature to cooling tower - T_{L2}	78.8	^oF
	26	^oC
Exit temperature from cooling tower - T_{L1}	60.8	^oF
	16	^oC
Ambient Temperature - T_{AMB}	16	^oC
	289.15	K
Reference Temperature - T_{REF}	16	^oC
	289.15	K
Length of tank	1.5	m
Height of tank	2	m
Width of tank	1.5	m
Volume of plating soln tank	4.5	m^3
Volume of plating soln in tank	3	m^3
Initial Mass of plating tank $M_{PT\|t=0}$	3000	kg
Initial Temperature of tank $T_{PT\|t=0}$	26	^oC
Volumetric flow rate of water	0.003	m^3/s
Time to pass through cooling tower - $Time_{CT}$	395.80	s
	6.60	min
Surface area of top of tank	2.25	m^2
Rate of Mass $Evap_{PT}$	0.0033	$L/m^2.hr$
Mass $Evap_{PT}$	2.04E-06	kg/s
	8.09E-04	kg
Re-circulating flow rate of water	0.79	gal/s
	47.55	gal/min

Rate of Mass $Evap_{CT}$	0.73	gal/min
Mass $Evap_{CT}$	0.05	kg/s
	18.04	kg
Mass flow rate of H_{PS}	3	kg/s
Mass H_{PS}	1187.40	kg
Mass flow rate of C_{PS}	2.95	kg/s
Mass C_{PS}	1169.36	kg
Mass of plating tank at time 2 - $M_{PT\|t=2}$	2981.98	kg
Thickness of metal plate	0.001	m
Length of metal piece	0.05	m
Width of metal piece	0.05	m
Square meter of metal plate	0.0025	m^2
No. of metal pieces	10	
CD	150	A/m^2
V	6	V
E_{ELEC}	8.91	KJ
Density of metal piece - mild steel	7801	kg/m^3
Cp of mild steel	0.47	$KJ/kg.^oC$
E_{CMP}	9.22E-01	KJ
M_{CPS}	2.95	kg/s
Cp of C_{PS}	4.18	KJ/kg.K
E_{CPS}	0.00	KJ
Conduction and Convection Losses from Side 1 = L*H		
Plating bath material of construction	mild steel	
Thermal conductivity of mild steel	0.19	W/m.K
Heat transfer co-efficient of water	280	$W/m^2.K$
Thickness of steel - Δx	0.001	m
Heat transfer co-efficient of air	11.3	$W/m^2.K$
Area for heat transfer	3	m^2
Q	616.46	W
	0.62	KW
Conduction and Convection Losses from Side 2 = W*H		
Plating bath material of construction	mild steel	
Thermal conductivity of mild steel	0.19	W/m.K
Heat transfer co-efficient of water	280	$W/m^2.K$
Thickness of steel - Δx	0.001	m
Heat transfer co-efficient of air	11.3	$W/m^2.K$
Area for heat transfer	3	m^2
Q	616.46	W
	0.62	KW

Conduction and Convection Losses from Bottom of Tank = W*L		
Plating bath material of construction	mild steel	
Thermal conductivity of mild steel	0.19	W/m.K
Heat transfer co-efficient of water	280	$W/m^2.K$
Thickness of steel - Δx	0.001	m
Heat transfer co-efficient of air	11.3	$W/m^2.K$
Area for heat transfer	2.25	m^2
Q	231.17	W
	0.23	KW
Convection Losses from Top of Tank = W*L		
Plating bath material of construction	mild steel	
Heat transfer co-efficient of air	11.3	$W/m^2.K$
Area for heat transfer	2.25	m^2
Q	254.25	W
	0.25	KW
Total conduction and convection losses	680	KJ
Mass Evaporated from plating tank	2.04E-06	kg/s
Critical temperature for water - T_C	647.3	K
Reduced temperature - T_R	0	
C_1	52053000	
C_2	0.3199	
C_3	-0.212	
C4	0.26	
Latent heat of vapourisation	43836310.69	J/kmol
	2435350.59	J/kg
	2435.35	KJ/kg
E_{EVAP}	1.97	KJ
Temperature of plating bath - T_{PB}	296	K
	23.16	^oC
Steady State Temperature Region	**Value**	**Unit**
Humidity - X_1	0.0096	kg H_2O/kg air
Saturation humidity - X_2	0.0138	kg H_2O/kg air
Mass of water evaporated in cooling tower for 1 hour	54.43	kg
Surface area of top of tank	2.25	m^2
Rate of Mass EvapPT	0.0028	$L/m^2.hr$
Mass EvapPT	0.000002	kg/s
	0.0062	kg
Total mass evaporated	54.44	kg

Table 44: Data for operating line and loci for verification 3

Operating Line					
Slope	3489.17		Temperature (^0C)	16	26

Y- Intercept	-15448.30		Enthalpy (J/kg)	40378.37	75270.03
Enthalpy of entering air (J/kg)	40378.37				
Point 1					
Temperature (^{0}C)	16	16	16	16	
Enthalpy (J/kg)	28377.2	30238	32098.8	40378.37	
Locus Point					
Slope	-4249.27		Temperature (^{0}C)	16	15.32
Y- Intercept	108366.61		Enthalpy (J/kg)	40378.37	43267.87
Point 2					
Temperature (^{0}C)	16.5	16.5	16.5	16.5	
Enthalpy (J/kg)	28377.2	30238	40378.37	42100.6	
Locus Point					
Slope	-4249.27		Temperature (^{0}C)	16.5	15.86
Y- Intercept	112213.47		Enthalpy (J/kg)	42100.6	44820.13
Point 3					
Temperature (^{0}C)	17	17	17	17	
Enthalpy (J/kg)	28377.2	30238	40378.37	43728.8	
Locus Point					
Slope	-4249.27		Temperature (^{0}C)	17	16.38
Y- Intercept	115966.31		Enthalpy (J/kg)	43728.8	46363.34
Point 4					
Temperature (^{0}C)	17.5	17.5	17.5	17.5	
Enthalpy (J/kg)	28377.2	30238	40378.368	45589.6	
Locus Point					
Slope	-4249.27		Temperature (^{0}C)	17.5	16.92
Y- Intercept	119951.74		Enthalpy (J/kg)	45589.6	48054.17
Point 5					
Temperature (^{0}C)	18	18	18	18	
Enthalpy (J/kg)	28377.2	30238	40378.37	47450.4	
Locus Point					
Slope	-4249.27		Temperature (^{0}C)	18	17.47
Y- Intercept	123937.17		Enthalpy (J/kg)	47450.4	49702.51
Point 6					
Temperature (^{0}C)	18.5	18.5	18.5	18.5	18.5
Enthalpy (J/kg)	28377.2	30238	40378.37	47450.4	49078.6
Locus Point					
Slope	-4249.27		Temperature (^{0}C)	18.5	17.99
Y- Intercept	127690.00		Enthalpy (J/kg)	49078.6	51245.73
Point 7					

Temperature (^{0}C)	19	19	19	19	19
Enthalpy (J/kg)	28377.2	30238	40378.37	47450.4	50706.8
Locus Point					
Slope	-4249.27		Temperature (^{0}C)	19	18.48
Y- Intercept	131442.84		Enthalpy (J/kg)	50706.8	52916.42
Point 8					
Temperature (^{0}C)	19.5	19.5	19.5	19.5	19.5
Enthalpy (J/kg)	28377.2	30238	40378.37	47450.4	52567.6
Locus Point					
Slope	-4249.27		Temperature (^{0}C)	19.5	19
Y- Intercept	135428.27		Enthalpy (J/kg)	52567.6	54692.23
Point 9					
Temperature (^{0}C)	20	20	20	20	20
Enthalpy (J/kg)	28377.2	30238	40378.37	47450.4	54195.8
Locus Point					
Slope	-4249.27		Temperature (^{0}C)	20	19.5
Y- Intercept	139181.10		Enthalpy (J/kg)	54195.8	56320.43
Point 10					
Temperature (^{0}C)	20.5	20.5	20.5	20.5	20.5
Enthalpy (J/kg)	28377.2	30238	40378.37	47450.4	56056.6
Locus Point					
Slope	-4249.27		Temperature (^{0}C)	20.5	20.05
Y- Intercept	143166.53		Enthalpy (J/kg)	56056.6	57968.77
Point 11					
Temperature (^{0}C)	21	21	21	21	21
Enthalpy (J/kg)	28377.2	30238	40378.368	47450.4	57684.8
Locus Point					
Slope	-4249.27		Temperature (^{0}C)	21	20.5
Y- Intercept	146919.37		Enthalpy (J/kg)	57684.8	59809.43
Point 12					
Temperature (^{0}C)	21.5	21.5	21.5	21.5	21.5
Enthalpy (J/kg)	28377.2	30238	40378.37	47450.4	59545.6
Locus Point					
Slope	-4249.27		Temperature (^{0}C)	21.5	21.05
Y- Intercept	150904.80		Enthalpy (J/kg)	59545.6	61457.77
Point 13					
Temperature (^{0}C)	22	22	22	22	22
Enthalpy (J/kg)	28377.2	30238	40378.37	47450.4	61173.8
Locus Point					
Slope	-4249.27		Temperature (^{0}C)	22	21.5

Y- Intercept	154657.63		Enthalpy (J/kg)	61173.8	63298.43
Point 14					
Temperature (^{0}C)	22.5	22.5	22.5	22.5	22.5
Enthalpy (J/kg)	28377.2	30238	40378.37	47450.4	63034.6
Locus Point					
Slope	-4249.27		Temperature (^{0}C)	22.5	22.01
Y- Intercept	158643.06		Enthalpy (J/kg)	63034.6	65116.74
Point 15					
Temperature (^{0}C)	23	23	23	23	23
Enthalpy (J/kg)	28377.2	30238	40378.37	47450.4	64662.8
Locus Point					
Slope	-4249.27		Temperature (^{0}C)	23	22.5
Y- Intercept	162395.90		Enthalpy (J/kg)	64662.8	66787.43
Point 16					
Temperature (^{0}C)	23.5	23.5	23.5	23.5	23.5
Enthalpy (J/kg)	28377.2	30238	40378.37	47450.4	66523.6
Locus Point					
Slope	-4249.27		Temperature (^{0}C)	23.5	22.96
Y- Intercept	166381.33		Enthalpy (J/kg)	66523.6	68818.20
Point 17					
Temperature (^{0}C)	24	24	24	24	24
Enthalpy (J/kg)	28377.2	30238	40378.37	47450.4	68151.8
Locus Point					
Slope	-4249.27		Temperature (^{0}C)	24	23.43
Y- Intercept	170134.16		Enthalpy (J/kg)	68151.8	70573.88
Point 18					
Temperature (^{0}C)	24.5	24.5	24.5	24.5	24.5
Enthalpy (J/kg)	28377.2	30238	40378.37	47450.4	70012.6
Locus Point					
Slope	-4249.27		Temperature (^{0}C)	24.5	23.9
Y- Intercept	174119.59		Enthalpy (J/kg)	70012.6	72562.16
Point 19					
Temperature (^{0}C)	25	25	25	25	25
Enthalpy (J/kg)	28377.2	30238	40378.368	47450.4	71640.8
Locus Point					
Slope	-4249.27		Temperature (^{0}C)	25	24.38
Y- Intercept	177872.43		Enthalpy (J/kg)	71640.8	74275.34
Point 20					
Temperature (^{0}C)	25.5	25.5	25.5	25.5	25.5
Enthalpy (J/kg)	28377.2	30238	40378.37	47450.4	73501.6

Locus Point					
Slope	-4249.27		Temperature (^{0}C)	25.5	24.85
Y- Intercept	181857.86		Enthalpy (J/kg)	73501.6	76263.62
Point 21					
Temperature (^{0}C)	26	26	26	26	26
Enthalpy (J/kg)	28377.2	30238	40378.37	47450.4	75270.03
Locus Point					
Slope	-4249.27		Temperature (^{0}C)	26	25.3
Y- Intercept	185750.93		Enthalpy (J/kg)	75270.03	78244.52

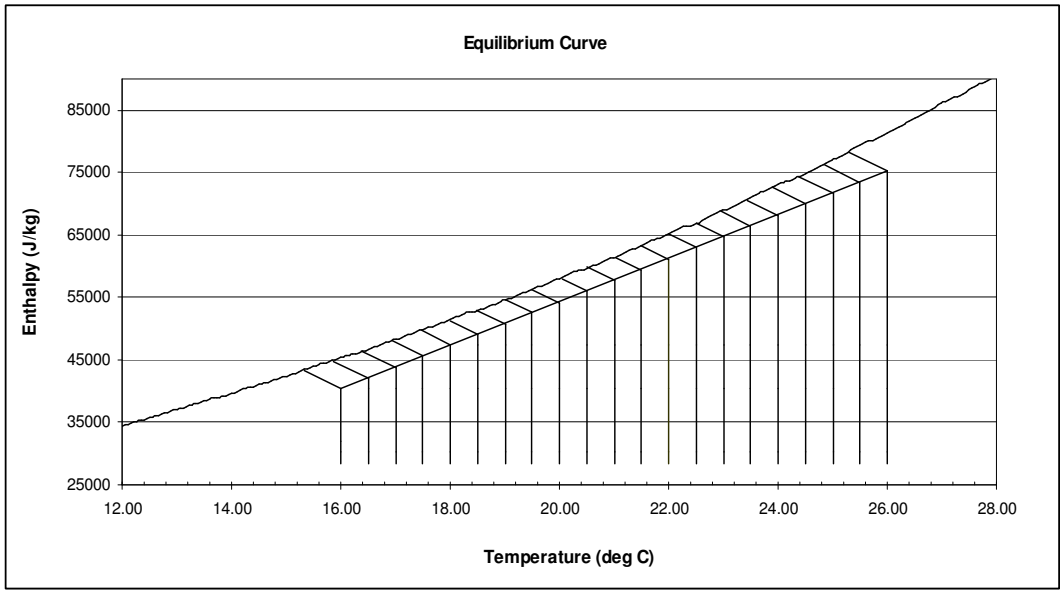

Figure 46: Equilibrium curve with operating line and loci for verification 3

Table 45: Data for construction of area under the curve graph for verification 3

Temperature (^{0}C)	Hy (J/kg)	Hyi (J/kg)	Hyi – Hy (J/kg)	1/Hyi - Hy
16	40378.37	43267.87	2889.50	3.46E-04
16.5	42100.60	44820.13	2719.53	3.68E-04
17	43728.80	46363.34	2634.54	3.80E-04
17.5	45589.60	48054.17	2464.57	4.06E-04
18	47450.40	49702.51	2252.11	4.44E-04
18.5	49078.60	51245.73	2167.13	4.61E-04
19	50706.80	52916.42	2209.62	4.53E-04
19.5	52567.60	54692.23	2124.63	4.71E-04
20	54195.80	56320.43	2124.63	4.71E-04
20.5	56056.60	57968.77	1912.17	5.23E-04
21	57684.80	59809.43	2124.63	4.71E-04
21.5	59545.60	61457.77	1912.17	5.23E-04
22	61173.80	63298.43	2124.63	4.71E-04
22.5	63034.60	65116.74	2082.14	4.80E-04
23	64662.80	66787.43	2124.63	4.71E-04

Temperature (^{0}C)	Hy (J/kg)	Hyi (J/kg)	Hyi – Hy (J/kg)	1/Hyi - Hy
23.5	66523.60	68818.20	2294.60	4.36E-04
24	68151.80	70573.88	2422.08	4.13E-04
24.5	70012.60	72562.16	2549.56	3.92E-04
25	71640.80	74275.34	2634.54	3.80E-04
25.5	73501.60	76263.62	2762.02	3.62E-04
26	75270.03	78244.52	2974.49	3.36E-04

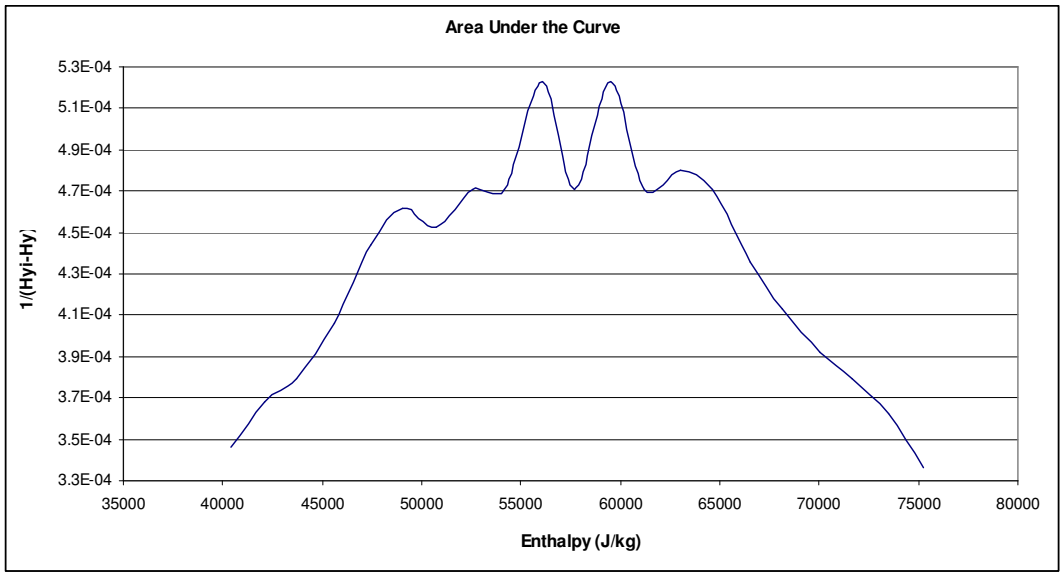

Figure 47: Area under the curve for verification 3

Table 46: Results of graphical solution of integral for verification 3

Area	ΔX	ΔY	ΔX * ΔY
Area 1	2000	3.46E-04	6.92E-01
Area 2	2000	3.70E-04	7.40E-01
Area 3	2000	3.87E-04	7.74E-01
Area 4	2000	4.22E-04	8.44E-01
Area 5	2000	4.57E-04	9.14E-01
Area 6	2000	4.53E-04	9.05E-01
Area 7	2000	4.69E-04	9.38E-01
Area 8	2000	4.74E-04	9.47E-01
Area 9	2000	5.18E-04	1.04E+00
Area 10	2000	4.86E-04	9.72E-01
Area 11	2000	4.99E-04	9.97E-01
Area 12	2000	4.76E-04	9.52E-01
Area 13	2000	4.74E-04	9.48E-01
Area 14	2000	4.39E-04	8.78E-01
Area 15	2000	4.10E-04	8.20E-01
Area 16	2000	3.89E-04	7.78E-01
Area 17	2891.67	3.73E-04	1.08E+00
Total			**15.21**

Annexure D4: Microsoft excel results for verification 4

Table 47: Calculation of cooling tower height for verification 4

Calculation of diffusivity coefficient	**Value**	**Unit**
Molecular mass of diffusing component, M_A	18	kg/kmol
Molecular mass of non diffusing component, M_B	29	kg/kmol
Va	12.7	
Vb	20.1	
Pressure of system, P	1	atm
Temperature of water	302.15	K
D_{AB}	2.57E-05	m^2/s
Calculation of gas phase mass transfer coefficient	**Value**	**Unit**
Pressure of the system	101325	Pa
Temperature of the entering water, T_{L2}	29	oC
	302.15	K
Humidity of the air stream	0.0083	kg H_2O/kg air
Partial pressure of water in the bulk air stream - P_{A2}	0.000	Pa
Partial pressure at the interface - P_{A1}	4010.05	Pa
Log mean partial pressure, P_{BM}	99306.48	Pa
Diameter of cooling tower	1	m
Cross sectional area of cooling tower	0.196	m^2
Air mass flow rate	5	kg/s
G	24.45	$kg/s.m^2$
Temperature of air	14	^oC
	287.15	K
Density of air	1.23	kg/m^3
Viscosity of air	1.80E-05	Pa.s
Volumetric flow rate	3.90	m^3/s
Velocity	19.87	m/s
Reynolds number	680094.01	>2100 - turbulent flow
Schmidt number	0.567	range is 0.5 - 3
Sherwood number	1322.99	
kc'	6.81E-02	m/s
R	8314	m^3.Pa/kmol.K
k_G	2.91E-08	$kmol/s.m^2$.Pa
a	900	m^2/m^3
k_Ga	2.62E-05	$kmol/s.m^3$.Pa
Calculation of slope of operating line	**Value**	**Unit**
Water mass flow rate	4	kg/s
L	20.37	$kg/s.m^2$
Specific heat capacity of water, C_L	4187	KJ/kg.K
Slope	3489.17	
H_{Y1}	35046.756	J/kg.K

H_{Y2}	87384.256	J/kg.K
Calculation of slope of locus	**Value**	**Unit**
Heat transfer co-efficient of water - h_L	280	$W/m^2.K$
Molecular mass of air -M_B	29	kg/kmol
Slope	-3273.17	
Calculation of cooling tower height	**Value**	**Unit**
Integral	35.36	
Height, z	11.23	m

Table 48: Calculation of plating bath temperature for verification 4

Unsteady state temperature region	**Value**	**Unit**
Inlet temperature to cooling tower - T_{L2}	84.2	^oF
	29	^oC
Exit temperature from cooling tower - T_{L1}	57.2	^oF
	14	^oC
Ambient Temperature - T_{AMB}	14	^oC
	287.15	K
Reference Temperature - T_{REF}	14	^oC
	287.15	K
Length of tank	1.5	m
Height of tank	2	m
Width of tank	1.5	m
Volume of plating soln tank	4.5	m^3
Volume of plating soln in tank	3	m^3
Initial Mass of plating tank $M_{PT\|t=0}$	3000	kg
Initial Temperature of tank $T_{PT\|t=0}$	29	^oC
Volumetric flow rate of water	0.0040	m^3/s
Time to pass through cooling tower - $Time_{CT}$	551.18	s
	9.19	min
Surface area of top of tank	2.25	m^2
Rate of Mass $Evap_{PT}$	0.0039	$L/m^2.hr$
Mass $Evap_{PT}$	0.000002	kg/s
	0.00134	kg
Re-circulating flow rate of water	1.06	gal/s
	63.40	gal/min
Rate of Mass $Evap_{CT}$	1.46	gal/min
Mass $Evap_{CT}$	0.09	kg/s
	50.24	kg
Mass flow rate of H_{PS}	4	kg/s
Mass H_{PS}	2204.73	kg
Mass flow rate of C_{PS}	3.91	kg/s
Mass C_{PS}	2154.49	kg
Mass of plating tank at time 2 - $M_{PT\|t=2}$	2949.78	kg
Thickness of metal plate	0.001	m

Length of metal piece	0.05	m
Width of metal piece	0.05	m
Square meter of metal plate	0.0025	m^2
No. of metal pieces	10	
CD	150	A/m^2
V	6	V
E_{ELEC}	12.40	KJ
Density of metal piece - mild steel	7801	kg/m^3
Cp of mild steel	0.473	$KJ/kg.^oC$
E_{CMP}	1.38	KJ
M_{CPS}	3.91	kg/s
Cp of C_{PS}	4.18	KJ/kg.K
E_{CPS}	0.00	KJ
Conduction and Convection Losses from Side 1 = L*H		
Plating bath material of construction	mild steel	
Thermal conductivity of mild steel	0.19	W/m.K
Heat transfer co-efficient of water	280	$W/m^2.K$
Thickness of steel - Δx	0.001	m
Heat transfer co-efficient of air	11.3	$W/m^2.K$
Area for heat transfer	3	m^2
Q	924.69	W
	0.92	KW
Conduction and Convection Losses from Side 2 = W*H		
Plating bath material of construction	mild steel	
Thermal conductivity of mild steel	0.19	W/m.K
Heat transfer co-efficient of water	280	$W/m^2.K$
Thickness of steel - Δx	0.001	m
Heat transfer co-efficient of air	11.3	$W/m^2.K$
Area for heat transfer	3	m^2
Q	924.69	W
	0.92	KW
Conduction and Convection Losses from Bottom of Tank = W*L		
Plating bath material of construction	mild steel	
Thermal conductivity of mild steel	0.19	W/m.K
Heat transfer co-efficient of water	280	$W/m^2.K$
Thickness of steel - Δx	0.001	m
Heat transfer co-efficient of air	11.3	$W/m^2.K$
Area for heat transfer	2.25	m^2
Q	346.76	W
	0.35	KW

Convection Losses from Top of Tank = W*L		
Plating bath material of construction	mild steel	
Heat transfer co-efficient of air	11.3	$W/m^2.K$
Area for heat transfer	2.25	m^2
Q	381.38	W
	0.38	KW
Total conduction and convection losses	1420.68	KJ
Mass Evaporated from plating tank	0.000002	kg/s
Critical temperature for water - T_C	647.3	K
Reduced temperature - T_R	0.47	
C_1	52053000	
C_2	0.3199	
C_3	-0.212	
C4	0.25795	
Latent heat of vapourisation	43727823.48	J/kmol
	2429323.53	J/kg
	2429.32	KJ/kg
E_{EVAP}	3.25	KJ
Temperature of plating bath - T_{PB}	295.81	K
	22.66	^oC
Steady State Temperature Region	**Value**	**Unit**
Humidity - X_1	0.0083	kg H_2O/kg air
Saturation humidity - X_2	0.012	kg H_2O/kg air
Mass of water evaporated in cooling tower for 1 hour	63.94	kg
Surface area of top of tank	2.25	m^2
Rate of Mass EvapPT	0.0027	$L/m^2.hr$
Mass EvapPT	0.000002	kg/s
	0.0061	kg
Total mass evaporated	63.94	kg

Table 49: Data for operating line and loci for verification 4

Operating Line					
Slope	3489.17		Temperature (^{0}C)	14	29
Y- Intercept	-13801.58		Enthalpy (J/kg)	35046.76	87384.26
Enthalpy of entering air (J/kg)	35046.76				
Point 1					
Temperature (^{0}C)	14	14	14	14	
Enthalpy (J/kg)	28377.2	30238	32098.8	35046.76	
Locus Point					
Slope	-3273.17		Temperature (^{0}C)	14	13.22
Y- Intercept	80871.08		Enthalpy (J/kg)	35046.76	37599.83

Point 2					
Temperature (^{0}C)	15	15	15	15	
Enthalpy (J/kg)	28377.2	30238	35046.76	38379	
Locus Point					
Slope	-3273.17		Temperature (^{0}C)	15	14.3
Y- Intercept	87476.49		Enthalpy (J/kg)	38379	40670.22
Point 3					
Temperature (^{0}C)	16	16	16	16	
Enthalpy (J/kg)	28377.2	30238	35046.76	41868	
Locus Point					
Slope	-3273.17		Temperature (^{0}C)	16	15.43
Y- Intercept	94238.66		Enthalpy (J/kg)	41868	43733.70
Point 4					
Temperature (^{0}C)	17	17	17	17	
Enthalpy (J/kg)	28377.2	30238	35046.76	45357	
Locus Point					
Slope	-3273.17		Temperature (^{0}C)	17	16.52
Y- Intercept	101000.83		Enthalpy (J/kg)	45357	46928.12
Point 5					
Temperature (^{0}C)	18	18	18	18	
Enthalpy (J/kg)	28377.2	30238	35046.76	48846	
Locus Point					
Slope	-3273.17		Temperature (^{0}C)	18	17.61
Y- Intercept	107762.99		Enthalpy (J/kg)	48846	50122.53
Point 6					
Temperature (^{0}C)	19	19	19	19	19
Enthalpy (J/kg)	28377.2	30238	35046.76	48846	52335
Locus Point					
Slope	-3273.17		Temperature (^{0}C)	19	18.65
Y- Intercept	114525.16		Enthalpy (J/kg)	52335	53480.61
Point 7					
Temperature (^{0}C)	20	20	20	20	20
Enthalpy (J/kg)	28377.2	30238	35046.76	48846	55824
Locus Point					
Slope	-3273.17		Temperature (^{0}C)	20	19.7
Y- Intercept	121287.32		Enthalpy (J/kg)	55824	56805.95
Point 8					
Temperature (^{0}C)	21	21	21	21	21
Enthalpy (J/kg)	28377.2	30238	35046.76	48846	59313

Locus Point					
Slope	-3273.17		Temperature (^{0}C)	21	20.7
Y- Intercept	128049.49		Enthalpy (J/kg)	59313	60294.95
Point 9					
Temperature (^{0}C)	22	22	22	22	22
Enthalpy (J/kg)	28377.2	30238	35046.76	48846	62802
Locus Point					
Slope	-3273.17		Temperature (^{0}C)	22	21.68
Y- Intercept	134811.66		Enthalpy (J/kg)	62802	63849.41
Point 10					
Temperature (^{0}C)	23	23	23	23	23
Enthalpy (J/kg)	28377.2	30238	35046.76	48846	66291
Locus Point					
Slope	-3273.17		Temperature (^{0}C)	23	22.65
Y- Intercept	141573.82		Enthalpy (J/kg)	66291	67436.61
Point 11					
Temperature (^{0}C)	24	24	24	24	24
Enthalpy (J/kg)	28377.2	30238	35046.756	48846	69780
Locus Point					
Slope	-3273.17		Temperature (^{0}C)	24	23.58
Y- Intercept	148335.99		Enthalpy (J/kg)	69780	71154.73
Point 12					
Temperature (^{0}C)	25	25	25	25	25
Enthalpy (J/kg)	28377.2	30238	35046.76	48846	73269
Locus Point					
Slope	-3273.17		Temperature (^{0}C)	25	24.5
Y- Intercept	155098.16		Enthalpy (J/kg)	73269	74905.58
Point 13					
Temperature (^{0}C)	26	26	26	26	26
Enthalpy (J/kg)	28377.2	30238	35046.76	48846	76758
Locus Point					
Slope	-3273.17		Temperature (^{0}C)	26	25.39
Y- Intercept	161860.32		Enthalpy (J/kg)	76758	78754.63
Point 14					
Temperature	27	27	27	27	27
Enthalpy	28377.2	30238	35046.76	48846	80247
Locus Point					
Slope	-3273.17		Temperature (^{0}C)	27	26.3
Y- Intercept	168622.49		Enthalpy (J/kg)	80247	82538.22

Point 15					
Temperature (^{0}C)	28	28	28	28	28
Enthalpy (J/kg)	28377.2	30238	35046.76	48846	83736
Locus Point					
Slope	-3273.17		Temperature (^{0}C)	28	27.14
Y- Intercept	175384.65		Enthalpy (J/kg)	83736	86550.92
Point 16					
Temperature (^{0}C)	29	29	29	29	29
Enthalpy (J/kg)	28377.2	30238	35046.76	48846	87384.26
Locus Point					
Slope	-3273.17		Temperature (^{0}C)	29	28.01
Y- Intercept	182306.08		Enthalpy (J/kg)	87384.26	90624.69

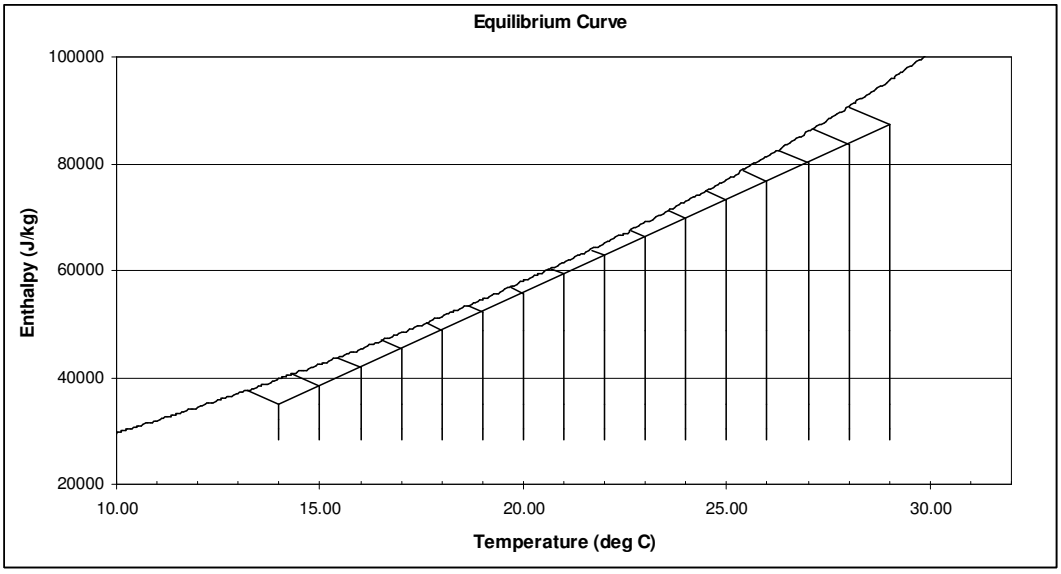

Figure 48: Equilibrium curve with operating line and loci for verification 4

Table 50: Data for construction of area under the curve graph for verification 4

Temperature (^{0}C)	Hy (J/kg)	Hyi (J/kg)	Hyi – Hy (J/kg)	1/Hyi - Hy
14	35046.76	37599.83	2553.07	3.92E-04
15	38379.00	40670.22	2291.22	4.36E-04
16	41868.00	43733.70	1865.70	5.36E-04
17	45357.00	46928.12	1571.12	6.36E-04
18	48846.00	50122.53	1276.53	7.83E-04
19	52335.00	53480.61	1145.61	8.73E-04
20	55824.00	56805.95	981.95	1.02E-03
21	59313.00	60294.95	981.95	1.02E-03
22	62802.00	63849.41	1047.41	9.55E-04
23	66291.00	67436.61	1145.61	8.73E-04
24	69780.00	71154.73	1374.73	7.27E-04
25	73269.00	74905.58	1636.58	6.11E-04
26	76758.00	78754.63	1996.63	5.01E-04

Temperature (^{0}C)	Hy (J/kg)	Hyi (J/kg)	Hyi – Hy (J/kg)	1/Hyi - Hy
27	80247.00	82538.22	2291.22	4.36E-04
28	83736.00	86550.92	2814.92	3.55E-04
29	87384.26	90624.69	3240.43	3.09E-04

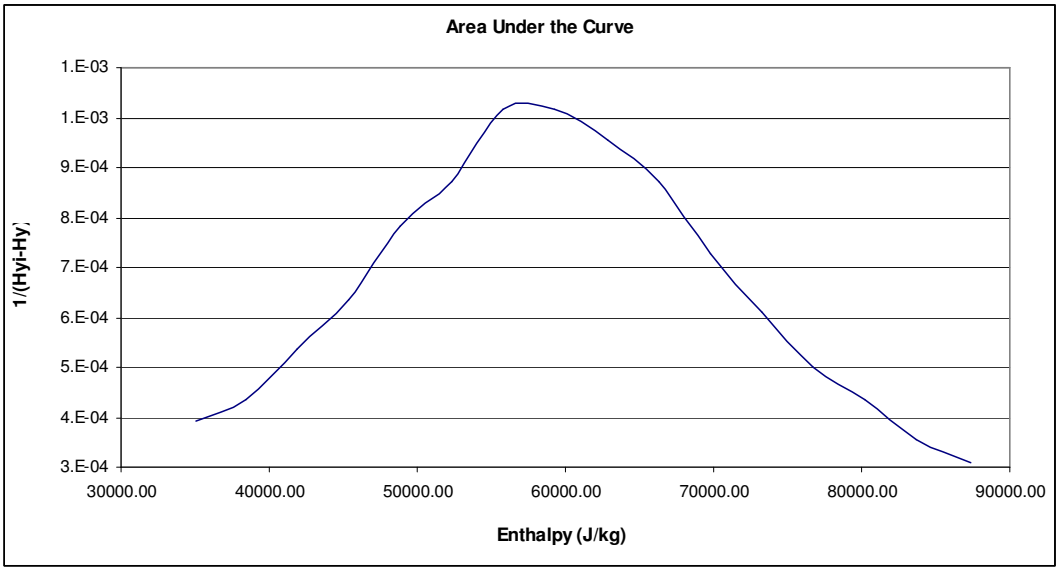

Figure 49: Area under the curve for verification 4

Table 51: Results of graphical solution of integral for verification 4

Area	ΔX	ΔY	ΔX * ΔY
Area 1	3000	3.9169E-04	1.175E+00
Area 2	3000	4.3000E-04	1.290E+00
Area 3	3000	5.1000E-04	1.530E+00
Area 4	3000	5.9300E-04	1.779E+00
Area 5	3000	7.0800E-04	2.124E+00
Area 6	3000	8.1500E-04	2.445E+00
Area 7	3000	9.0000E-04	2.700E+00
Area 8	3000	1.0230E-03	3.069E+00
Area 9	3000	1.0200E-03	3.060E+00
Area 10	3000	9.7000E-04	2.910E+00
Area 11	3000	9.0800E-04	2.724E+00
Area 12	3000	8.0000E-04	2.400E+00
Area 13	3000	6.8200E-04	2.046E+00
Area 14	3000	5.8800E-04	1.764E+00
Area 15	3000	4.9500E-04	1.485E+00
Area 16	3000	4.4000E-04	1.320E+00
Area 17	3000	3.6900E-04	1.107E+00
Area 18	1337.5	3.2500E-04	4.347E-01
			35.36

Annexure D5: Microsoft excel results for verification 5

Table 52: Calculation of cooling tower height for verification 5

Calculation of diffusivity coefficient	**Value**	**Unit**
Molecular mass of diffusing component, M_A	18	kg/kmol
Molecular mass of non diffusing component, M_B	29	kg/kmol
va	12.7	
vb	20.1	
Pressure of system, P	1	atm
Temperature of water	305.15	K
D_{AB}	2.62E-05	m^2/s
Calculation of gas phase mass transfer coefficient	**Value**	**Unit**
Pressure of the system	101325	Pa
Temperature of the entering water, T_{L2}	32	oC
	305.15	K
Humidity of the air stream	0.0063	kg H_2O/kg air
Partial pressure of water in the bulk air stream - P_{A2}	0.000	Pa
Partial pressure at the interface - P_{A1}	4760.71	Pa
Log mean partial pressure, P_{BM}	98925.55	Pa
Diameter of cooling tower	1	m
Cross sectional area of cooling tower	0.196	m^2
Air mass flow rate	6	kg/s
G	30.56	$kg/s.m^2$
Temperature of air	12	^oC
	285.15	K
Density of air	1.24	kg/m^3
Viscosity of air	1.79E-05	Pa.s
Volumetric flow rate	4.85	m^3/s
Velocity	24.68	m/s
Reynolds number	854220.72	>2100 - turbulent flow
Schmidt number	0.552	range is 0.5 - 3
Sherwood number	1583.61	
kc'	8.30E-02	m/s
R	8314	m^3.Pa/kmol.K
k_G	3.58E-08	$kmol/s.m^2$.Pa
a	900	m^2/m^3
k_Ga	3.23E-05	$kmol/s.m^3$.Pa
Calculation of slope of operating line	**Value**	**Unit**
Water mass flow rate	5	kg/s
L	25.46	$kg/s.m^2$
Specific heat capacity of water, C_L	4187	KJ/kg.K
Slope	3489.17	
H_{Y1}	27958.43	J/kg.K

H_{Y2}	97741.76	J/kg.K
Calculation of slope of locus	**Value**	**Unit**
Heat transfer co-efficient of water - h_L	280	$W/m^2.K$
Molecular mass of air -M_B	29	kg/kmol
Slope	-2658.66	
Calculation of cooling tower height	**Value**	**Unit**
integral	44.11	
Height, z	14.22	m

Table 53: Calculation of plating bath temperature for verification 5

Unsteady state temperature region	**Value**	**Unit**
Inlet temperature to cooling tower - T_{L2}	89.6	^oF
	32	^oC
Exit temperature from cooling tower - T_{L1}	53.6	^oF
	12	^oC
Ambient Temperature - T_{AMB}	12	^oC
	285.15	K
Reference Temperature - T_{REF}	12	^oC
	285.15	K
Length of tank	1.5	m
Height of tank	2	m
Width of tank	1.5	m
Volume of plating soln tank	4.5	m^3
Volume of plating soln in tank	3	m^3
Initial Mass of plating tank $M_{PT\|t=0}$	3000	kg
Initial Temperature of tank $T_{PT\|t=0}$	32	^oC
Volumetric flow rate of water	0.005	m^3/s
Time to pass through cooling tower - $Time_{CT}$	558.47	s
	9.31	min
Surface area of top of tank	2.25	m^2
Rate of Mass $Evap_{PT}$	0.0046	$L/m^2.hr$
Mass $Evap_{PT}$	0.000003	kg/s
	0.0016	kg
Re-circulating flow rate of water	1.32	gal/s
	79.25	gal/min
Rate of Mass $Evap_{CT}$	2.43	gal/min
Mass $Evap_{CT}$	0.15	kg/s
	84.84	kg
Mass flow rate of H_{PS}	5	kg/s
Mass H_{PS}	2792.37	kg
Mass flow rate of C_{PS}	4.85	kg/s
Mass C_{PS}	2707.53	kg
Mass of plating tank at time 2 - $M_{PT\|t=2}$	2915.18	kg
Thickness of metal plate	0.001	m

Length of metal piece	0.05	m
Width of metal piece	0.05	m
Square meter of metal plate	0.0025	m^2
No. of metal pieces	10	
CD	150	A/m^2
V	6	V
E_{ELEC}	12.57	KJ
Density of metal piece - mild steel	7801	kg/m^3
Cp of mild steel	0.473	$KJ/kg.^oC$
E_{CMP}	1.84	KJ
M_{CPS}	4.85	kg/s
Cp of C_{PS}	4.18	KJ/kg.K
E_{CPS}	0.00	KJ
Conduction and Convection Losses from Side 1 = L*H		
Plating bath material of construction	mild steel	
Thermal conductivity of mild steel	0.19	W/m.K
Heat transfer co-efficient of water	280	$W/m^2.K$
Thickness of steel - Δx	0.001	m
Heat transfer co-efficient of air	11.3	$W/m^2.K$
Area for heat transfer	3	m^2
Q	1232.92	W
	1.23	KW
Conduction and Convection Losses from Side 2 = W*H		
Plating bath material of construction	mild steel	
Thermal conductivity of mild steel	0.19	W/m.K
Heat transfer co-efficient of water	280	$W/m^2.K$
Thickness of steel - Δx	0.001	m
Heat transfer co-efficient of air	11.3	$W/m^2.K$
Area for heat transfer	3	m^2
Q	1232.92	W
	1.23	KW
Conduction and Convection Losses from Bottom of Tank = W*L		
Plating bath material of construction	mild steel	
Thermal conductivity of mild steel	0.19	W/m.K
Heat transfer co-efficient of water	280	$W/m^2.K$
Thickness of steel - Δx	0.001	m
Heat transfer co-efficient of air	11.3	$W/m^2.K$
Area for heat transfer	2.25	m^2
Q	462.34	W
	0.46	KW

Convection Losses from Top of Tank = W*L		
Plating bath material of construction	mild steel	
Heat transfer co-efficient of air	11.3	$W/m^2.K$
Area for heat transfer	2.25	m^2
Q	508.50	W
	0.51	KW
Total conduction and convection losses	1919.29	KJ
Mass Evaporated from plating tank	0.000003	kg/s
Critical temperature for water - T_C	647.3	K
Reduced temperature - T_R	0.471419744	
C_1	52053000	
C_2	0.3199	
C_3	-0.212	
C4	0.25795	
Latent heat of vapourisation	43618286.19	J/kmol
	2423238.12	J/kg
	2423.24	KJ/kg
E_{EVAP}	3.91	KJ
Temperature of plating bath - T_{PB}	295.58	K
	22.43	^oC
Steady State Temperature Region	**Value**	**Unit**
Humidity - X_1	0.0063	kg H_2O/kg air
Saturation humidity - X_2	0.0104	kg H_2O/kg air
Mass of water evaporated in cooling tower for 1 hour	88.56	kg
Surface area of top of tank	2.25	m^2
Rate of Mass EvapPT	0.0027	$L/m^2.hr$
Mass EvapPT	0.000002	kg/s
	0.005993469	kg
Total mass evaporated	88.57	kg

Table 54: Data for operating line and loci for verification 5

Operating Line					
Slope	3489.17		Temperature (^0C)	12	32
Y-Intercept	-13911.57		Enthalpy (J/kg)	27958.43	97741.76
Enthalpy of entering air (J/kg)	27958.43				
Point 1					
Temperature (^0C)	12	12	12	12	
Enthalpy (J/kg)	25818.6	26516.4	27214.2	27958.43	
Locus Point					
Slope	-2658.66		Temperature (^0C)	12	10.74
Y-Intercept	59862.31		Enthalpy (J/kg)	27958.43	31308.34

Point 2					
Temperature (^{0}C)	13	13	13	13	
Enthalpy (J/kg)	25818.6	26516.4	27958.43	31401	
Locus Point					
Slope	-2658.66		Temperature (^{0}C)	13	11.95
Y-Intercept	65963.54		Enthalpy (J/kg)	31401	34192.59
Point 3					
Temperature (^{0}C)	14	14	14	14	
Enthalpy (J/kg)	25818.6	26516.4	27958.43	34890	
Locus Point					
Slope	-2658.66		Temperature (^{0}C)	14	13.1
Y-Intercept	72111.19		Enthalpy (J/kg)	34890	37282.79
Point 4					
Temperature (^{0}C)	15	15	15	15	
Enthalpy (J/kg)	25818.6	26516.4	27958.43	38379	
Locus Point					
Slope	-2658.66		Temperature (^{0}C)	15	14.2
Y-Intercept	78258.85		Enthalpy (J/kg)	38379	40505.93
Point 5					
Temperature (^{0}C)	16	16	16	16	
Enthalpy (J/kg)	25818.6	26516.4	27958.43	41868	
Locus Point					
Slope	-2658.66		Temperature (^{0}C)	16	15.35
Y-Intercept	84406.51		Enthalpy (J/kg)	41868	43596.13
Point 6					
Temperature (^{0}C)	17	17	17	17	17
Enthalpy (J/kg)	25818.6	26516.4	27958.43	41868	45357
Locus Point					
Slope	-2658.66		Temperature (^{0}C)	17	16.5
Y-Intercept	90554.16		Enthalpy (J/kg)	45357	46686.33
Point 7					
Temperature (^{0}C)	18	18	18	18	18
Enthalpy (J/kg)	25818.6	26516.4	27958.43	41868	48846
Locus Point					
Slope	-2658.66		Temperature (^{0}C)	18	17.52
Y-Intercept	96701.82		Enthalpy (J/kg)	48846	50122.16
Point 8					
Temperature (^{0}C)	19	19	19	19	19
Enthalpy (J/kg)	25818.6	26516.4	27958.43	41868	52335

Locus Point					
Slope	-2658.66		Temperature (^{0}C)	19	18.6
Y-Intercept	102849.48		Enthalpy (J/kg)	52335	53398.46
Point 9					
Temperature (^{0}C)	20	20	20	20	20
Enthalpy (J/kg)	25818.6	26516.4	27958.43	41868	55824
Locus Point					
Slope	-2658.66		Temperature (^{0}C)	20	19.65
Y-Intercept	108997.13		Enthalpy (J/kg)	55824	56754.53
Point 10					
Temperature (^{0}C)	21	21	21	21	21
Enthalpy (J/kg)	25818.6	26516.4	27958.43	41868	59313
Locus Point					
Slope	-2658.66		Temperature (^{0}C)	21	20.65
Y-Intercept	115144.79		Enthalpy (J/kg)	59313	60243.53
Point 11					
Temperature (^{0}C)	22	22	22	22	22
Enthalpy (J/kg)	25818.6	26516.4	27958.43	41868	62802
Locus Point					
Slope	-2658.66		Temperature (^{0}C)	22	21.64
Y-Intercept	121292.45		Enthalpy (J/kg)	62802	63759.12
Point 12					
Temperature (^{0}C)	23	23	23	23	23
Enthalpy (J/kg)	25818.6	26516.4	27958.43	41868	66291
Locus Point					
Slope	-2658.66		Temperature (^{0}C)	23	22.61
Y-Intercept	127440.10		Enthalpy (J/kg)	66291	67327.88
Point 13					
Temperature (^{0}C)	24	24	24	24	24
Enthalpy (J/kg)	25818.6	26516.4	27958.43	41868	69780
Locus Point					
Slope	-2658.66		Temperature (^{0}C)	24	23.52
Y-Intercept	133587.76		Enthalpy (J/kg)	69780	71056.16
Point 14					
Temperature (^{0}C)	25	25	25	25	25
Enthalpy (J/kg)	25818.6	26516.4	27958.43	41868	73269
Locus Point					
Slope	-2658.66		Temperature (^{0}C)	25	24.48
Y-Intercept	139735.42		Enthalpy (J/kg)	73269	74651.50

Point 15					
Temperature (^{0}C)	26	26	26	26	26
Enthalpy (J/kg)	25818.6	26516.4	27958.428	41868	76758
Locus Point					
Slope	-2658.66		Temperature (^{0}C)	26	25.35
Y-Intercept	145883.07		Enthalpy (J/kg)	76758	78486.13
Point 16					
Temperature (^{0}C)	27	27	27	27	27
Enthalpy (J/kg)	25818.6	26516.4	27958.428	41868	80247
Locus Point					
Slope	-2658.66		Temperature (^{0}C)	27	26.25
Y-Intercept	152030.73		Enthalpy (J/kg)	80247	82240.99
Point 17					
Temperature (^{0}C)	28	28	28	28	28
Enthalpy (J/kg)	25818.6	26516.4	27958.43	41868	83736
Locus Point					
Slope	-2658.66		Temperature (^{0}C)	28	27.08
Y-Intercept	158178.39		Enthalpy (J/kg)	83736	86181.96
Point 18					
Temperature (^{0}C)	29	29	29	29	29
Enthalpy (J/kg)	25818.6	26516.4	27958.43	41868	87225
Locus Point					
Slope	-2658.66		Temperature (^{0}C)	29	27.9
Y-Intercept	164326.04		Enthalpy (J/kg)	87225	90149.52
Point 19					
Temperature (^{0}C)	30	30	30	30	30
Enthalpy (J/kg)	25818.6	26516.4	27958.43	41868	90714
Locus Point					
Slope	-2658.66		Temperature (^{0}C)	30	28.75
Y-Intercept	170473.70		Enthalpy (J/kg)	90714	94037.32
Point 20					
Temperature (^{0}C)	31	31	31	31	31
Enthalpy (J/kg)	25818.6	26516.4	27958.43	41868	94203
Locus Point					
Slope	-2658.66		Temperature (^{0}C)	31	29.5
Y-Intercept	176621.36		Enthalpy (J/kg)	94203	98190.99
Point 21					
Temperature (^{0}C)	32	32	32	32	32
Enthalpy (J/kg)	25818.6	26516.4	27958.43	41868	97741.76
Locus Point					

Slope	-2658.66		Temperature (^{0}C)	32	30.3
Y-Intercept	182818.78		Enthalpy (J/kg)	97741.76	102261.48

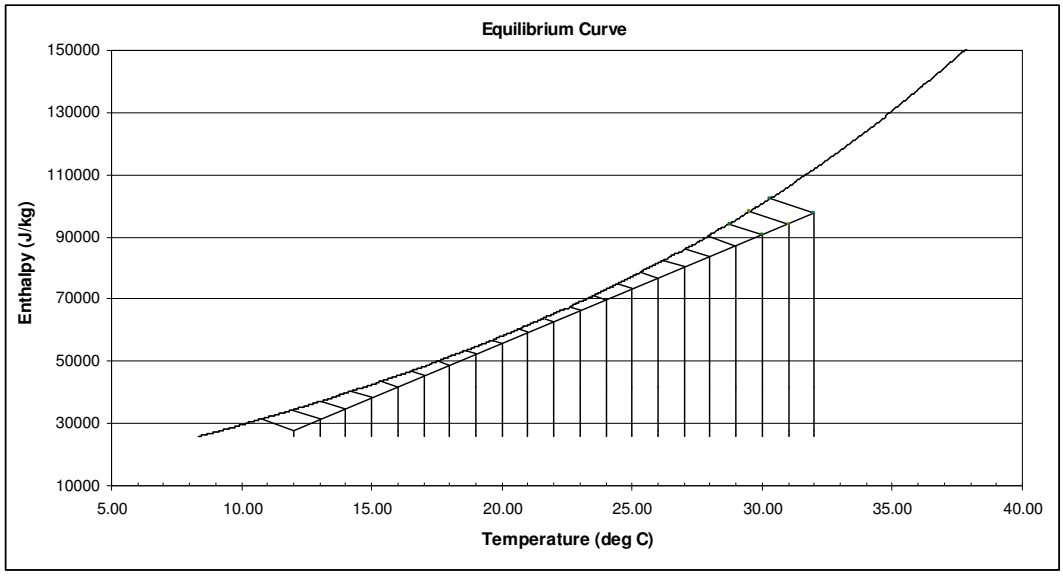

Figure 50: Equilibrium curve with operating line and loci for verification 5

Table 55: Data for construction of area under the curve graph for verification 5

Temperature (^{0}C)	Hy (J/kg)	Hyi (J/kg)	Hyi – Hy (J/kg)	1/Hyi - Hy
12	27958.43	31308.34	3349.91	2.99E-04
13	31401.00	34192.59	2791.59	3.58E-04
14	34890.00	37282.79	2392.79	4.18E-04
15	38379.00	40505.93	2126.93	4.70E-04
16	41868.00	43596.13	1728.13	5.79E-04
17	45357.00	46686.33	1329.33	7.52E-04
18	48846.00	50122.16	1276.16	7.84E-04
19	52335.00	53398.46	1063.46	9.40E-04
20	55824.00	56754.53	930.53	1.07E-03
21	59313.00	60243.53	930.53	1.07E-03
22	62802.00	63759.12	957.12	1.04E-03
23	66291.00	67327.88	1036.88	9.64E-04
24	69780.00	71056.16	1276.16	7.84E-04
25	73269.00	74651.50	1382.50	7.23E-04
26	76758.00	78486.13	1728.13	5.79E-04
27	80247.00	82240.99	1993.99	5.02E-04
28	83736.00	86181.96	2445.96	4.09E-04
29	87225.00	90149.52	2924.52	3.42E-04
30	90714.00	94037.32	3323.32	3.01E-04
31	94203.00	98190.99	3987.99	2.51E-04
32	97741.76	102261.48	4519.72	2.21E-04

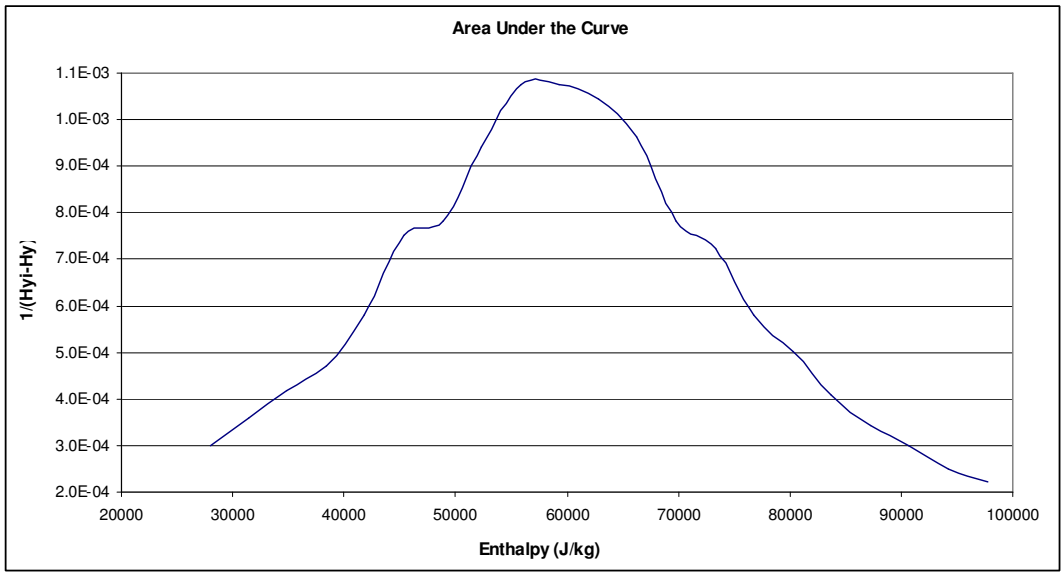

Figure 51: Area under the curve for verification 5

Table 56: Results of graphical solution of integral for verification 5

Area	**∆X**	**∆Y**	**∆X * ∆Y**
Area 1	3000	2.99E-04	8.96E-01
Area 2	3000	3.50E-04	1.05E+00
Area 3	3000	4.00E-04	1.20E+00
Area 4	3000	4.48E-04	1.34E+00
Area 5	3000	5.10E-04	1.53E+00
Area 6	3000	6.35E-04	1.91E+00
Area 7	3000	7.63E-04	2.29E+00
Area 8	3000	7.85E-04	2.36E+00
Area 9	3000	9.20E-04	2.76E+00
Area 10	3000	1.05E-03	3.15E+00
Area 11	3000	1.08E-03	3.25E+00
Area 12	3000	1.07E-03	3.20E+00
Area 13	3000	1.03E-03	3.08E+00
Area 14	3000	9.36E-04	2.81E+00
Area 15	3000	7.80E-04	2.34E+00
Area 16	3000	7.30E-04	2.19E+00
Area 17	3000	6.10E-04	1.83E+00
Area 18	3000	5.29E-04	1.59E+00
Area 19	3000	4.53E-04	1.36E+00
Area 20	3000	3.82E-04	1.15E+00
Area 21	3000	3.32E-04	9.96E-01
Area 22	3000	2.98E-04	8.94E-01
Area 23	3783.33	2.55E-04	9.65E-01
Total			**44.11**